

PNEUMOVIRUS INFECTION AND EFFECTS ON DENDRITIC CELLS OF MICE

A Thesis Submitted to the College of
Graduate Studies and Research
In Partial Fulfillment of the Requirements
For the Degree of Master of Science
In the Department of Veterinary Microbiology
University of Saskatchewan
Saskatoon

By

NATASA ARSIC

Keywords: dendritic cell, virus, RSV, PVM, lung

© Copyright Natasa Arsic, July, 2008. All rights reserved.

Permission to Use

In presenting this thesis in partial fulfilment of the requirements for a Postgraduate degree from the University of Saskatchewan, I agree that the Libraries of this University may make it freely available for inspection. I further agree that permission for copying of this thesis in any manner, in whole or in part, for scholarly purposes may be granted by the professor or professors who supervised my thesis work or, in their absence, by the Head of the Department or the Dean of the College in which my thesis work was done. It is understood that any copying or publication or use of this thesis or parts thereof for financial gain shall not be allowed without my written permission. It is also understood that due recognition shall be given to me and to the University of Saskatchewan in any scholarly use which may be made of any material in my thesis.

Requests for permission to copy or to make other use of material in this thesis in whole or part should be addressed to:

Head of the Department of Veterinary Microbiology

University of Saskatchewan

Saskatoon, Saskatchewan,

S7N 5B4, CANADA

ABSTRACT

Respiratory syncytial virus (RSV) is the primary viral pathogen responsible for lower respiratory tract disease in neonates and young children worldwide. By the age of two, virtually all children have been infected with RSV, and approximately 40% of them develop lower respiratory tract infections. In addition to acute morbidity, an association between RSV infection in early childhood and later development of recurrent wheezing and airway hyperresponsiveness (AHR) has been repeatedly demonstrated.

In this work we established a method for propagating pneumonia virus of mice (PVM) in a baby hamster kidney-21 (BHK-21) cell line. We also modified the standard plaque assay method and established a reliable and, most importantly, reproducible way to quantitate PVM. In our work we used PVM strain 15 to successfully establish an *in vivo* animal model for RSV disease in Balb/c and C57/Bl mice. Different susceptibility/resistance patterns to a pathogen exist for different mouse strains. In the case of Balb/c and C57/Bl mice, these patterns are well characterized for several pathogens including *Leishmania major* and adenovirus type 1. Our comparative study demonstrated clear differences in susceptibility to PVM strain 15 infection between Balb/c and C57/Bl mice; Balb/c mice being more susceptible.

In peripheral sites, dendritic cells (DCs) serve as sentinel cells that take up and process antigens. Numerous studies revealed that certain pathogens stimulate changes in DC phenotypic characteristics and thus contribute to functional alterations that lead to inappropriate T cell activation and disease augmentation. To examine effects of PVM on DCs, we infected bone marrow dendritic cells (BM-DCs) derived from both mouse strains with PVM, and evaluated their phenotypic and functional characteristics 24 hours

post infection. Under these experimental conditions, PVM infected BM-DCs did not show a significant increase in the expression of costimulatory and major histocompatibility complex class II (MHC II) molecules compared to uninfected controls. Furthermore, there were no changes in the ability of PVM-infected DCs to take up soluble antigen. The production of IL-12p70, the pivotal cytokine in the development of a Th1-type response, by the PVM-infected BM-DCs was not significantly different from uninfected cells. In addition, there was no significant impact of PVM infection on the ability of DCs to induce naïve T cell proliferation.

ACKNOWLEDGEMENTS

Many people have contributed to this thesis, but first and foremost, I wish to thank Dr. Sylvia van den Hurk for giving me a chance to work in her laboratory. I also wish to thank the members of my advisory committee, Dr. Lorne Babiuk, Dr. Philip Griebel, Dr. Hugh Townsend for their guidance and support, and Dr. Baljit Singh as my external examiner. I wish to thank Dr. Kuldip Mirakhur and Barry Carroll for their assistance with organizing and conducting animal experiments. Dr. Susantha Gomis for histopathology analysis, Terry Beskorwayne for his help with FACS analysis and Dr. Helene Rosenberg for generously sharing her PVM α -N antibody with me. I would also like to thank Laura Latimer for technical help and Joyce Sander for her precious administrative assistance and words of encouragement in times of need. I wish to thank Terry Beskorwayne, Dr. Shaun Labiuk, Dr. Natalia Vasilenko, Dr. Vladislav Lobanov and John Mapletoft for being my friends during this journey. To my parents, my husband and my daughter, I thank you for standing by me throughout the years.

Dedication

To my parents, Boro and Radoslava Poljasevic, for teaching me to be everything that I am today.

To my husband Srdjan and my daughter Tatjana without whom all of this would not matter.

TABLE OF CONTENTS

PERMISSION TO USE	i
ABSTRACT	ii
ACKNOWLEDGEMENTS	iii
DEDICATION	iv
TABLE OF CONTENTS	vi
LIST OF FIGURES	x
LIST OF ABBREVIATIONS	xiii

1. INTRODUCTION AND LITERATURE REVIEW

1.1 The Burden of Respiratory Syncytial Virus Disease	1
1.2 Epidemiology of Respiratory Syncytial Virus Disease	3
1.3 Virus Classification and Characteristics	4
1.4 Acute and Delayed Pathology of Respiratory Syncytial Virus Infection	7
1.5 Host Characteristics Affecting Pathogenesis	9
1.6 Role of Immunity in Pathogenesis of Respiratory Syncytial Virus Infection	12
1.6.1 Involvement of Innate Immunity	13
1.6.2 Involvement of Cytotoxic T Cells (CD8)	15
1.6.3 Involvement of CD4 T Cells	17
1.6.3.1 Involvement of γ/δ T-Cells	21
1.6.4 Impact of Humoral Immunity	21

1.7 Involvement of Dendritic Cells	24
1.8 Animal Models for Studying Respiratory Syncytial Virus	29
1.9 Pneumonia Virus of Mice	32
1.9.1 Virus Classification and Characteristics	32
1.9.2 Rationale for use as Animal Model for Respiratory Syncytial Virus Infection	33
2.0 HYPOTHESES AND OBJECTIVES	35
3.0 MATERIALS AND METHODS	36
3.1 Media, Cell Lines, and Virus	36
3.2 Stock Virus Preparation	37
3.3 Virus Plaque Assay	38
3.3.1 Immunohistochemistry	39
3.4 Pneumonia Virus of Mice Inactivation by Ultraviolet Irradiation	40
3.5 Mouse Strains	41
3.6 Challenge of Mice with Pneumonia Virus of Mice	41
3.7 Collection of Lungs for Virus Quantitation and Histopathology	42
3.8 Generation of Bone Marrow-derived Murine Dendritic Cells	43
3.9 Flow Cytometric Analysis	44
3.10 Endocytosis Assay	45
3.11 Isolation of Lymphocytes	46
3.12 Nylon Wool Columns for Spleen-derived T Cells	47
3.13 Mixed Lymphocyte Reaction (MLR)	48
3.14 Enzyme-linked Immunosorbent Assays	49

3.15 Immunoblotting	50
4.0 RESULTS	51
4.1 Virus Propagation and Quantitation	51
4.1.1 Virus Propagation	51
4.1.2 Virus Quantification	55
4.2. Establishment of an Intranasal Pneumonia Virus of Mice Challenge	
Model in Balb/c Mice	57
4.2.1 Body Weight Loss	57
4.2.2 Clinical Illness and Survival	59
4.2.3 Viral Titers in the Lungs	62
4.2.4 Macroscopic and Microscopic Pulmonary Lesions in Balb/c	
Mice	64
4.3 Establishment of an Intranasal Pneumonia Virus of Mice Challenge	
Model in C57/Bl Mice	66
4.3.1 Body Weight Loss	66
4.3.2 Clinical Illness and Survival	68
4.3.3 Viral Titers in the Lungs	68
4.3.4 Macroscopic and Microscopic Pulmonary Lesions in C57/Bl	
Mice	72
4.4 Comparative Study of Pneumonia Virus of Mice Infection of	
Balb/c and C57/Bl Mice	74
4.4.1 Influence of the Volume of Inoculum on Pneumonia Virus	
of Mice Infection of Balb/c and C57/Bl Mice	74

4.4.2 Clinical Illness and Survival	77
4.4.3 Viral Titers in the Lungs	79
4.5 In Vitro BM-DC Studies	82
4.5.1. Confirmation of BM-DCs Infection with Pneumonia Virus of Mice by Western Blot	82
4.5.2. Phenotypic Changes of Pneumonia Virus of Mice infected BM-DCs	85
4.5.3. Functional Changes of Pneumonia Virus of Mice infected BM-DCs	90
4.5.3.1 Endocytosis	90
4.5.3.2 Mixed Lymphocyte Reaction	95
4.5.3.3 IL-12 p70 Production by Pneumonia Virus of Mice infected BM-DCs	100
5.0 DISCUSSION	102
5.1 Virus Propagation and Quantitation	102
5.2 Susceptibility / resistance to Pneumonia Virus of Mice infection of Balb/c and C57/Bl Mice	104
5.3 Phenotypic and Functional Changes in BM-DCs upon Pneumonia Virus of Mice Infection	108
6.0 GENERAL DISCUSSION AND CONCLUSIONS	112
7.0 REFERENCES	115

LIST OF FIGURES

Figure 4.1.1	Body weight loss in Balb/c mice challenged intranasally with high or low dose PVM grown at 33 ^o C or 37 ^o C	53
Figure 4.1.2	Clinical signs of Balb/c mice during day six post infection	54
Figure 4.1.3	Appearance of PVM-infected BHK-21 cells 48 hours post infection	56
Figure 4.2.1	Body weight changes compared to day 0 for PVM-infected Balb/c mice	58
Figure 4.2.2	Clinical signs of Balb/c mice during six days post infection	61
Figure 4.2.3	Viral titers of Balb/c mice inoculated with 100 PFU or 500 PFU	63
Figure 4.2.4	Representative macroscopic and microscopic observations in the lung tissue of PVM infected Balb/c mice	65
Figure 4.3.1	Body weight changes compared to day 0 for PVM-infected C57/Bl mice	67
Figure 4.3.2	Clinical signs of C57/Bl mice during 10 days post infection	70
Figure 4.3.3	Viral titers of C57/Bl mice inoculated with 100 PFU or 3000 PFU	71
Figure 4.3.4	Representative macroscopic and microscopic observations in the lung tissue of PVM infected C57/Bl mice	73

Figure 4.4.1	Body weight changes compared to day 0 of PVM-infected Balb/c and C57/Bl mice	76
Figure 4.4.2	Clinical signs of Balb/c and C57/Bl mice for six or seven days post infection	78
Figure 4.4.3	Virus recovered from PVM challenged Balb/c and C57/Bl mice	80
Figure 4.4.4	Comparison of viral titers between Balb/c and C57/Bl mice	81
Figure 4.5.1	The presence of PVM N protein in bone marrow derived DCs cultured for 24 hours with PVM or UV-inactivated PVM	84
Figure 4.5.2.1	Phenotypic changes of PVM-infected BM-DCs, measured by the expression of costimulatory surface markers	87
Figure 4.5.2.2	Phenotypic changes of PVM-infected BM-DCs measured by the expression of costimulatory surface markers	88
Figure 4.5.2.3	Comparison of the expression of costimulatory surface markers between Balb/c and C57/Bl mice	89
Figure 4.5.3.1.1	Uptake of FITC-labeled dextran from medium by BM-DCs	92
Figure 4.5.3.1.2	Comparison of uptake of FITC-labeled dextran from medium by BM-DCs from Balb/c and C57/Bl derived BM-DCs	93
Figure 4.5.3.1.3	Influence of PVM infection on the uptake of FITC-labeled dextran from medium by BM-DCs	94

Figure 4.5.3.2.1	Induction of naïve T cell proliferation by Balb/c BM-DCs subjected to different treatments	97
Figure 4.5.3.2.2	Induction of naïve T cell proliferation by C57/Bl BM-DCs subjected to different treatments	98
Figure 4.5.3.2.3	Comparison of the ability of PVM-infected BM-DCs to induce naïve T cell proliferation in allogeneic MLR in Balb/c and C57/Bl BM-DCs	99
Figure 4.5.3.3	IL-12p70 production by PVM-infected Balb/c and C57/Bl BM-DCs	101

LIST OF ABBREVIATIONS

Ag	Antigen
AHR	Airway hyperresponsiveness
AP	Alkaline phosphatase
APC	Antigen presenting cells
ARDS	Acute respiratory distress syndrome
ATCC	American type culture collection
BCIP	5-bromo-4-chloro-3-indolyl-phosphate
BHK-21	Baby hamster kidney-21
BRSV	Bovine respiratory syncytial virus
BSC-1	Monkey African green kidney epithelial cells
CCA	Chimpanzee coryza agent
CPM	Counts per minute
CTL	Cytotoxic T cells
DC	Dendritic cell
DMEM	Dulbecco's modified eagle medium
DsRNA	Double-stranded RNA
EDTA	Ethylenediaminetetraacetic acid
ELISA	Enzyme-linked immunosorbant assay
F protein	Fusion protein
FBS	Fetal bovine serum
FI-RSV	Formalin-inactivated respiratory syncytial virus
FITC	Fluorescein isothiocyanate
GM-CSF	Granulocyte-macrophage colony-stimulating factor
HEPES	4-(2-hydroxyethyl)-1-piperazineethanesulfonic acid
HIV	Human immunodeficiency virus
HRSV	Human respiratory syncytial virus
ICAM	Intercellular adhesion molecule
IFN	Interferon
Ig	Immunoglobulin
IL	Interleukin
kDa	Kilo Dalton
LPS	Lipopolysaccharide
LRT	Lower respiratory tract
LRTI	Lower respiratory tract infections
mAb	Monoclonal antibody
MCP	Monocyte chemotactic protein
MEM	Minimum essential medium
MHC	Major histocompatibility complex
MIP	Macrophage inflammatory protein
MLR	Mixed lymphocyte reaction

MOI	Multiplicity of infection
mRNA	Messenger ribonucleic acid
NBT	Nitroblue tetrazolium chloride
NK	Natural killer
NO	Nitric oxide
ORF	Open reading frame
PBMC	Peripheral blood mononuclear cell
PBS	Phosphate-buffered saline
PFU	Plaque-forming units
PG	Prostaglandin
PVM	Pneumonia virus of mice
RANTES	Regulated on activation, normal T cell expressed and secreted
RNA	Ribonucleic acid
RSV	Respiratory syncytial virus
RT	Room temperature
SDS-PAGE	Sodium dodecyl sulfate polyacrylamide gel electrophoresis
SEM	Standard error of the mean
SH	Small hydrophobic
SP	Surfactant protein
STAT	Signal transducers and activators of transcription
TBS	Tris-buffered saline
TBST	Tris-buffered saline Tween-20
TCR	T cell receptor
Th	T helper cell
Th1	Type-1 CD4+ T helper cell
Th2	Type-2 CD4+ T helper cell
TLR	Toll-like receptor
TNF	Tumor necrosis factor
URT	Upper respiratory tract
URTI	Upper respiratory tract infection
UV	Ultraviolet

1.0 Introduction and Literature Review

1.1 The Burden of Respiratory Syncytial Virus Disease

Respiratory syncytial virus (RSV) is the primary viral pathogen responsible for lower respiratory tract disease in neonates and young children worldwide (187). RSV causes a seasonal infection, frequently seen in early winter and spring. Virus is transmitted either by large aerosolized droplets, direct contact with respiratory secretions, or via fomites (80, 104). The economic and medical impact of RSV infections in infants is illustrated by the fact that approximately two-thirds of infants are infected with RSV before the age of two (102). Respiratory syncytial virus (RSV) is responsible for an estimated 64 million pediatric hospitalizations worldwide (319). In the United State 125,000 infants and young children are hospitalized due to RSV infections annually, with associated costs of \$400,000,000 per year (261). Unfortunately, up to 2% of hospitalized infants develop respiratory insufficiency and die (6).

In addition to acute morbidity, an association between RSV infection in early childhood and later development of recurrent wheezing and airway hyperresponsiveness (AHR) has been repeatedly demonstrated (183, 238, 265). RSV has also been found to be an important cause of severe respiratory illness among senior citizens (81, 88). In patients with severe combined immunodeficiency disease, RSV pneumonia can lead to respiratory failure with mortality rates of 70–100% (129). Since infection can occur in the presence of circulating antibodies, re-infection is common in all age groups (200).

Apart from host-related characteristics involved in increased susceptibility to severe RSV infections including premature birth, immunodeficiency disorders and host genotype (47, 186, 310), it is speculated that the severe outcome of RSV infections in some younger children is partially caused by the direct cytopathic effect of the virus itself and partially by a defective immunological response (52, 185). Based on results collected while studying infants vaccinated with formalin-inactivated RSV (FI-RSV), it is widely believed that a connection between the severity of RSV disease and imbalance in the Th1- and Th2-lymphocyte response to the vaccine exists. Furthermore, many studies demonstrated that CD8⁺ and CD4⁺ T cells are involved in the inhibition of viral replication as well as RSV-induced pathology (4, 42). Collectively, these studies demonstrate that a fine balance exists between the protective and disease-generating effects of T cells during RSV infection.

Although scientists believed that increased RSV pathology was antibody-mediated, the protective role of antibodies against RSV disease has been demonstrated in several animal models, including cotton rats and monkeys (125, 229). It was demonstrated that passively administered antibody can diminish the frequency of severe RSV-induced illness in at-risk children (110), suggesting that active immunization may indeed be possible. These findings were confirmed in humans by the fact that administration of RSV immunoglobulins and humanized monoclonal antibodies against RSV decreased the incidence and severity of bronchiolitis in high-risk children (110). However, an effective vaccine against RSV infection does not exist.

1.2. Epidemiology of Respiratory Syncytial Virus Disease

Respiratory syncytial virus is distributed globally, and epidemics of RSV take place every winter in temperate climates, and perennially in tropical regions (122). Epidemiological studies of RSV demonstrated the existence of two groups of RSV. Antigenic RSV Group A and RSV Group B were identified based on their different reactivities with monoclonal antibodies against the viral antigens (7, 197). In view of the fact that genetic variability also exists within each group, this may contribute to several strains circulating in a community and repeated infections with RSV (128, 295). The same hypothesis could also be applied to RSV infections of infants under six months of age despite the presence of circulating maternal antibodies against one of the viral strains (196). It was found that the G glycoprotein shows the greatest antigenic diversity among the different RSV strains and that variation in the G glycoprotein may have a considerable effect on the efficiency of transmission (41, 147, 283). During an outbreak, both strains are concurrently present in the community, and season-to-season variation is found in the predominant A strain (5, 181).

In northern regions RSV outbreaks consistently begin each October and continue through April, with the peak period usually taking place between January and March (122). In a community, virus is most commonly transmitted by aerosols, but transmission by direct contact with respiratory secretions or via fomites is also widespread (122). It was shown that RSV in respiratory secretions can survive on surfaces for over six hours. The duration and degree of viral shedding shows a relationship with the clinical severity of disease. Viral shedding can last as long as four weeks in RSV-infected infants, compared to only three to four days in the case of RSV-infected older children and adults (69, 172). Exceptionally high virulence of RSV is

demonstrated by the fact that during community epidemics up to 100 % of children in day care centers could be infected (126). RSV infections are also a major threat to the health of infants in the pediatric wards. During an outbreak, pediatric wards personnel and infected infants who are admitted into hospital are the major source of infection. Since RSV causes mild upper respiratory tract infections in otherwise healthy individuals, up to 50% of personnel may be infected and actively transmit RSV infection without dramatic symptoms that would require absence from work (122). In contrast, the highest risk of morbidity due to RSV infection in infants less than six months of age, emphasizes the significance of RSV nosocomial infections (290).

By the age of two virtually all children have been infected with RSV, and approximately 40% of them develop lower respiratory tract infections and 2% need hospitalization. In the infants that require hospitalization, the mortality rate is approximately 1% (215). Studies in humans showed a direct correlation between large family size and increasing incidence of disease (117). Infants are usually exposed to RSV through contact with school-age siblings who generally show only mild upper respiratory tract infection (URTI) symptoms. Most commonly, life threatening infections are seen in children that already suffer from pre-existing cardiorespiratory disease or are immunocompromised (215). RSV has also been found to be an important cause of severe respiratory illness among senior citizens and immunocompromised individuals (81, 88).

1.3 Virus Classification and Characteristics

Shortly after it was discovered in 1956, RSV was quickly recognized as a major viral pathogen responsible for extensive outbreaks of respiratory tract infections in infants and

immunocompromised individuals world-wide. The virus was discovered accidentally, when a group of chimpanzees in a colony outside of Washington DC exhibited some mild upper respiratory tract infection symptoms. Morris and associates recovered virus from one of the chimpanzees after realizing that people handling the sick animals also became sick. Based on similarities between the Long strain and the Schneider strains isolated from infected humans and Chimpanzee coryza agent (CCA) isolated from sick chimpanzees, Chanock and colleagues included characteristics of all different strains and created the term Respiratory Syncytial Virus (49, 50).

Newly isolated virus was classified as a member of the genus *Pneumovirus*, of the family Paramyxoviridae. The family Paramyxoviridae also contains the *Paramyxovirus* and *Morbillivirus* genera. Other members of the genus *Pneumovirus* are bovine RSV (BRSV) and Pneumonia virus of mice (PVM), which cause respiratory tract disease in calves and mice respectively (36). RSV is a medium-sized enveloped, negative sense RNA virus. The RSV genome is a single strand of nonsegmented RNA composed of approximately 15,000 nucleotides. A model for RSV transcription and replication and the complex role that RSV polymerase plays in this process was recently reviewed by Cowton *et al.* (62). The viral genome replicates within the cytoplasm of lung epithelial cells and alveolar macrophages, and encodes 10 viral proteins, G, F, SH, M, N, P, L, M2, NS1 and NS2 (75).

Out of those 10 proteins, the G, F, and SH proteins are transmembrane surface proteins. The fusion (F) protein is a transmembrane glycoprotein 68 kDa in size, and composed of two disulphide-linked subunits. Subunit F1 is 48 kDa while subunit F2 is 20 kDa in size. The F protein mediates viral penetration and cell-to-cell spread by the fusion of the viral or infected-cell membrane with target cell membrane. It is believed that the F protein exists in metastable

conformation that is changed into a fusogenic conformation by contact with the receptor on the target cell membrane. This change brings highly hydrophobic residues of F1 in close proximity of the target membrane and allows fusion (193). This fusion of infected cell membranes results in characteristic syncytium formation, the hallmark of RSV infection (36). It is significant to mention that antibodies produced to the epitopes of the F protein by the host cells can neutralize virus. Transmembrane surface protein G is a 70 kDa glycoprotein. Heavily glycosylated G glycoprotein shows structural homologies with the CX3C chemokine fractaline and mediates viral attachment by binding to human CX3CR1 surface receptor. Similar to the F protein, the G protein can stimulate the production of effective anti-RSV antibodies (36, 80). Although antigenic diversity between the different RSV strains could be due to antigenic differences in the G, F, N and P RSV proteins, the attachment G protein is the most variable protein. In some instances, the amino acid homology of the attachment G protein between the A and B RSV isolates can be as low as 53% (36). These strain variations could be yet another mechanism by which RSV evades host immune responses. The third transmembrane surface protein is a small hydrophobic protein (SH), 14 kDa in size. The function of the transmembrane surface protein SH is not clear, but it has been reported that SH is not required for viral replication and syncytium formation (38).

There are also four nucleocapsid-associated proteins: N, P, L, and M2. These proteins associate with the genomic RNA to form the viral nucleocapsid. Nucleoprotein N is a 45 kDa protein that protects genomic and antigenomic RNA and mediates transition from transcription to replication. Matrix protein M2 has two transcripts: the M2 ORF-1, which serves as a transcription anti-termination factor and the M2 ORF-2 which functions as a RNA regulatory protein (80). Matrix proteins M2 ORF-1 and M2 ORF-2 have molecular masses of 22 kDa and

12 kDa respectively. Phosphoprotein P (33 kDa) and polymerase protein L (250 kDa) are nucleocapsid-associated proteins that act as a polymerase co-factor and RNA-dependent RNA polymerase, respectively (80). Matrix protein M is a small 25 kDa protein, which mediates the association between the viral nucleocapsid and the envelope (212).

Finally, the non-structural viral proteins NS1 and NS2 are two small 13.8 and 14.5 kDa viral products that accumulate in infected cells but are almost untraceable in mature virions (212). Only recently, the non-structural proteins NS1 and NS2 were correlated to species-specific inhibition of and resistance to α/β interferons via interferon regulatory factor 3 (33, 255).

1.4 Acute and Delayed Pathology of Respiratory Syncytial Virus Infection

RSV causes a seasonal infection, most frequently in winter and spring. Virus is transmitted either by large aerosolized droplets, or direct contact with respiratory secretions, or via fomites (80, 104). The incubation period of RSV respiratory disease is approximately five days (151, 279). RSV does not show systemic spread and primarily replicates in the epithelial cells of the nasopharynx (120).

It is believed that the mechanism by which the virus spreads from the upper respiratory tract to the lower respiratory tract involves direct viral spread along the respiratory mucosa by induction of cell fusion and syncytium formation or viral transfer via aspiration of nasopharyngeal secretions (262). Several studies reported that alveolar macrophages are infected with RSV *in vivo*, implicating an additional potential mechanism for the spread of RSV to the lower respiratory tract (190, 218).

Primary infantile RSV infection is usually a mild upper respiratory tract infection that in 40% of cases progresses into a mild lower respiratory tract infection (278). The onset of symptoms depends on the age of the infected individual. While infants can show signs and symptoms of infection within hours or days of inoculation, adults and older children may not have symptoms of RSV infection for several days after the infection. In most cases, the symptoms of RSV mimic the common cold. Symptoms of RSV infection can be mild, moderate or severe, the latter mostly seen in infants younger than 30 weeks of age. Signs of lower respiratory tract involvement usually develop 1–3 days after the onset of rhinorrhea, the most prominent upper respiratory tract symptom (19). Apart from the stuffy nose and nasal flaring accompanied by low-grade fever, symptoms such as deep cough, shortness of breath and wheezing usually mark the occurrence of viral spread into the bronchi and bronchioles. Infants tend to be irritable and have irregular feedings due to the breathing difficulties. Bronchiolitis is the hallmark of lower respiratory tract involvement during RSV infection (80). Typically, bronchiolar epithelial necrosis and loss of specialized functions such as ciliary motility due to ciliated epithelial cell destruction are observed (1). Small airways (75- 250 microns) first show characteristic pathological bronchiolitis features. Peribronchiolar infiltration by lymphocytes, eosinophils, neutrophils and macrophages, followed by submucosal edema and increased mucus secretion inevitably lead to hyperinflation and collapse of distal lung tissue (117). In severe cases, RSV pneumonia with interstitial infiltration of mononuclear cells is also common (69). It is important to point out that RSV infection is not a severe disease in the majority of RSV infected children and otherwise healthy adults, and the exact pathology in this population is not well known since they never seek doctors' attention (215).

There are various reports that RSV bronchiolitis experienced in the first year of life is often associated with recurrent childhood wheezing (183, 267, 275). Several studies also demonstrated that approximately half of all children hospitalized for treatment of RSV bronchiolitis have later episodes of childhood wheezing or lung function abnormalities (148, 205, 287). This association usually disappears by the age of 12, but in some cases it can progress into asthma. It was shown that children with RSV bronchiolitis during the first six months of their lives had significantly higher incidences of asthma than children in a control group (266). So far, studies that show a direct cause and an effect relationship between RSV bronchiolitis and asthma have not been performed. Further, more recent studies indicate that pre-existing alterations in lung function early in life is a more important sign of recurrent wheezing later in life than a history of RSV bronchiolitis (268).

There is also a belief that viral persistence could account for the delayed effect of RSV infection. Persistent infection of a macrophage-like cell line *in vitro* as well as macrophages in several animal models *in vivo* has been demonstrated (34, 112, 297, 298). Also, studies in mice showed reappearance of infectious virus after suppression of T cells in mice that had been infected with RSV and recovered (259). Presently, studies on long-term infection in humans show contradicting results, and the need for future research is apparent (89, 318).

1.5 Host Characteristics Affecting Pathogenesis

The specific mechanisms which determine why RSV infection causes severe disease in some children and only mild symptoms and signs of infection in others are not well understood. Environmental conditions such as family size, socio-economic status, day care attendance, and

parental smoking, have been associated with exacerbated disease (219, 270, 320). The presence of underlying illnesses like congenital heart disease or pulmonary disease with diminished lung function or premature birth (< 35 weeks gestation) are also associated with increased incidence of severe RSV infections (108, 178, 182).

Differences in the severity of the infection caused by RSV can also be understood by taking the different host factors involved in the pathogenesis of the disease into consideration. Each year during a RSV outbreak approximately 5-10% of otherwise healthy adults are re-infected with RSV, but the clinical representation of the disease is never dramatic in nature (90, 118). Several studies have revealed that age may play a significant role in disease severity (92, 203, 251). While the majority of RSV infections in older children and adults are mild in nature, infections of neonates and elderly individuals may result in severe consequences. The immunological immaturity of an immune response in neonates and the deteriorating immune response in the elderly may be associated with an imbalanced RSV-specific immune response that favors disease augmentation (14, 189). The lack of lung elasticity in neonates and the elderly is also a significant contributing factor for increased disease susceptibility in this population (99, 214). Animal studies using a mouse model revealed that mice infected very early in life (up to 1 week of age) showed increased severity of disease symptoms including enhanced IL-4 production, increased cell recruitment to the lung, and increased eosinophilia and neutrophilia upon secondary infection later in life (68). Although severe RSV infections are usually observed in young infants, in one study 21 percent of acute respiratory infections in a senior care center were caused by RSV (91). Furthermore, re-infection within a senior population is common and usually severe in nature (204).

The immune status of an infected person also plays a significant role in the pathogenesis of the disease. The role of RSV as an opportunistic pathogen is clearly seen in cases of severely immunosuppressed patients after bone marrow transplantations. In this population, RSV infections are more severe with a mortality rate ranging from 30 to 100% (317). Human immunodeficiency virus (HIV) is an important cause of immunosuppression in humans (80). HIV infected patients show prolonged virus shedding (48) and a more severe manifestation of disease (1) after RSV infection. Fortunately, severe respiratory complications and mortalities are uncommon (156). Since the exacerbated disease is induced mostly by an excessive immune response (289), a more severe manifestation of a disease in immunocompromised individuals clearly indicates the need for control of viral replication by cell-mediated immunity. Otherwise, RSV will cause progressive cytopathic damage to the lung tissue that will inevitably lead to respiratory failure (43).

Several studies were performed in an effort to investigate possible relations between RSV group A and B and clinical severity of RSV infections. The results were inconclusive, since some investigators were able to find a direct correlation between group A strain infection and more severe disease (304), while others failed to do so (158). Interestingly, in two studies infections with group B strain were reported as more severe (135, 280).

Since variation in the severity of RSV infections in human populations exists, possible influences of host genotype on the disease phenotype were investigated. Several animal studies demonstrated a significant influence of host genotype on the severity of disease (142, 274). In one study, susceptibility to RSV infection was examined in 8 different inbred mouse strains. The most resistant strain was C57BL/6J, while BALB/cJ was a moderately susceptible strain, and AKR/J mice were found to be the most permissive strain (274). Upon examination of clinical

signs and viral titers recovered from backcross progeny infected with RSV, authors concluded that susceptibility to RSV has to be influenced by multiple genes (274). In a separate study, interferon (IFN)- γ dependent resistance to eosinophilia in C57BL/6 mice compared to BALB/cJ was also confirmed (142). A genetic association with the severity of RSV infection in human studies has been found for IL-8 , IL-4, IL-6, IL-10, CD14 and surfactant protein (SP)-A and SP-D, (54, 103, 114, 118, 119, 133, 272, 286). During the RSV infection surface glycoprotein F activates MyD88 pathway via pattern recognition receptor TLR4 and CD14 (163). Awomoyi *et al.* recently showed that hyporesponsiveness of TLR4 could be associated with two single nucleotide polymorphisms (SNPs) in the ectodomain of TLR. They also suggested that TLR4 SNPs could be correlated to premature birth, indicating the reason for increased incidents of severe RSV infection in this population (16). In light of all these findings, it is apparent that additional research is necessary to further investigate the causative role of these and other genetic factors in the severity of RSV infections. Consequently, development of easier screening and appropriate implementation of prophylactic measures for infants at high risk should be put in place.

1.6 Role of Immunity in pathogenesis of Respiratory Syncytial Virus infection

Similar to other respiratory infections, both innate and acquired immune factors are required for recovery from RSV infection. Although necessary, immune factors involved in resolution of RSV infection play a substantial role in disease pathogenesis. This is confirmed by the fact that RSV is not a highly cytopathic virus (157). For example, human studies demonstrated absence of clinical improvement in cases where viral load in infected children was

decreased up to 30-fold by administration of protective antibodies (180). Also, an association of genetic polymorphisms for IL-8, and IL-4 with severity of RSV infection further implicates immunopathology rather than just the cytopathic effect of the virus as a cause for augmentation of clinical disease (141).

1.6.1 Involvement of Innate Immunity

Innate immune cells and their products are the first line of defense against RSV and other pathogens. The importance of this arm of the immune response is exemplified by its role not only in immediate defense but also in its ability to initiate and shape the development of the specific, acquired immune response.

During the establishment of RSV infection, respiratory epithelial cells and resident macrophages are predominantly targeted by the virus. Epithelial cells recognize RSV via interaction of toll like receptor 4 (TLR4) and RSV surface protein F. This interaction triggers the host cellular response characterized by the upregulation of the STAT and NF-kB pathways, which leads to changes in cellular gene expression and increased production of several cytokines, chemokines, surfactants and cell surface molecules (25, 115).

For instance, it was reported that hospitalized RSV-infected infants have decreased concentrations of surfactant protein A in the broncho-alveolar lavage fluid (153). In addition, *in vitro* studies revealed surface protein A's ability to neutralize RSV infection by binding to the fusion F protein, supporting its role in RSV pathology (98).

Following RSV infection, lung epithelial cells show an increase in the expression of several cell-adhesion molecules including ICAM-1 (involved in the retention of neutrophils at

the site of infection) as well as class I major histocompatibility complex (MHC-I) molecules (13) that are involved in antigen-presentation (95). Furthermore, IL-1 α , IL-6, IL-11, granulocyte-macrophage colony-stimulating factor (GM-CSF) and tumor necrosis factor α (TNF- α) are only some of the proinflammatory and immunomodulatory cytokines produced by RSV-infected lung epithelial cells (12, 85, 192, 208, 213).

Both human and animal studies confirmed the enhancement of chemokine production during RSV infection (116, 165, 207). Chemokines are chemoattractant cytokines produced by monocytes and epithelial cells that mediate recruitment to the respiratory tract during RSV infection (122). Given that pathological damage of the lung tissue during severe RSV infections is characterized by the influx of innate immune cells, the importance of chemokines in disease pathogenesis can not be overlooked. Chemokines such as CXCL8 (IL-8), CCL2 (monocyte chemoattractant protein-1 (MCP-1)), CCL3 (macrophage inflammatory protein-1 α (MIP-1 α)) and CCL5 (regulated on activation, normal T cell expressed and secreted (RANTES)) are repeatedly implicated as mediators in severe RSV infections (300).

It was shown that upregulation of neutrophil and T cell chemoattractant CXCL8 (IL-8) could be linked to the severity of bronchiolitis mediated by excessive pulmonary neutrophilia (103). Neutrophils, which represent over 90% of cells in the URT and over 70% in the LRT during RSV infection, play both protective and disease-inducing roles during RSV infection (87). Neutrophils express their protective role against RSV by destroying virus-infected cells via lytic enzymes that are released during the process of neutrophil degranulation (305). Unfortunately, the cytotoxic effect is non-specific and in addition to virus-infected cells many surrounding healthy cells are inevitably damaged. CCL5 is a second cytokine that is very often associated with severe illness after RSV infection. Stimulated by IFN- γ , IL-1 α , IL-1 β , and TNF- α , CCL5

serves as a potent chemoattractant for monocytes, memory T cells, and eosinophils. Resembling the action of neutrophils, eosinophils also lack specificity in their action, and inflict damage to healthy by-stander cells in addition to RSV-infected ones (103).

The importance of CCL5 in disease severity is further supported by the observation that increased levels of CCL5 were found in nasal lavage fluids from infants with RSV bronchiolitis compared to those that were RSV-infected but without augmented clinical signs of disease (209). A different study also revealed an increase in IL-12 production and significant reduction in airway hyperreactivity following treatment with anti-CCL5 antibodies (288).

The role chemokines play in directing the development of an acquired immune response was demonstrated by comparative studies of chemokine expression profiles during Th1- or Th2-type responses induced by RSV in BALB/c mice. While increased levels of CCL2, CCL11 (chemoattractive mediator for eosinophils), and CXCL10 were found during a Th2-biased response, the Th1-type response was marked by an increase in CCL3 levels (67, 258).

These data collectively demonstrate the important role chemokines play in determining both the level of pulmonary inflammation and the type of immune cells recruited to the site of infection. The role of dendritic cells (DCs), one of the specialized cellular members of the innate immune response, will be discussed.

1.6.2 Involvement of Cytotoxic T Cells (CD8)

Abundant evidence supports the view that RSV-specific cytotoxic T cells (CTL) act as a key immune factor involved in viral clearance (4). Similar to their role in other viral infections,

CD8 T cells migrate to the site of RSV infection and act either by secreting cytokines that activate other immune cells or by inducing apoptosis of infected epithelial cells via perforin/granzyme or Fas/FasL mechanisms (179). Apart from their protective role in RSV infections, there is a growing body of evidence that supports the belief that an exaggerated CTL response is responsible for more severe manifestations of RSV disease (56).

On the other hand, studies of lung tissue from fatal cases of RSV infection in infants revealed almost complete absence of natural killer (NK) and CD8 T cells, indicating an inadequate immune response as a reason for fatality. Furthermore, the amount of lymphocyte – derived cytokines was also negligible (315).

It is important to mention that CD8 T cells serve as a principal source of IFN- γ and that mouse studies showed conflicting results regarding the role of lymphocyte–derived cytokines like IFN- γ with regards to the disease severity. While some studies performed with IFN- γ knockout mice uncovered a decrease in lung airway obstruction of RSV-infected compared to wild-type animals (301), other studies showed an absolute requirement for the presence of IFN- γ for protection (224).

Both protective and detrimental effects of CTLs in RSV infection were demonstrated in several mouse animal studies. For instance, studies with immunodeficient mice with prolonged persistent infection, showed that the presence of adequate amounts of RSV-specific CD8 T cells leads to complete clearance of RSV (105). Similar results were obtained from adoptive transfer studies in mice, where termination of RSV infection was observed following the transfer of RSV-specific CD8 T cells (4, 42). Human studies also confirmed a protective role for CTLs. For example, in two independent studies an association between a significant decrease in clinical symptoms and an increase in the number of CTLs in the peripheral blood was observed in

previously infected adults (18, 145). Nevertheless, adaptive transfer studies also showed that if large numbers of RSV-specific CTLs were transferred to RSV-infected mice, viral clearance was accompanied by acute pulmonary damage, which in some cases progressed into terminal damage (42).

As previously mentioned, RSV infections tend to be more severe in infants under six months of age (161). The role CD8 T cells play in this interesting trend was very elegantly demonstrated in a study by Chiba *et al.* who measured the cytotoxic activity in infants six months of age or older and five months of age or younger. Astonishingly, 60% of older infants showed cytotoxic activity compared to only 25% of younger infants, indicating inappropriate RSV specific CTL response as a possible cause for more severe manifestations of RSV infection in younger infants (53).

Mouse studies also showed that RSV-specific CD8 T cells that migrate to the lungs of infected mice show signs of functional impediment characterized by a decrease in cytotoxic capacity and production of anti-viral cytokines (299). This finding indicates the presence of tissue-specific CD8 down-regulatory mechanisms that can possibly impede proper CD8 T cell function. At this point, the true nature of CTL involvement in the immunopathology of RSV disease is still incompletely understood, and future research is necessary to resolve present dilemmas.

1.6.3. Involvement of CD4 T Cells

Like CD8 T cells, CD4 T cells are involved in protection as well as RSV disease augmentation (4). The CD4 T cells are generally divided into two classes. The first class

represents the Th1 subset of CD4 T cells and is characterized by production of specific cytokines, namely IL-2, IFN- γ , and TNF- α . The Th2 subset of CD4 T cells, is characterized by production of IL-4, IL-5, IL-6, IL-10 and IL-13 (175).

In order to explain the enhancement of RSV disease as a result of the type of immune response generated, the most useful model was derived from studies using FI-RSV conducted in 1966 and 1967. Those studies revealed that prior vaccination with FI-RSV led to more severe disease upon infection with RSV. Vaccinated children did not show a decrease in the rate of infection following RSV exposure, and most significantly, 80% of vaccinated children needed hospitalization. Among those hospitalized, two died while the remaining patients showed a wide range of respiratory illnesses including pneumonia, bronchiolitis, rhinitis, or bronchitis (155).

Postmortem microscopic examination of the deceased patients showed intense inflammatory cell infiltrate, including mono- and polymorphonuclear cells, and massive eosinophilia (201). It is of interest that a recent paper by Prince *et al*, 2001 (227) disputes that eosinophilia is a primary marker of vaccine-enhanced RSV disease as the eosinophils observed earlier might actually have been neutrophils. Furthermore, other groups found neutrophilic alveolitis without the presence of eosinophilia in calves (97) and green monkeys (150).

The most commonly accepted explanation for the disease-augmenting response to the vaccine is the development of an imbalance in the Th1- and Th2-lymphocyte response. Clinical and histological findings in infants vaccinated with FI-RSV confirmed an unusual immune shift toward a Th2-type response, in contrast to the expected Th1-type response seen during the majority of viral infections (109). Additionally, mice vaccinated with FI-RSV showed a T cell-mediated increase in lung pathology that was reversed upon treatment with IL-4- and IL-10-specific monoclonal antibodies (58, 59, 308). It is interesting to mention that several studies

demonstrated a predominant Th1-type response in murine models of RSV infection (17, 18, 43). Contrary to non-vaccinated animals, in vaccine studies different types of responses were reported depending on the type of vaccine used. For example, a Th1-type response with predominant secretion of IFN- γ , IL-2 and production of IgG2a was seen in animals vaccinated with the F protein, while a Th2-type response was seen in animals vaccinated either with FI-RSV or RSV G protein (23, 146).

With respect to the RSV G protein, an interesting discovery was made while studying mice vaccinated with this protein. Varga *et al.* showed that upon re-infection of mice vaccinated with RSV G protein, the majority of G-specific CD4 T cells express the V β 14 T cell receptor (303). The involvement of this G-specific CD4 T cell subset in the severity of RSV disease was confirmed when the pulmonary disease enhancement was diminished upon elimination of these V β 14-bearing CD4 T cells (224). Moreover, increased lung eosinophilia was reported in naïve mice following passive administration of RSV G-specific CD4 T cells (3).

Conflicting findings regarding the role of CD4 T cells are numerous and derived from both mouse and human studies. For instance, passive transfer studies showed augmentation of lung pathology in mice that received CD4 T cells. However, the decrease in pulmonary virus titers of infected mice upon treatment with CD4 T cell-enriched splenocytes demonstrated a protective role for CD4 T cells (4, 42).

Studies in humans confirmed the contradictory results from the animal model studies. For instance, the role of IFN- γ , the hallmark cytokine of a Th1-type response, was investigated in several human studies. A comparison of IFN- γ in nasopharyngeal washing between children with severe and mild manifestations of RSV disease revealed increased production of IFN- γ in children with severe clinical disease (302). In another study, IFN- γ was also found to be the most

abundant cytokine in patients with clinically severe disease (35). In contrast, a strong Th2-biased response marked by increased IL-4 production and pulmonary eosinophilia was found while studying RSV infected infants 12 month of age or younger (161). A Th2-type response with high IL-4 vs. IFN- γ ratios and low IFN γ , IL-12 and IL-18 mRNA expression was also found in another study with infants with acute bronchiolitis (171).

Cortisol is a glucocorticosteroid involved in inhibition of IFN- γ production through its direct action on T cells or indirectly through a decrease in IL-12 production. A recent study by Pinto *et al.* showed a correlation between decreased IL-12 and IFN- γ production by PBMCs of infants with severe RSV disease and high plasma cortisol levels in this population compared to uninfected or RSV-infected infants with mild clinical manifestations (223).

Taken together, these results without a doubt prove the ability of RSV to induce both Th1- and Th2-type responses, so further studies on the involvement of Th1- and Th2-types of responses in disease augmentation are necessary (36).

Repeated re-infection with RSV in all age groups (119, 126) demonstrates the apparent absence of long-lived protective immunity against RSV. It has been repeatedly shown that RSV-specific memory T cells are able to proliferate upon subsequent RSV challenge and that these memory cells are mostly stored in the spleen (216, 242). In their work Richter *et al.* experimentally proved that memory T cells found at the site of infection belonged to the “short lived” effector memory T cells (characterized by IFN- γ but no IL-2 production), indicating the absence of “long-lived” IL-2 producing central-memory T cells as a possible reason for the lack of long-lasting protection (149, 242, 249, 250).

1.6.3.1 Involvement of γ/δ T-cells

Although, rarely examined, a minor T-cell population characterized by the expression of gamma-delta chain on the T cell receptor (γ/δ TCR) has also been implicated in the immunopathogenesis of RSV infection (10). Contrary to α/β T cells, this T cell subset has the unique ability to recognize proteins directly, independent of the major histocompatibility complex (175). In one longitudinal study of human infants infected with RSV, acute RSV-induced bronchiolitis was linked to decreased IFN- γ production by γ/δ T-cells. Two years later, the infants that had reduced amounts of IFN- γ in the peripheral blood during the acute phase of RSV-induced bronchiolitis were more likely to develop recurrent wheezing (10). This observation provided evidence for a possible role for γ/δ T-cells. Perhaps a change in IFN- γ production from this subset of T cells biases the α/β T cell immune response toward a Th2-type response by altering the cytokine microenvironment.

1.6.4 Impact of Humoral Immunity

The protective role of RSV-specific antibodies is well documented in both human and animal studies (125, 169, 229). IgM, IgA, and IgG of both serum and secretory type are present upon RSV infection. Although they can be raised against the majority of RSV proteins, the antibodies specific for the F and G proteins are most important for protection (100, 211, 296, 306). Though useful for protection against RSV, the antibody response is not enough for resolution of RSV infection and involvement of cellular immunity is required for viral clearance.

In RSV-infected patients, secretion of IgM starts after five to eight days and IgM can be detected up to three months post-infection. Secretory IgA is induced during the first two to five days after infection and is particularly important in protecting the upper respiratory tract. Although short in duration during primary infection, this antibody can persist for a longer time following re-infection (198). Both free and cell-bound IgA is detected in nasopharyngeal secretions and reaches peak titers between day eight and thirteen post-infection (188).

In contrast to IgA, serum IgG is inefficient in protection of the upper respiratory tract. Instead, their protective role is mostly confined to the lower respiratory compartment (228, 264). During primary infection, the IgG response is slow and reaches peak titers 20-30 days after the onset of symptoms. As expected, the secondary response is faster and significantly higher titers are reached seven days post infection (312).

The role of IgE in RSV disease is not completely understood. An association of IgE with persistent childhood wheezing after RSV infections early in life has been suspected in numerous studies (314). Symptoms like rhinorrhea, wheezing and a dry cough usually seen with RSV disease could all be induced by mast cell activation and histamine release mediated by IgE. In addition, increased levels of RSV-specific free IgE in infants that have RSV-related wheezing was reported (314). As a result, IgE is frequently implicated in the immunopathology of RSV disease (311, 313).

The unfortunate augmentation of disease after re-infection in children vaccinated with FI-RSV in the mid 1960s led researchers to believe in an antibody-mediated intensification of RSV disease for many years. This idea was abandoned following the establishment of a protective role for RSV-specific antibodies in numerous animal studies including cotton rats, mice and monkeys (229, 282). Studies in humans also showed a decrease in the frequency of infections as well as a

reduction in the clinical severity of RSV disease in patients that received RSV-specific immunoglobulins and humanized monoclonal antibodies against RSV (110).

As previously mentioned, RSV disease is more severe in infants younger than six months of age (51, 52). However, all full-term infants have transplacentally transferred RSV-specific antibodies with titers that are similar to maternal titers but decrease over time (21, 154). Furthermore, reports of increased severity of RSV disease in infants with low RSV antibody titers confirmed the protective role of maternal antibodies (101).

It is not clear why infants between two and six months of age show signs of more severe clinical disease after RSV infection. One explanation could be that titers of maternally transferred antibodies fall below protective concentrations two months post-delivery (247). For example, it was reported that the secreted form of the G protein, sG, accounts for 80% of the total amount of G protein in the first 24 hours post-infection, compared to only twenty percent in the progeny virus (127). Thus, it is possible that decreased levels of maternally transferred antibodies, after the first few months of life, are more easily inactivated by this secretory form of the G protein. Another explanation could be that passively transferred maternal antibodies interfere with the infant's own immune response (199). It was shown that children older than six months of age generally have protective IgM, IgA and IgG levels that are significantly higher than those in their younger counterparts, demonstrating the importance of age in the establishment of an appropriate antibody response against RSV (275).

1.7. Dendritic cell involvement

Numerous studies implicated DCs as important, if not crucial, in the induction of the immune response against RSV. What is unique about these specialized cellular members of the innate immune response is their ability to effectively initiate an antigen-specific response in naive T cells (132).

Dendritic cells are antigen presenting cells (APC) that originate in bone marrow and circulate in blood as CD34 precursor cells. This precursor population can differentiate into macrophages, granulocytes or DCs depending on the presence of external growth factors (143, 144). The presence of GM-CSF and TNF- α , for example, initiate development of DCs from human cord blood-derived CD34 precursor cells *in vitro* (44).

Two different subsets of DCs that differ in phenotype, localization and function have been identified in mice (11, 144, 253, 254). Both plasmacytoid and myeloid DC populations express β_2 integrin CD11c, costimulatory molecules CD40 and CD86, as well as class II major histocompatibility complex (MHC) (134, 152). Several markers are used to distinguish between these two populations. The most reliable one is CD45R, also known as B220, which is present on plasmacytoid and absent on myeloid DCs. On the other hand, myeloid DCs are characterized by the expression of β_2 integrin CD11b (15, 71). As mentioned earlier, these two subsets also show different localizations and functions. Plasmacytoid dendritic cells are predominantly localized to the T cell-rich areas of secondary lymphoid organs, compared to the peripheral tissue localization of myeloid DCs. Furthermore, plasmacytoid DCs are less phagocytic and produce higher levels of IL-12 than myeloid DCs (170, 237, 276). In contrast, myeloid DCs prime allogeneic CD4 and CD8 T cells more efficiently than plasmacytoid DCs *in vitro* (162, 284).

In agreement with their role as sentinel cells, DCs are located at the sites of the body where maximal microbial encounters take place. Those sites include the skin, lung and intestines (166). Although derived from a common precursor, DCs show phenotypical heterogeneity depending on the site where they reside. Interestingly, significant phenotypic heterogeneity was also found among DCs within different compartments of the respiratory tract itself (166). The exact roles of all these phenotypically different DCs have not yet been completely elucidated, but most probably these differences are related to slight differences in their function.

Dendritic cells circulate in blood as precursor DCs before entering into peripheral tissues where they become resident immature DCs that constantly monitor their environment. Under inflammatory conditions, inflammatory chemokines such as macrophage inflammatory protein (MIP)-1 α and β monocytes chemotactic protein (MCP) are produced by epithelial cells, and act as potent migratory attractants for immature DCs through a chemokine receptor CCR-6-dependent mechanism (226). Following the migratory signal, immature DCs accumulate rapidly at the site of inflammation where they take up and process antigens. Several specialized mechanisms facilitate this extremely efficient function of immature DCs. Their capacity to take up soluble antigens through macropinocytosis and their ability to phagocytose microbial particles and mediate endocytosis via cell surface receptors like Ig Fc, mannose and DEC-205 receptors, are some of the mechanisms involved in antigen uptake (184, 248, 277, 285). Furthermore, immature DCs have a unique MHC class II compartment that allows them to rapidly process and present antigens via MHC II molecules (45, 222).

Following antigen uptake and processing, DCs migrate via afferent lymphatics toward the draining lymph nodes where they interact with naive T cells and initiate antigen-specific immune responses (61, 93, 225). This migration is facilitated by the upregulation of chemokine receptor

CCR7 whose ligand MIP-3 β is constitutively expressed in T cell areas of the draining lymph nodes (107). After antigen uptake, DC maturation takes place. The most effective inducers of DC maturation are LPS, dsRNA, CpG oligonucleotides, CD40L on T cells, and inflammatory cytokine such as TNF α (46, 273). During the process of maturation, immature DCs undergo significant morphological and functional changes including a decreased capacity to take up and process antigens and increase in the expression of the Ag-presenting molecule MHC class II and accessory molecules such as CD40, CD80 (B7-1), and CD86 (B7-2) (167, 236). Furthermore, loss of sensitivity to inflammatory cytokines and increased responsiveness to lymphoid cytokines is accomplished by changes in the types of secretory chemokines and chemokine receptors, such as CCR6 and CCR7, that immature and mature DCs express (166).

Numerous studies revealed the pivotal role DCs play in the development of tolerance, memory and Th1/Th2 polarization (37, 72, 220). One of the simplest models that explains DC-T cell interaction describes the factors involved in the appropriate initiation of the adaptive immune response. According to this model, the type of response mounted depends on the type and quantity of antigen presented via MHC molecules, the existence of adequate amounts of costimulatory molecules and the presence of an appropriate cytokine microenvironment. For example, inappropriate expression of costimulatory molecules leads to T cells anergy and apoptosis (173). Furthermore, secretion of IL-12 by DCs was found to play an important role in finalizing T cell differentiation into Th1 or Th2 effector cells. While IL-12 production by DCs leads to a Th1-bias, the absence of IL-12 production is linked to a Th2-type response (173).

With respect to RSV, a constant increase in the number of mature DCs was found in a mice infected with RSV revealing the potential of RSV to induce DC maturation during the establishment of infection (24). Human studies also showed an increased production of Th2-type

cytokines, IL-10 and IL-4, and a decrease in the Th1-type cytokine IFN- γ by cord blood-derived DCs in RSV-infected infants (20). In their study, Boogaard *et al.* reported differential activation of myeloid and plasmacytoid bone marrow-derived DCs upon RSV infection *in vitro* (31). While myeloid DCs infected with RSV showed up-regulation of costimulatory maturation markers and enhanced T cell proliferation, plasmacytoid DCs failed to induce these kinds of changes, but instead produced significant amounts of IFN- α , an important cytokine during an antiviral response (31). In contrast, a different study also showed up-regulation of maturation markers, but the ability of RSV infected-monocyte-derived human DCs to induce T cell proliferation was decreased and the cytokine production was suppressed (70).

The role of DCs in determining the type of effector T cell proliferation was supported by a mouse study in which the majority of lung DCs were of the myeloid CD8 α^- type in contrast to the plasmacytoid CD8 α^+ phenotype (173). *In vitro* studies showed that production of high levels of the Th2 cytokines IL-4, IL-5 and IL-10 was mediated by CD8 α^- , while a predominantly Th1 cytokine profile with IFN- γ and IL-2 production was seen in T cells activated by CD8 α^+ dendritic cells (121, 236).

As previously mentioned, RSV infections are frequently more severe in infants, and the maturational state of DCs in infants was implicated as one of the possible causes for age-dependent augmentation of RSV infections. Animal studies showed a post-natal delay in the development of the class II MHC (Ia) DC population in the respiratory tract and a low density within respiratory epithelia, compared with other tissues. These differences ceased to exist in older animals (202). Collectively, these results classify DCs as pivotal cells during an innate immune response, and identify their role in orchestrating the development of an adaptive immune response against a given microbial insult.

Given that the maturation state of DCs could be altered depending on the local microenvironment, mainly by the presence of proinflammatory and immunomodulatory cytokines produced by RSV-infected lung epithelial cells, the role of epithelial cells in immune regulatory mechanisms was a predictable field of research in the last few years. For instance, even though the precise regulatory mechanisms that keep DCs in peripheral sites in the immature state are unknown, it was proposed that there are a number of tissue-derived factors capable of inhibiting DC maturation. These include IL-10, which is known to inhibit DC maturation and block Th1-priming via inhibition of IL-12 secretion (177). Prostaglandin (PG)E₂ also inhibits production of IL-12, nitric oxide (NO) and epithelial cadherin, all expressed by the epithelial cells (73, 281). The degree of cross-talk between epithelial cells and DCs has been closely observed in the gastro-intestinal tract and the skin (32, 206). A study done by Rimoldi *et al.* confirmed the regulatory role of intestinal epithelial cells for DCs. They demonstrated that intestinal DCs responded differently depending on the invasiveness of the bacteria and that complete induction of DC activation mediated by bacterial and epithelial cell factors was present only when invasive bacterial strains were used. This observation finding indicated epithelial cells and not DCs as central cells for recognition of “danger” signals (245). Skin studies also revealed an important role for epithelial cells in regulating DCs function. Ligation of epithelial-cell secreted E-cadherin to the surface receptors on DCs abrogated DC maturation, and hence influenced their function (243).

Apart from the influence of epithelial factors such as IL-10, (PG)E₂, and NO on the function of lung DCs, the mechanisms by which airway epithelial cells influence DC migration, maturation and activation are not completely understood. Research in this field is stalled due to the logistical difficulties linked to isolation of satisfactory numbers of airway DCs. Thus, the

need to develop satisfactory models for studying DC interactions with epithelial cells and other cellular factors is paramount.

1.8. Animal Models for Studying Respiratory Syncytial Virus

Animal models are crucial to understand the mechanism of disease enhancement during RSV infection and for the development of safe and effective vaccines. Although not ideal in all aspects, animal models are useful in predicting the effects of key genetic and environmental factors involved in pathogenesis, as well as identifying protective antigens. A number of animal models have been used to study RSV disease, and the effect of FI-RSV, which is the best studied model of RSV disease augmentation, is amazingly similar in all species studied, including mice, cotton rats, cattle, and primates (74, 227, 257, 307).

Almost seventeen years after unsuccessful attempts by Coates and Chanock (55) to establish a murine animal model for RSV, Prince *et al.* (233) successfully established resistance /susceptibility patterns for RSV infection in twenty inbred mouse strains. This work allowed insight into RSV-induced immunopathogenesis which had been not possible before. Of special value were the studies that depict different cytokine profiles induced by various immunization strategies. For example, it is widely accepted that enhanced disease in the FI-RSV mouse model is influenced by T cells. Studies in FI-RSV-immunized Balb/c mice showed a noticeable increase in the expression of IL-5, IL-10 and IL-13, which are common Th2-type cytokines. There was a corresponding decrease in the expression of IL-12, indicating a bias toward a Th2-type response as a possible cause of increased inflammation (308). Unfortunately, slightly different cytokine profiles were observed in different strains of mice, indicating a future need for large-scale

parallel studies (40). In any case, mouse models have several advantages compared to other animal models. The availability of inbred, congenic, knock-out and transgenic strains, the vast array of specific immunological reagents, the easy availability and the low cost of mice are only some of the advantages of this model (40).

Cotton rats are another very useful model for studying RSV infection. As early as the nineteen-seventies, when Dreizin *et al.* (82) investigated histological changes in the lungs of RSV-infected cotton rats, the usefulness of this animal model was obvious. Since cotton rats are 100-fold more susceptible to RSV when compared to mice, and also show increased immunological responsiveness (106, 230), it was not surprising that cotton rats developed FI-RSV vaccine-induced augmented RSV disease that closely mimicked that in humans (232). Many therapeutic studies were performed using cotton rats, including studies on the effect of ribavirin on viral replication (139) and prevention of pulmonary infection by serum neutralizing antibodies (110, 229, 231). Some of these studies provided the basis for the establishment of preventive RSV Ig treatment for children at risk in 1996 (40). Although useful, the use of the cotton rat animal models have limitations due to the lack of inbreeding and the scarcity of immunological reagents.

Bovine RSV is a bovine respiratory pathogen that causes disease in cattle similar to that seen in humans infected with RSV (217). Formalin-inactivated BRSV causes enhanced disease in BRSV-infected cattle in a way that closely resembles the symptoms seen in children vaccinated with FI-RSV (257). On the other hand, a different study demonstrated reduction in pulmonary pathology in BRSV-infected animals vaccinated with FI-BRSV prior to infection (316). The major benefit of the BRSV infection model is the possibility to study an infection in

its natural host. However, the high cost, the necessity of large animal facilities and the lack of inbred strains makes the work with this model challenging.

Non-human primate models of RSV infection have been established for chimpanzees (22), owl monkeys (234, 240), rhesus monkeys (22), African green monkeys (150), cebus monkeys (241), squirrel monkeys (22), bonnet monkeys (269), and baboons (130). Unfortunately, clinical and radiological signs of pulmonary RSV disease were demonstrated only in a few cases. For example, significant histopathological changes in the lungs of rhesus monkeys infected with RSV were documented, but only mild clinical disease was observed (22). A study with African green monkeys demonstrated similar histopathological changes in FI-RSV animals to those described in children who died after immunization, but the low number of animals used in this study leaves the results open to interpretation (150). Similarly, studies in chimpanzees, genetically the closest relatives of humans, described primary RSV infection (22), but, the conclusions from this study were based on findings derived from only four animals, and an insight into the nature of the infection was restricted to nasal tissue examination only. Furthermore, the enhancement of disease in FI-RSV-vaccinated chimpanzees was never scrutinized (57, 63-66, 140).

Collectively, the necessity for larger numbers of animals to be included in these kinds of studies in order to get significant results creates a major setback. Also, the lack of immunological reagents further complicates research in this field. Keeping in mind that the use of chimpanzees, closest to humans genetically, is severely limited due to the extremely high cost associated with purchasing and housing of these animals, the prospect for using this model in the future is very limited.

1.9 Pneumonia Virus of Mice

1.9.1. Virus Classification and Characteristics

As previously mentioned, Pneumonia Virus of Mice (PVM) is a murine counterpart of human RSV (HRSV) and a member of the genus *Pneumovirus*, of the family Paramyxoviridae (291). In 1939, Horsfall and Hahn isolated PVM from lung tissue of asymptomatic mice. Surprisingly, passage of this lung tissue supernatant into healthy mice resulted in disease characterized by fatal pneumonia (137, 138). Numerous studies also demonstrated the ability of PVM to infect other laboratory rodent species (291), and several wild rodent species and mammals including humans were found to be seropositive for PVM as well (84, 136, 191, 221, 235). In addition, Pringle and Eglin reported that close to 80% of the population in the United Kingdom tested seropositive for PVM, indicating wide-spread human infection with this or serologically closely related viruses (235).

Characterized by Krempl and colleagues, the genome of this virus without doubt shows similarities in gene order with other members of the *Pneumovirus* genus. The genome of PVM encodes 10 mRNAs that are translated into 12 major proteins, 11 of which are equivalent to HRSV proteins (160). In their study, Krempl and colleagues demonstrated that apart from the absence of overlapping ORFs in P mRNA, the PVM gene map, NS1-NS2-N-P-M-SH-F-G-M2-L, was a precise match with that of HRSV, thus indicating PVM as the phylogenetically closest known relative of HRSV (160).

Presently, two strains of PVM are used in research laboratories, PVM strain 15 which is available at American Type Culture Collection (ATCC) and strain J3666 which was maintained

by serial passage in mice. Although several research groups reported strain 15 as nonpathogenic in mice (28, 60, 76), recent studies demonstrated that the severity of the disease and clinical signs in mice infected by J3666 and the ATCC-acquired strain 15 were virtually impossible to differentiate (77, 159). A comparison of the genome sequences between J3666 and strain 15 showed a limited number of differences (291).

It is believed that both strains originated from the same virus isolate, but that the strain 15 virus maintained in BSC-1 primate cells acquired a deletion in the cytoplasmic tail of the G protein (239). Most probably this mutated virus was used in the studies that initially reported the inability of PVM strain 15 to cause disease in different strains of mice. In 2004, an analysis of the complete gene sequence of the ATCC-acquired strain 15 confirmed the absence of any G protein mutations, providing additional evidence that strain 15 is not an intrinsically non-pathogenic strain (159).

1.9.2. Rationale for use as Animal Model for Respiratory Syncytial Virus Infection

Although several groups have studied RSV pathogenesis in rodent models (27, 307, 309), RSV is not a murine pathogen and does not closely duplicate the clinical disease in humans. A comparative study of the characteristics of RSV infection in humans and mice and PVM infection in mice very elegantly illustrated that mice infected with HRSV showed only mild mononuclear cell infiltration and no eosinophil recruitment. Acute respiratory distress syndrome (ARDS) (60, 76, 78) was also absent. Furthermore, the inoculum required for the initial infection was up to 2 million plaque-forming units (PFU) and the peak lung viral titers were lower than the titer of the inoculum, suggesting an inability of the virus to successfully replicate in mouse lungs

(79). In contrast, PVM is a natural rodent Pneumovirus pathogen. Intranasal inoculation with as little as 30 PFU leads to massive virus replication in situ, with virus titers reaching as high as 10^8 pfu/g in lung tissue 5-7 days post inoculation, depending on the strain of mouse used (76). Depending on the size of the inoculum, virus replication is associated with a severe inflammatory bronchiolitis and pneumonia that in some cases progresses to ARDS and death (79). Several studies also demonstrated that the chemokine response to PVM in mice imitates those described for severe HRSV infections (29, 30, 123). Virus replication is accompanied by a substantial influx of granulocytes, comparable to what has been observed for severe RSV infection in humans (79, 111, 123). Severe infections with PVM lead to significant morbidity and mortality of infected animals, yet another feature not seen in mice infected with HRSV.

Although there is still uncertainty as to what degree PVM infection in mice is analogous to HRSV infection in infants, an investigation of the process of PVM infection in its natural host has the potential for detection of relevant markers for HRSV infection in humans.

2.0 Hypothesis

I tested a hypothesis that infection with Pneumovirus leads to impaired phenotypic and functional profiles of BM-DCs.

This hypothesis was tested using following objectives:

1. Establishment of procedures for propagation and quantitation of PVM strain 15 in BHK-21 cells
2. Evaluation of the effects of PVM infection in Balb/c and C57/Bl mice in vivo
3. Evaluation of the effects of live and killed PVM on the functional properties of BM-DCs in Balb/c and C57/Bl mice ex vivo.

3.0 Materials and Methods

3.1 Media, Cell lines, and Virus

Baby hamster kidney (BHK-21) cells (ATCC CCL-10) were obtained from the American Type Culture Collection (Rockville, MD, USA). BHK-21 cells were maintained in minimum essential medium (MEM) (Invitrogen Canada Inc., GIBCO, Burlington, ON, Canada) with 2 mM L-glutamine and 1.5 g/L sodium bicarbonate, 0.1 mM non-essential amino acids, 1.0 mM sodium pyruvate, and 10% fetal bovine serum (FBS) (SeraCare Life Science, Oceanside, CA, USA). Cells were propagated in T-150 (150 cm²) tissue culture flasks (Falcon™ BD Bioscience, San Jose, CA, USA) and incubated at 37 °C, 5% CO₂. After 2-3 days of incubation, 100% confluent BHK-21 monolayers were collected and a single cell suspension was transferred to new T-150 tissue culture flasks. Harvesting of the 100% confluent BHK-21 cells monolayer was performed by replacing the culture medium with 10 ml Versene (0.07 mM disodium ethylenediaminetetraacetic acid (EDTA), 1.10 mM dextrose, 2.68 mM potassium chloride, 137 mM sodium chloride and 9.58 mM sodium phosphate monobasic; Sigma-Aldrich Canada Ltd., Oakville, ON, Canada) and 0.5% of trypsin. Rounding up of the cells was confirmed by examination of cells under the microscope. Once the cells were rounded up, the versene-trypsin solution was taken of the cells and after a single forceful tap at the bottom of the flask, the cells were collected by gently pipetting culture media over the cell monolayer. BHK-21 cells are fast growing cells and were subcultured three times per week at 1:4 ratios.

Pneumonia Virus of Mice (PVM) Strain 15 was obtained from the American Type Culture Collection (Rockville, MD, USA), and maintained in Dulbecco's Modified Eagle

Medium High Glucose 1X (DMEM-Glutamax) (Invitrogen Canada Inc., GIBCO, Burlington, ON, Canada) supplemented with 10 mM Hepes (Invitrogen Canada Inc., GIBCO, Burlington, ON, Canada), 0.1 mM non-essential amino acids (Invitrogen Canada Inc., GIBCO, Burlington, ON, Canada), 50 µg/ml Gentamicin Reagent (Invitrogen Canada Inc., GIBCO, Burlington, ON, Canada) and 2% heat-inactivated FBS (SeraCare Life Science, Oceanside, CA, USA), referred later as complete DMEM.

3.2 Stock Virus Preparation

Pneumonia Virus of Mice was propagated in BHK-21 cells. Briefly, 100% confluent BHK-21 cells cultured in T-150 flasks were subcultured 1:3 one day before infection with PVM. The next day the cells were between 65% and 75% confluent. Cell culture medium was replaced with DMEM-Glutamax supplemented as above. The cells were infected with PVM at a multiplicity of infection (MOI) of 1. Flask filter caps were sealed with parafilm (Pechiney Plastic Packaging, Menasha, WI, USA) to prevent CO₂ loss and contamination, and incubated for three hours at 37 °C with constant rocking on a rocker platform (Labnet International, INC, Woodbridge, NY, USA). Subsequently, an additional four milliliter of DMEM-Glutamax medium was added and infected cells were incubated at 37 °C and 5% CO₂ until rounding up of the cells was visible under the microscope. Once a cytopathic effect was present, usually three days post infection, infected cells were collected by scraping them from the surface of the flask with a 25 cm cell scraper (Falcon™ BD Bioscience, San Jose, CA, USA). Collected cells and culture medium were aliquoted, stored at -80 °C, and used as a virus stock.

3.3 Virus Plaque Assay

In order to quantitate PVM, a standard plaque assay was used with slight modifications. BHK-21 cells were collected from a 100% confluent monolayer using versene-trypsin treatment as described in section 3.1. The single cell suspension was counted using a Bright-Line haemocytometer (Hausser Scientific, Horsham, PA, USA), and the cell concentration was adjusted to 8×10^5 cells per milliliter by addition of the appropriate volume of MEM with 2 mM L-glutamine and Earle's salts adjusted to contain 1.5 g/L sodium bicarbonate, 0.1 mM non-essential amino acids, 1.0 mM sodium pyruvate, and 10% FBS. Twenty-five microliters cells and 75 μ l MEM, were added per well of flat-bottom 96-well microtiter plates (Corning Incorporated, Corning, NY, USA) using a multichannel pipettor and sterile pipette tips. The cells were incubated for 24 hours at 37 °C and 5% CO₂, and infected with PVM by replacing the culture medium with 100 μ l ten-fold serial dilutions of virus in DMEM-Glutamax supplemented as above.

All dilutions were made in triplicate wells. Following a three hours incubation at 37 °C and 5% CO₂ the culture medium was replaced with 200 μ l per well of DMEM-Glutamax supplemented as above. Flat-bottom 96-well microtiter plates (Corning Incorporated, Corning, NY, USA) were again incubated at 37 °C and 5% CO₂ for 48 hours. At this point the cells were ready for the immunostaining assay.

3.3.1. Immunohistochemistry

The culture medium was gently removed from the flat-bottom 96-well microtiter plate (Corning Incorporated, Corning, NY, USA) using a multichannel pipettor and replaced with 100 µl per well of cold acetone-methanol solution in a ratio of 3:1. After addition of acetone-methanol solution, the plates were incubated for 15 minutes at -20 °C. The acetone-methanol solution was gently removed and the cells were rinsed once with 100 µl ice-cold 1 X Phosphate-Buffered Saline (PBS) pH 7.3, 0.05 molarity (Invitrogen Canada Inc., GIBCO, Burlington, ON, Canada) per well. Subsequently, the cells were washed three times for five minutes with ice-cold PBS with constant rocking on the Rocker 35 rocking platform (Labnet International, INC, Woodbridge, NY, USA). After washing, 200 µl of 5% goat serum (Invitrogen Canada Inc., GIBCO, Burlington, ON, Canada) in PBS per well was added to the cells. The cells were incubated at room temperature (RT) for one hour on the rocking platform, and washed again twice for five minutes with PBS at RT and constant rocking on the Rocker 35 rocking platform (Labnet International, INC, Woodbridge, NY, USA). Subsequently, 100 µl N-specific rabbit polyclonal antibody diluted 1:800 in PBS with 1% goat serum (Invitrogen Canada Inc., GIBCO, Burlington, ON, Canada) was added to the cells. The cells were incubated at RT for one hour on the rocking platform, rinsed once with PBS and washed with rocking once for ten minutes and twice for five minutes. Fluorescein isothiocyanate (FITC)-conjugated goat anti-rabbit IgG (Zymed Laboratories Inc., San Francisco, CA, USA) diluted 1:800 in PBS with 1% goat serum (Invitrogen Canada Inc., GIBCO, Burlington, ON, Canada) was added at 100 µl per well. The cells were incubated for one hour with rocking in the dark. After the incubation the cells were washed three times for five minutes in the dark, and finally 100 µl PBS per well was added and

the plate was covered with aluminum foil to preserve the FITC signal. The plates were examined with an Axiovert microscope (Carl Zeiss Canada Ltd., Toronto, ON, Canada). The virus titer was determined as the number of plaques x dilution x 10 to convert to plaque forming units per milliliter.

3.4 Pneumonia Virus of Mice inactivation by ultraviolet irradiation

Ultraviolet (UV) irradiation of PVM was carried out in a specially designed cabinet with a germicidal fluorescent bulb (G8T5, General Electric, NY, USA) positioned at the top of the cabinet. An UVX digital radiometer (Ultra Violet Products, Inc., San Gabriel, CA, USA) was used to determine the exact dose of ultraviolet irradiation. An UV-dose of 3.7 mJ/cm²/sec was measured. Since different UV doses were measured depending on the distance of the UVX digital radiometer from the germicidal fluorescent bulb, all PVM samples were aliquoted in 35 mm tissue culture petri dishes (Corning Incorporated, Corning, NY, USA) in one milliliter volumes and kept at the same distance from the germicidal fluorescent bulb. PVM samples were exposed to UV-doses of 0, 222, 444, 666, 888, 1110, 1332, 1554, 1776, 1998 and 2220 mJ/cm². The temperature change inside the chamber was monitored over the ten-minute period, and a 6 °C change from 22 °C to 28 °C was observed.

The dose required for PVM inactivation was determined by measuring the ability of UV-irradiated samples to produce plaques on a BHK-21 cell monolayer. The plaque assay was performed as described in 3.3.

3.5 Mouse strains

In this study two series of experiments were performed, one using Balb/c (I-A^d) mice and the other one using C57/Bl (I-A^b) mice. The mice were 8 weeks of age and purchased from Charles River Laboratories Inc. (Wilmington, MA, USA).

Balb/c Albino mice originated from stock acquired by H.Bagg in 1913, while C57BL/6 originated from stock acquired from Jax F32 in 1951. Balb/c, the prototypic Th2 strain, is highly susceptible to *Leishmania major*, in contrast to resistant C57BL/6, CBA/J and C3H/HeJ, which usually are Th1 responding strains (168, 260). Balb/c is resistant to mouse adenovirus type 1 in contrast to C57BL/6 (113).

3.6 Challenge of mice with Pneumonia Virus of Mice

Prior to infection, PVM stock virus was thawed and transferred to 1.5 ml eppendorf tubes under sterile conditions. To release cell-associated virus, virus was sonicated five times with a high-intensity ultrasonic processor (Betatek Inc, Toronto, ON, Canada) for 30 seconds. Ice was present in the sonication tube at all times. The necessary dilutions were made using complete DMEM without FBS as a diluent. The tubes were kept on ice at all times. On day 0, three to six 8 week-old mice were put under light anesthesia using isoflurane (Baxter Corporation, Mississauga, ON, Canada), and inoculated intranasally with 30, 100, 300 or 3000 pfu in a total volume of 30 µl or 50 µl. The precise numbers of mice used in each experiment are provided in the figure legends. Control mice were inoculated intranasally with complete DMEM without FBS. A standard method was used to evaluate the infectious process from day 0 to day seven

post inoculation based on weight measurement, clinical signs and changes in overall appearance. On day seven the mice were euthanized and the lungs were evaluated for macroscopic and microscopic lesions as well as for virus replication.

3.7 Collection of Lungs for Virus Quantitation and Histopathology

Lungs from PVM-challenged and control mice were collected on day six or seven post-infection for virus quantitation and histopathology. Briefly, mice were euthanized by overdose with Halothane anesthesia (Halocarbon Products Corporation, River Edge, NJ, USA). The thorax was surgically opened and the right lung was collected in collection tubes. The collection tubes consisted of 2 ml screw-cap tubes (VWR International, Mississauga, ON, Canada) that were filled half-full with 2.4 mm zirconia beads (BioSpec Products Inc, Bartlesville, Oklahoma) and autoclaved. At the day of collection, the tubes were filled with 1.5 ml of lung medium under sterile conditions. Lung medium consisted of complete DMEM without FBS, supplemented with Aprotinin 1:1000 (v/v) (10 mg/ml) (Sigma-Aldrich Canada Ltd., Oakville, ON, Canada), Leupeptin 1:1000 (v/v) (10 mg/ml) (Sigma-Aldrich Canada Ltd., Oakville, ON, Canada), phenylmethylsulfonyl fluoride (PMSF) 1:100 (v/v) (100 mM) (Sigma-Aldrich Canada Ltd., Oakville, ON, Canada), and EDTA 1:5000 (v/v) (0.5 M). The collection tubes with lung medium were kept on ice before and after lung tissue collection. For lung homogenization a mini-beadbeater (BioSpec Products Inc, Bartlesville, OK, USA) was used for 10 seconds at 2500g, followed by centrifugation for one minute at 10000g. The resulting lung homogenate supernatants were used for virus titration as described in sections 3.3 and 3.4.

At the time of lung tissue collection, the left lung was collected from each animal for histopathology. Briefly, the trachea was clamped distally from the bifurcation of the trachea, and the left lung was perfused with buffered 10% neutral formalin (VWR International, Mississauga, ON, Canada). Collected lungs were placed in histological cassettes and kept in 10% buffered neutral formalin (VWR International, Mississauga, ON, Canada) until they were mounted on slides and stained with haematoxylin and eosin.

3.8 Generation of Bone Marrow-derived Murine Dendritic Cells

A procedure for generation of bone marrow-derived murine DCs was developed according to a procedure by Lutz *et al.* (174), with minor modifications. Female BALB/c or C57/Bl mice were sacrificed by Halothane overdose (Halocarbon Products Corporation, River Edge, NJ, USA) and skinned down. The femurs and tibiae of the mice were removed, washed in PBS and cleaned of the surrounding muscles by rubbing with Kleenex tissues. Subsequently, intact bones were left in 70% ethanol for two minutes for disinfection and washed with PBS. The ends of the bones were cut with scissors and the marrow was flushed with PBS using a syringe with a 0.45 mm diameter needle. Clusters within the marrow suspension were dispersed by vigorous pipetting. The cell suspension was centrifuged for eight minutes at 311g using a Sorvall Legend™ T/RT centrifuge (Kendro Laboratory Products, Newtown, CT, USA), and the resulting pellet was treated with 0.84% Tris-Ammonium Chloride (0.17 M Tris, 0.16 M NH₄Cl, pH 7.2) for five minutes. The reaction was stopped by adding PBS. The cells were washed twice with PBS and then resuspended in RPMI 1640 medium (Invitrogen Canada Inc., GIBCO, Burlington, ON, Canada), supplemented with 20 ng/ml murine GM-CSF (PeproTech Inc., Rocky Hill, NJ,

USA). The resuspended bone marrow cells were cultured in six-well tissue culture plates (Corning Incorporated, Corning, NY, USA) at an initial concentration of $\sim 1 \times 10^6$ /ml in a volume of 4 ml per well.

The cells were incubated at 37 °C and 5% CO₂ for three days. Subsequently, the medium was gently removed and 4 ml fresh complete RPMI 1640 medium supplemented with 20 ng/ml murine GM-CSF (PeproTech Inc., Rocky Hill, NJ, USA) was added per well. On day five 50% of the medium was replaced with fresh complete RPMI 1640 medium supplemented with medium containing 20 ng/ml murine GM-CSF.

3.9 Flow cytometric analysis

To evaluate how PVM proteins influence the expression of costimulatory molecules, DCs were infected with PVM, or UV-inactivated PVM at a MOI of 5, treated with an equivalent amount of BHK-21 cell lysate, or 1 µg per milliliter lipopolysaccharide (LPS), or left untreated. Twenty-four hours post treatment, the DCs were centrifuged at 311g using a Sorvall Legend™ T/RT centrifuge (Kendro Laboratory Products, Newtown, CT, USA) for 10 minutes and washed once in PBS. The collected single cell suspensions were counted with a bright-line hemacytometer (Hausser Scientific, Horsham, PA), and the cell concentrations were adjusted to 1×10^6 cells per milliliter by addition of appropriate volumes of PBS.

The DCs were plated at 5×10^5 cells per well in round-bottom 96-well tissue culture plates (Corning Incorporated, Corning, NY), and incubated on ice in the dark for 45 minutes with FITC-conjugated monoclonal antibody (mAb) specific for I-Ad (AMS-32-1), I-Ab (AF6-120.1), CD40 (3/23, rat IgG2a), CD86 (GL1, rat IgG2a), CD19 (1D3) or phycoerythrin (PE)-conjugated

anti-mouse CD11c (integrin α x chain) (HL3). Antibodies were purchased from BD Biosciences Pharmingen (BD Bioscience, San Jose, CA, USA). After incubation, the cells were washed three times with 200 μ l/well cold PBS and the final pellet was resuspended in 200 μ l 2% paraformaldehyde. A FACSCalibur flow cytometer (BD Bioscience, San Jose, CA, USA) was used for data acquisition and the data were analyzed with Cell Quest software (BD Bioscience, San Jose, CA, USA).

3.10 Endocytosis Assay

To evaluate how PVM proteins influence the capacity of DCs to take up soluble antigens from the culture medium, DCs infected with PVM, an UV inactivated PVM, or treated with BHK-21 cells lysate or 1 μ g/ml LPS, and untreated DCs were incubated with FITC-dextran (Sigma-Aldrich Canada Ltd., Oakville, ON, Canada) and endocytosis was monitored. Twenty-four hours post infection the DCs were collected, centrifuged at 311g using a Sorvall LegendTM T/RT centrifuge (Kendro Laboratory Products, Newtown, CT, USA) for 10 minutes and washed twice in complete RPMI 1640 (Invitrogen Canada Inc., GIBCO, Burlington, ON, Canada). The collected single cell suspensions were counted using a Bright-Line hemacytometer (Hausser Scientific, Horsham, PA, USA), and the cell concentration was adjusted to 2×10^6 cells per milliliter by addition of an appropriate volume of complete RPMI. Four hundred microliters of these cell suspensions were transferred into two 1.5 ml eppendorf tubes, at 200 μ l per tube, and 1 mg/ml FITC-dextran in PBS was added to each tube. Control tubes were wrapped with foil and left on ice for 30 minutes. A hole was made in the top of the test tubes in order to release pressure and the tubes were incubated at 37 $^{\circ}$ C for 30 minutes. After the incubation the cells

were centrifuged three times at 350g for five minutes in a table top centrifuge (EppendorfAG, Hamburg, Germany) at 4 °C. Each time the pellet was resuspended in 500 µl cold PBS. The final cell pellet was resuspended in 200 µl 2% paraformaldehyde in ddH₂O. Uptake of FITC-dextran by DCs was assessed by flow cytometry. A FACSCalibur (BD Bioscience, San Jose, CA, USA) was used for data acquisition and the data were analyzed with Cell Quest software (BD Bioscience, San Jose, CA, USA).

3.11 Isolation of Lymphocytes

Spleens from Balb/c and C57/Bl mice were collected in polypropylene 15 ml centrifuge tubes (Falcon™ BD Bioscience, San Jose, CA, USA) filled with five milliliter MEM supplemented with 10 mM Hepes and 50 µg/ml Gentamicin Reagent (Invitrogen Canada Inc., GIBCO, Burlington, ON, Canada). The spleens and media were poured into 100 µm cell strainers (Falcon™ BD Bioscience, San Jose, CA, USA) placed in petri dishes (VWR International, Mississauga, ON, Canada). Excess fat was removed and the spleens were cut into small pieces with scissors. Glass syringe plungers were used to gently tease spleens through the cell strainers. The cell strainers were washed with five milliliter MEM supplemented with 10 mM Hepes, and 50 µg/ml Gentamicin Reagent (Invitrogen Canada Inc., GIBCO, Burlington, ON, Canada). The cells were gently resuspended and returned to 15 ml centrifuge tubes on ice. After five minutes a Pasteur pipette was used for removal of clumps that may have settled. Then the cells were centrifuged at 311g using a Sorvall Legend™ T/RT centrifuge (Kendro Laboratory Products, Newtown, CT, USA) for 10 minutes at 4 °C. The resulting cell pellets were resuspended in one milliliter of 0.84% Tris-Ammonium Chloride (0.17 M Tris, 0.16 M NH₄Cl,

pH 7.2) and incubated for 30 seconds. After addition of 10 ml MEM supplemented with 10 mM Hepes, and 50 µg/ml Gentamicin Reagent (Invitrogen Canada Inc., GIBCO, Burlington, ON, Canada) the cells were washed twice and the final cell pellets were resuspended in two milliliters RPMI 1640 and kept on ice for T cell enrichment.

3.12 Nylon Wool Column for Spleen-derived T Cells

The splenocytes from C57BL/6 (H-2^b) or Balb/c (H-2^d) mice were isolated as described in 3.11 and resuspended in two millilitres complete RPMI 1640 medium with 10 % FBS. T cell-enriched populations were obtained using Nylon wool fiber Columns (Polysciences, Inc., Warrington, PA, USA). Briefly, the stopcock was removed from the sterile package and placed on the Luer tip of the syringe. The plunger was removed from the syringe, and the column was washed gently several times with complete RPMI 1640 medium at room temperature. The column was kept wet and free of air bubbles by gently tapping the sides of the column during the washes.

After making sure that the column was uniformly wet, the stopcock was closed and the prepared column was incubated for one hour at 37 °C. After the incubation the stopcock was opened and the medium was drained to the top of the nylon wool column. One to two times 10⁸ viable cells in a volume of 2 ml of medium were added per column, and medium was drained until the cells had entered the packed wool. After closing the stopcock, the column was washed with an additional 2 ml of medium until the wash medium entered the packed wool. The stopcock was closed again and an additional 5 ml of medium was added to the column.

Subsequently, the column was incubated for one hour at 37 °C. Nonadherent T-cells were collected after incubation by gently washing the column twice.

3.13 Mixed Lymphocyte Reaction (MLR)

Spleen-derived T-cells collected as described in sections 3.11 and 3.12 were counted using a bright-line hemacytometer (Hausser Scientific, Horsham, PA, USA) and the cell concentration was adjusted to 2×10^6 cells per milliliter by addition of the appropriate volume of complete RPMI with 10% FBS. These cells were used as the responder cells in the MLR. PVM-treated or control DCs were used as stimulator cells. The DCs were collected and centrifuged at 311g using a Sorvall Legend™ T/RT centrifuge (Kendro Laboratory Products, Newtown, USA) for 10 minutes and the resulting pellet was resuspended to a concentration of 2×10^5 cells per milliliter. These cells were then γ -irradiated (GamaCell 220, Cobalt 60 Irradiation Unit, Atomic Energy of Canada Ltd, Commercial Products Division, Ottawa, ON, Canada) at 5000 rads (6 minutes and 40 seconds at 749 RAD per minute). One hundred microliters of irradiated DCs were plated at four-fold dilutions in triplicate in round-bottom 96-well tissue culture plates (Corning Incorporated, Corning, NY). One hundred microliters T cells at a concentration of 2×10^6 cells per milliliter were then added to all wells. The resulting ratios of stimulator vs. responder cells were 1:10, 1:40, 1:160 and 1: 640. The cells were cultured in complete RPMI 1640, 10% FBS at 37 °C and 5% CO₂ for three or five days. Eighteen hours before collection the cell cultures were pulsed with 0.4 μ Ci/well of methyl ³[H] thymidine (Amersham Pharmacia Biotech, AB, Sweden). On days three and five the cells were collected using a Filter Mate harvester (Packard Bioscience Company, Meriden, Connecticut) and the

radioactivity was determined with a Microplate scintillation & luminescence counter (Packard Bioscience Company, Meriden, CT, USA). The results are expressed as mean counts per minute (CPM) of triplicate wells. All the results were corrected for background readings derived from wells with T cells only.

3.14 Enzyme-linked immunosorbent assay

For the quantitative determination of murine interleukin 12 p70 (IL-12 p70) concentrations in cell culture supernatants a Quantikine Mouse IL-12 p70 Immunoassay (R & D Systems, Inc, Minneapolis, MN, USA) was employed. Samples from PVM-treated and control cultures were collected, and small particulates were removed by centrifugation. The resulting cell culture supernatants were aliquoted and stored at -20 °C. The IL-12 p70 assay was used as per manufacturers recommendations. Briefly, all reagents, standards and samples were brought up to RT before they were prepared as per manufacturer's recommendations. Fifty microliters of assay diluent RD1-14 was then added to each well of the provided 96-well microplate that was pre-coated with monoclonal antibody specific for mouse IL-12 p70. Then 50 µl standard, control or sample was added in duplicate. After one minute of mixing the samples by gentle tapping on the edge of the plate, the plate was covered with adhesive strip and incubated for two hours at RT. During this time any IL-12 p70 present was bound to the immobilized antibody. Unbound substances were removed by washing five times with wash buffer, and then 100 µl of an enzyme-linked polyclonal antibody specific for mouse IL-12 p70 was added to all wells. The plates were incubated at RT for two hours, and washed again. After addition of 100 µl/well of substrate solution, the plates were incubated in the dark for 30 minutes at RT. The reaction was

stopped by addition of 100 μ l per well of stop solution. The enzyme reaction produces blue color that turns yellow when the reaction is stopped. The optical density was determined within 30 minutes, using a microplate spectrophotometer SpectraMAX 340PC (Molecular Devices Corporation, Sunnyvale, CA, USA). To correct for optical imperfections in the plate readings at 570 nm were subtracted from the readings at 450 nm.

3.15 Immunoblotting

Western blotting was carried out according to the method of Burnette (39), with some modifications. Briefly, proteins from PVM or UV-PVM infected BM-DCs were separated by sodium dodecyl sulfate polyacrylamide gel electrophoresis (SDS-PAGE), according to the method of Laemmli (164). Samples were resolved using 10% acrylamide and transferred electrophoretically to a nitrocellulose membrane (BioRad Laboratories, Hercules, CA, USA) in buffer containing 25 mM Tris-HCl, 192 mM glycine, and 20% (v/v) methanol, at 100 V for 1 hour. Following transfer, the membrane was blocked with Tris-buffered saline (TBS) containing 3% (w/v) skim milk powder, and then probed with rabbit α -N PVM antibodies, diluted 1:200 in TBS containing 1% skim milk. Following washing with TBS containing 0.05% (v/v) Tween-20 (TBST), the membrane was incubated with alkaline phosphatase (AP)-conjugated goat anti-rabbit IgG (Kirkegaard & Perry Laboratories, Gaithersburg, MD, USA), diluted 1:2,000 in TBS containing 1% skim milk. Bound antibody was visualized using SigmaFastTM 5-bromo-4-chloro-3-indolyl-phosphate (BCIP)/ nitroblue tetrazolium chloride (NBT) (Sigma-Aldrich Inc., St. Louis, MO, USA).

4.0 Results

4.1. Virus Propagation and Quantitation

4.1.1 Virus Propagation

Pneumonia Virus of Mice Strain 15 obtained from the American Type Culture Collection was propagated in a baby hamster kidney cell (BHK-21) line (ATCC CCL-10) as described in the material and methods section.

Although several research groups reported PVM strain 15 as nonpathogenic in mice (28, 60, 76), recent studies demonstrated that the disease severity and clinical observations in mice infected by J3666 and the ATCC-acquired PVM strain 15 were virtually impossible to differentiate (77, 159). Most probably, studies that reported PVM strain 15 as non-pathogenic in mice were performed with virus propagated in BSC-1 (monkey kidney) cells. This virus was shown to have a deletion in the cytoplasmic tail of the attachment glycoprotein (G) and this mutation was associated with the inability of PVM strain 15 to cause disease in different strains of mice (28, 60, 76). Since analysis of a complete gene sequence of PVM strain 15 from ATCC confirmed the absence of any G protein mutation, we decided to work with this virus strain (159).

Due to conflicting reports found in the literature regarding the optimal temperature for growth of PVM strain 15 in BHK-21 cells (124, 291), we propagated the virus at two different temperatures, 33 °C and 37 °C. Balb/c mice (six per group) were intranasally inoculated with high (5000 PFU) and low (30 PFU) inoculum doses of PVM grown at 33 °C or 37 °C. An

inoculum volume of 50 μ l per mouse was used. Changes in body weight were monitored for seven days post inoculation. Representative results from two animal trials are depicted in Figure 4.1.1. We were unable to statistically analyze differences between test groups, since the test animals from the same group were not individually assessed for weight changes. Instead the results for each day represent average body weight variation compared to day 0 for six mice per group. Nevertheless, a clear pattern was present in this and all following experiments. Animals from the groups that received a low 30 PFU dose experienced little or no changes in body weight regardless of whether the virus was grown at 33 °C or 37 °C. In contrast, animals inoculated with 5000 PFU showed weight loss on day four post infection. Furthermore, an apparent difference was found among animals challenged with a high inoculum dose, with animals inoculated with virus grown at 37 °C showing more dramatic body weight loss. Control animals did not lose any weight throughout the experiment.

Clinical signs were monitored based on a scoring system adapted from Morton and Griffiths (194). Three different categories of clinical signs were monitored: physical appearance, unprovoked behavior and the response to external stimulation. As shown in Figure 4.1.2, clinical signs confirmed that the animals inoculated with a high dose of virus grown at 37 °C showed more rapid and more severe disease progression. On day seven post infection, control mice and mice inoculated with 30 PFU of virus grown at 33 °C or 37 °C showed a 100% survival rate. Animals inoculated with 5000 PFU of PVM propagated at 33 °C or 37 °C showed 66.6% and 0% survival rates, respectively. Based on these results, we made the decision to propagate PVM strain 15 at 37 °C and to use this viral stock for further studies.

Figure 4.1.1- Body weight changes compared to day 0 for Balb/c mice (n=6), inoculated with high (5000 PFU) or low (30 PFU) doses of PVM strain 15, propagated either at 33 °C or 37 °C. Each point represents the average body weight change for six animals per group compared to preinoculation control values for these animals. The average preinoculation weight was 18.53 grams for the groups inoculated with virus propagated at 33 °C and 18.36 grams for the groups inoculated with virus propagated at 37 °C.

Figure 4.1.1

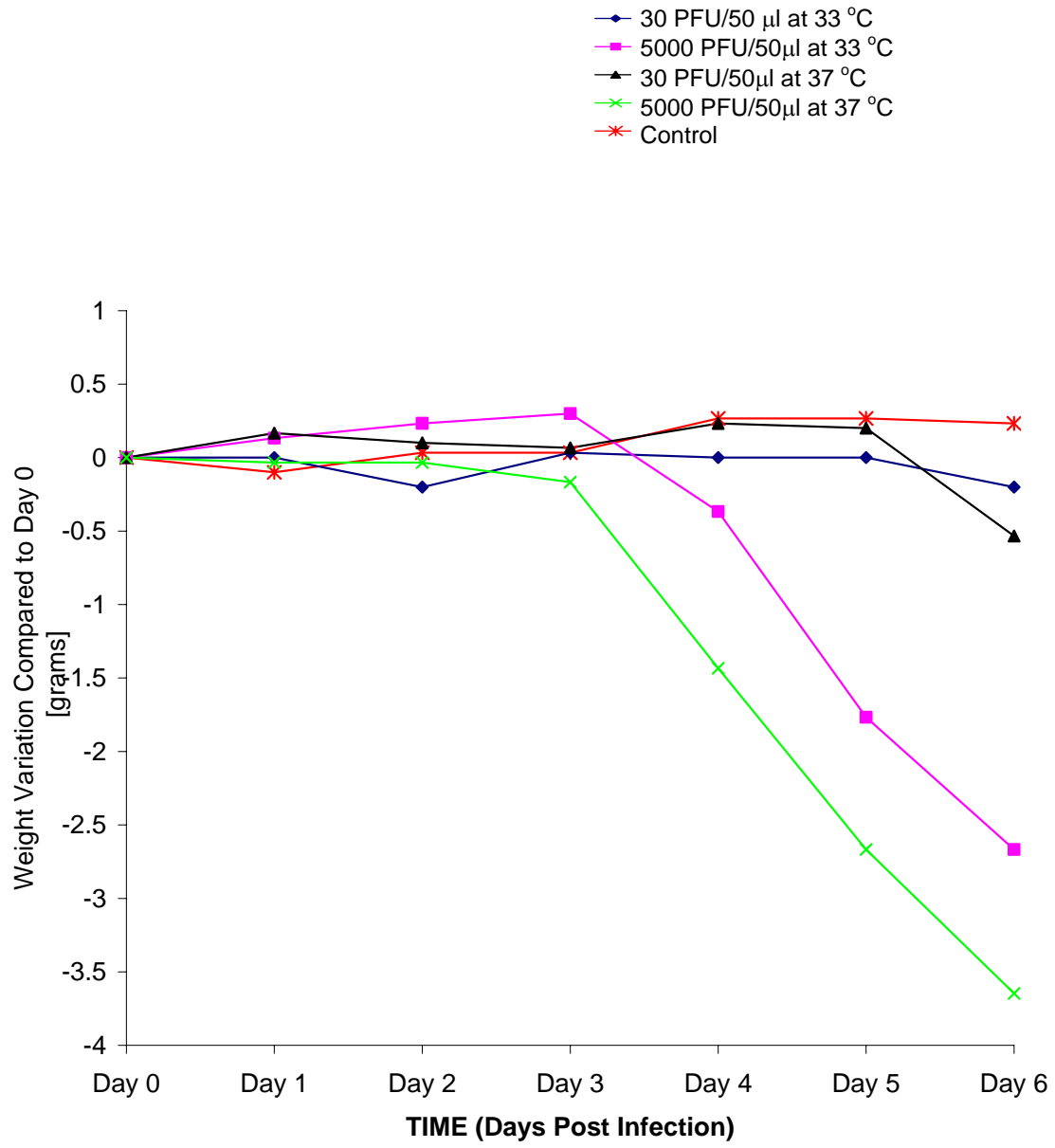
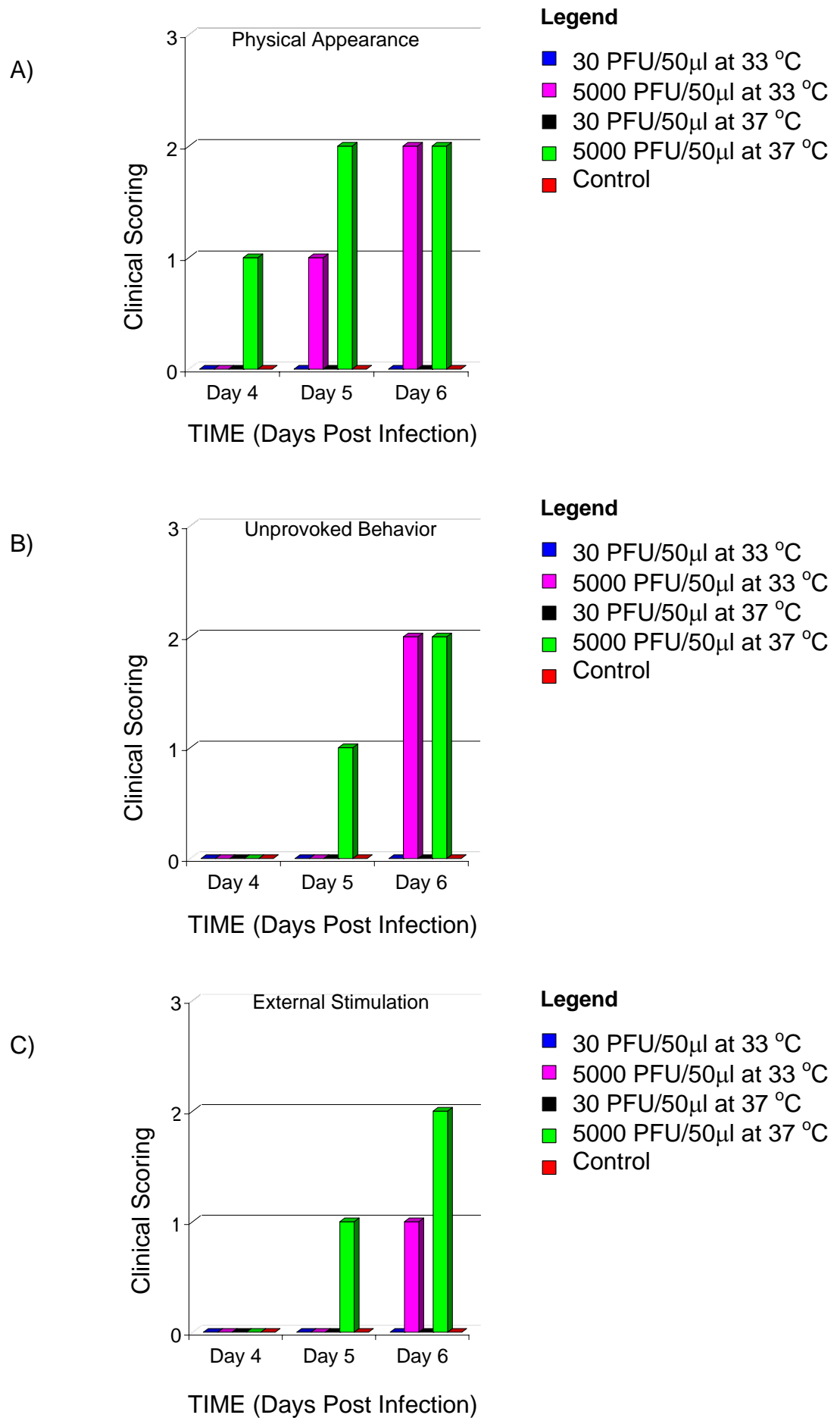


Figure 4.1.2 – Scoring of clinical signs for Balb/c mice during the six-day period post infection. Three categories of clinical signs were monitored: physical appearance, unprovoked behavior and response to external stimulation. The scoring system was as follows: Panel A (physical appearance) 0 - normal, 1 - lack of grooming, 2 - rough coat, nasal/ocular discharge, 3 - very rough coat, abnormal posture, enlarged pupils. Panel B (unprovoked behavior) 0 - normal, 1 - minor changes, 2 - abnormal; reduced mobility, decreased alertness, inactive. Panel C (behavioral response to external stimuli) 0 - normal, 1 - minor depression/exaggeration of response, 2 - moderately abnormal response, 3 - comatose. For all categories of clinical signs a score of 4 represents a dead animal.

Figure 4.1.2



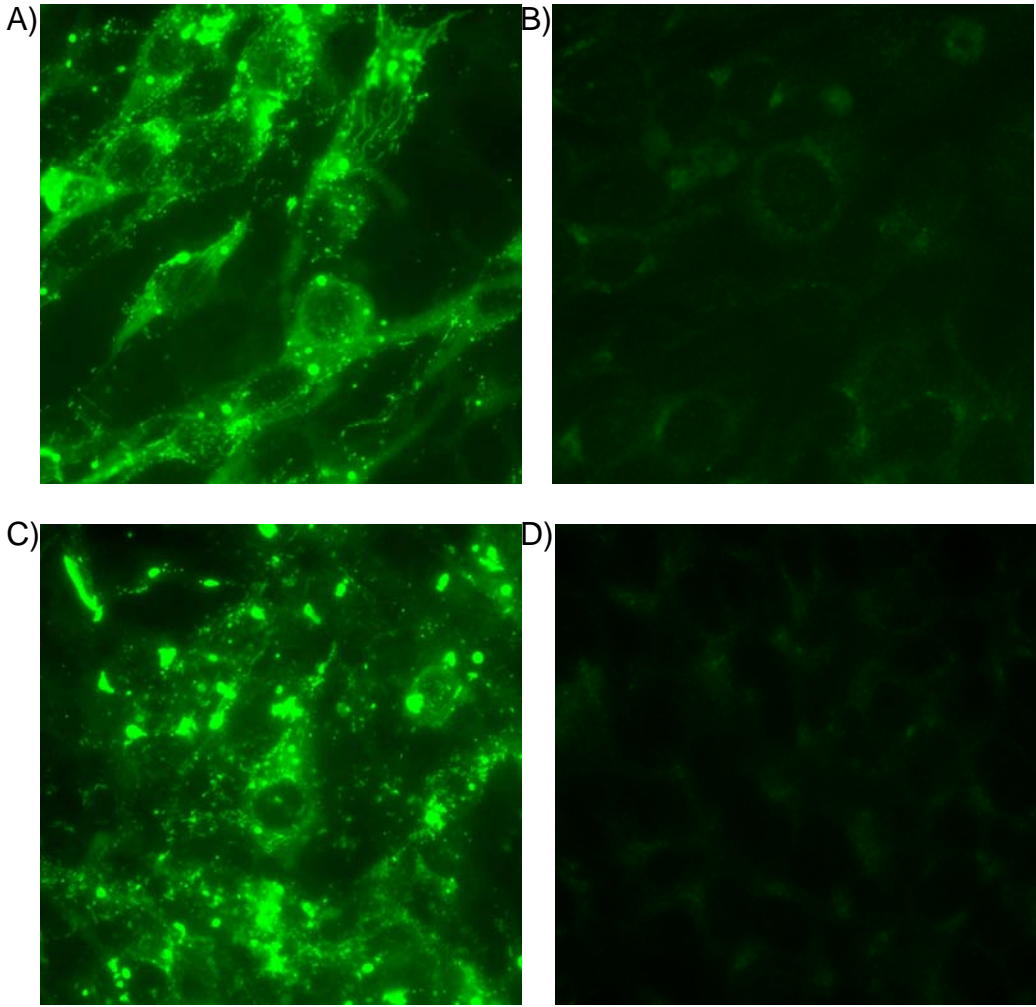
4.1.2 Virus Quantification

Several research groups have reported difficulties in consistent and reliable quantitation of PVM virus, mainly because the PVM-induced plaques develop slowly, have relatively indistinct borders, and are difficult to distinguish in cell cultures (83).

In order to overcome this problem we established an assay for the quantitation of PVM virus. Slight modifications of a standard plaque assay were employed, in which infected BHK-21 cells were immunostained with rabbit polyclonal primary antibodies specific for the N protein of PVM and goat α -rabbit FITC-labeled secondary antibodies. The resulting plaques were visualized by fluorescence microscopy. Appearance of fluorescently stained plaques is shown in Figure 4.1.3. Titers of PVM stock produced were measured to be 10^3 - 10^6 pfu/ml depending on the viral passage.

Figure 4.1.3 - Appearance of PVM-infected BHK-21 cells at 48 hours post infection. Infected cells were stained with rabbit polyclonal primary antibodies specific for the N protein of PVM and goat α -rabbit FITC-labeled secondary antibodies, and the resulting plaques were observed under the fluorescence microscope. Panels A and panel B represent original ATCC PVM strain 15-infected BHK-21 cells and mock-infected BHK-21 cells respectively. Panels C and panel D represent BHK-21 cells infected with a third passage of PVM propagated at 37 °C, and mock infected BHK-21 cells respectively. Cells infected with PVM appear as bright green colored cells. Original magnification 40 x.

Figure 4.1.3



4.2. Establishment of an Intranasal Pneumonia Virus of Mice Challenge Model in Balb/c Mice

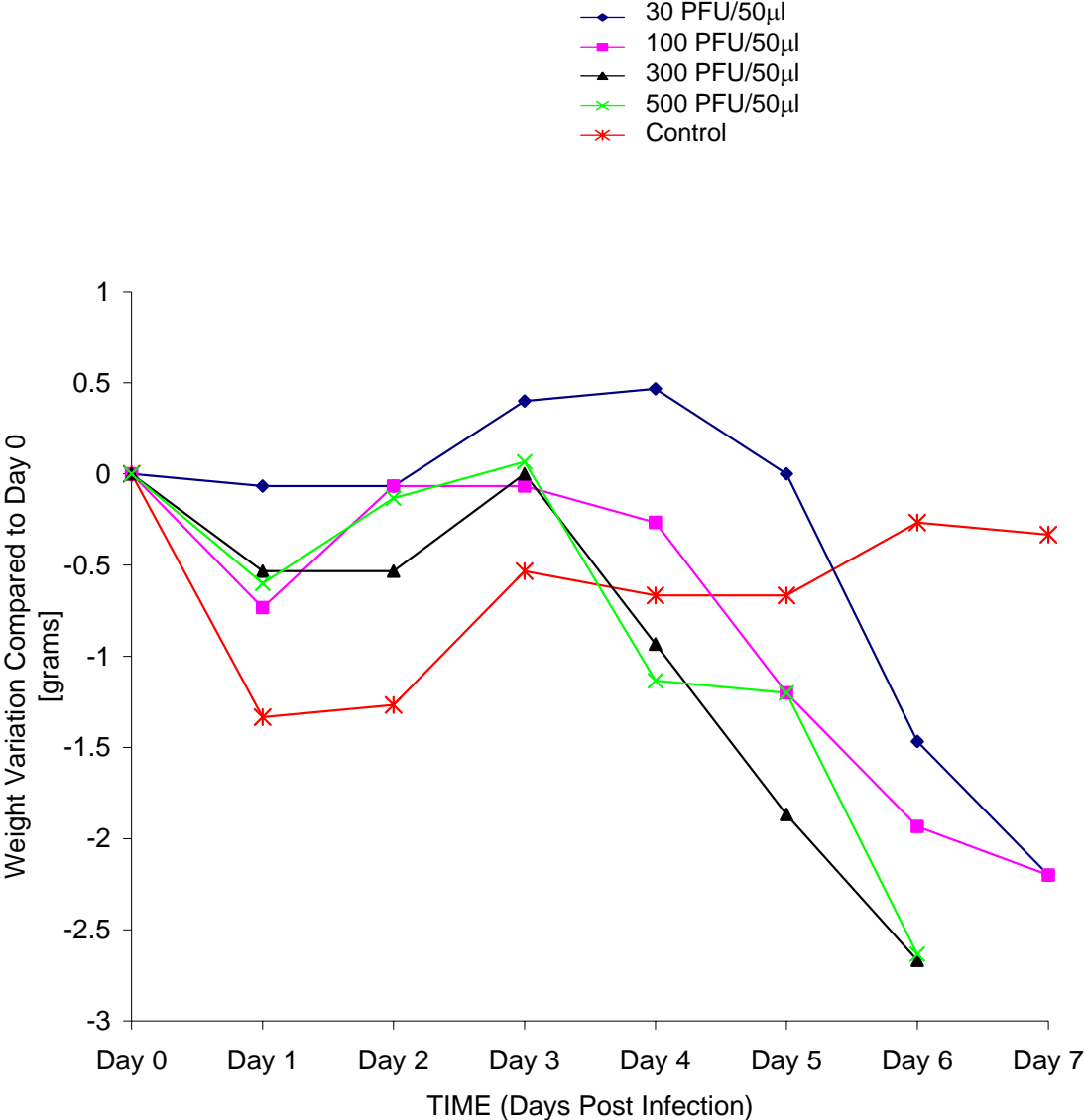
In order to assess the effects of PVM infection on clinical disease, we used standard methods for evaluation of the infectious process including clinical evaluation of infected animals based on weight measurement, and clinical signs, assessment of macroscopic and microscopic lung pathology, and evaluation of virus load in the lungs.

4.2.1 Body Weight Loss

Balb/c mice (three per group), were intranasally inoculated on day 0 with 0, 30, 100, 300 or 500 PFU of PVM strain 15 in a 50 μ l inoculum volume. Control animals were inoculated with the same volume of diluent. Clinical symptoms and body weights were monitored for seven days post infection. Figure 4.2.1 shows the weight variations compared to day 0 for five test groups. Initial body weight loss, most probably caused by stress inflicted by handling of the animals, was seen in all but one of groups. Following recovery, animals in the control group maintained their weight throughout the experiment. Gradual weight loss from four DPI was present in groups inoculated with 300 or 500 PFU, and the lowest weight of these animals was reached on day six, when they had lost more than 15% of their body weight. Less dramatic and somewhat delayed body weight loss was observed in animals inoculated with 100 or 30 PFU. In these animals loss in body weight started on day four or five respectively, and reached 10% on day seven post infection.

Figure 4.2.1 - Body weight changes compared to day 0 in PVM-infected Balb/c mice. Each point represents the mean body weight change for three mice per group compared to preinoculation values. The average preinoculation weight was 17.7 grams. On day 0 mice were inoculated with 0, 30, 100, 300, or 500 PFU of PVM strain 15. At day six post infection, all mice in the 300 PFU and 500 PFU groups were euthanized.

Figure 4.2.1



4.2.2 Clinical Illness and Survival

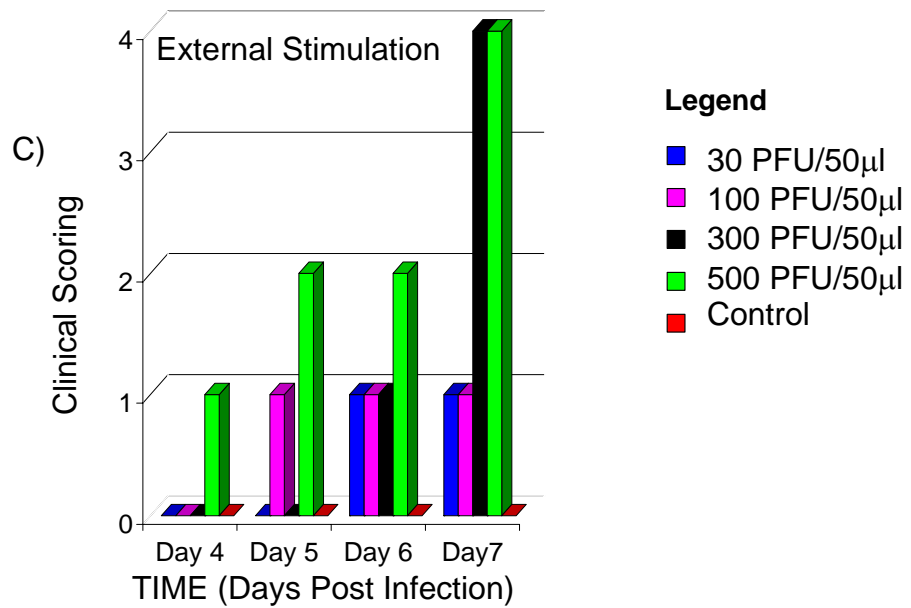
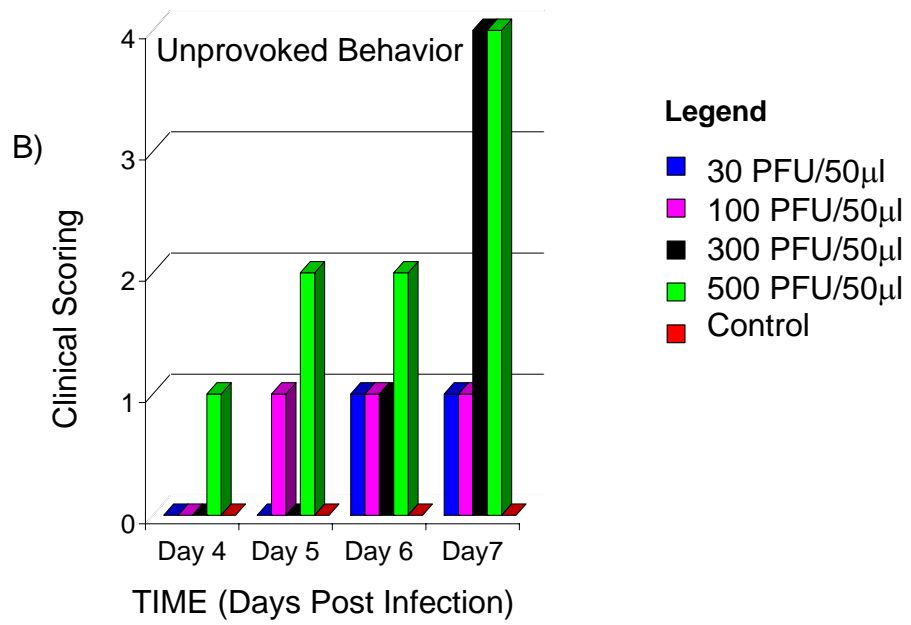
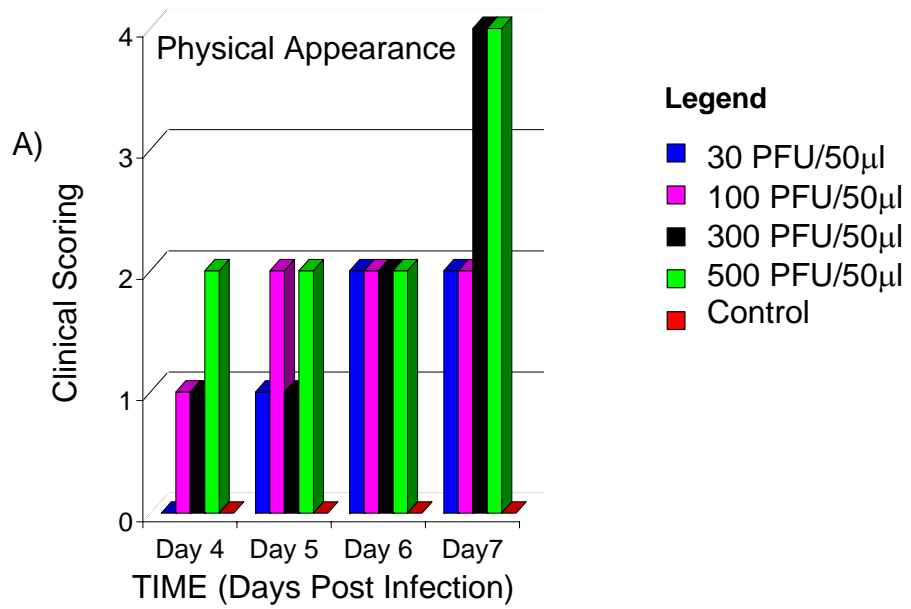
Clinical signs were monitored based on a scoring system adapted from Morton and Griffiths (194). Three categories of clinical signs were monitored: physical appearance, unprovoked behavior and the response to external stimulation. Additionally, the apparent increase in the respiratory rate of tested animals was monitored. The scoring system for all clinical signs was based on four points. A detailed explanation for scoring is presented in Figure 4.2.2.

While mice in the control group remained asymptomatic throughout the experiment, animals in all tested groups showed changes in their physical appearance, unprovoked behavior and response to external stimulation, as shown in panels A, B, and C of Figure 4.2.2. Most importantly, the extent of these changes corresponded to the dose of the virus that these animals received initially. Infected but not control mice showed changes in physical appearance characterized by decreased alertness and mobility, lack of grooming and prominent piloerection as well as up to ~ 30% increase in respiratory rate in groups that received the 300 and 500 PFU doses. As seen in Figure 4.2.2, (panel A), on day four post infection initial changes in physical appearance were observed in all experimented groups except the 30 PFU group, while only animals inoculated with 500 PFU showed changes in their unprovoked behavior (panel B) and external stimulation (panel C). On day six post infection animals from all experimental groups showed similar clinical signs with regards to physical appearance, while changes observed in unprovoked behavior and reaction to an external stimulation were increased in animals inoculated with 500 PFU. At day seven post infection animals that received 300 or 500 PFU had

to be euthanized so as to prevent unnecessary suffering. Survival rates for the other groups on day seven post infection was 100%.

Figure 4.2.2 – Scoring of clinical signs of Balb/c mice from day four till day six post PVM infection. Three categories of clinical signs were monitored: physical appearance, unprovoked behavior and the response to external stimulation. The scoring system was as follows : Panel A (physical appearance) 0 - normal, 1 - lack of grooming, 2 - rough coat, nasal/ocular discharge, 3 - very rough coat, abnormal posture, enlarged pupils. Panel B (unprovoked behavior) 0 - normal, 1 - minor changes, 2 - abnormal; reduced mobility, decreased alertness, inactive. Panel C (behavioral response to external stimuli) 0 - normal, 1 - minor depression/exaggeration of response, 2 - moderately abnormal response, 3 - comatose. For all categories of clinical signs a score of 4 represents a dead animal.

Figure 4.2.2

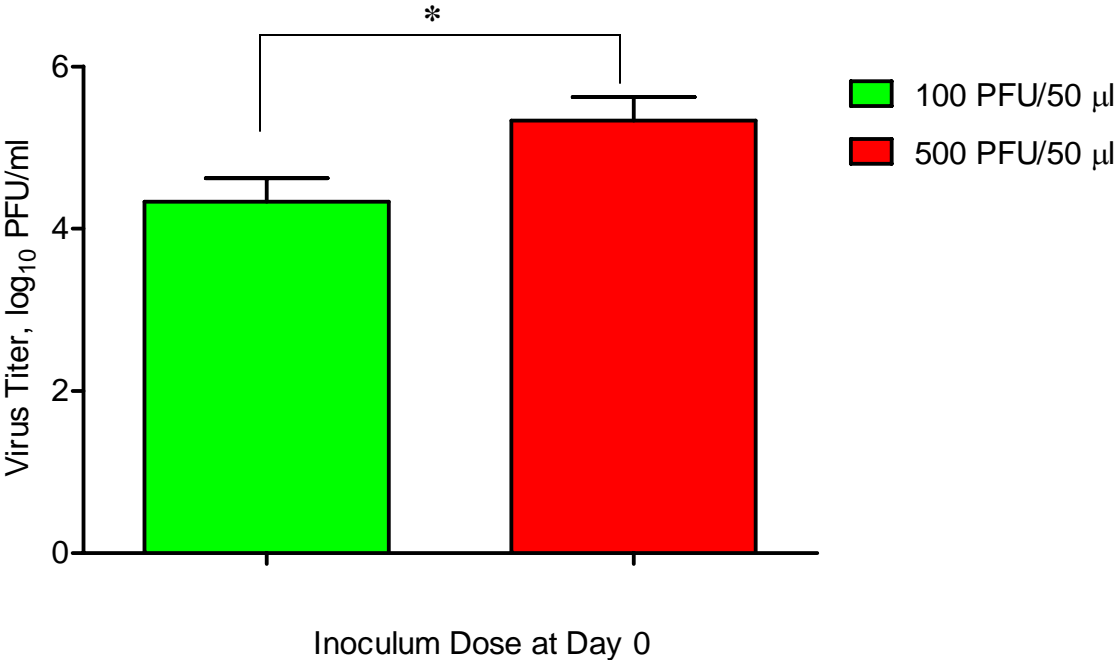


4.2.3 Viral Titers in the Lungs

On day six after PVM infection, lung homogenates from mice that had received intranasal inoculums of 100 or 500 PFU in a 50 μ l volume were selected and evaluated in a modified plaque assay to determine the extent of virus replication. As shown in Figure 4.2.3, viral titers were significantly different between these two groups. As expected, the viral titers reflected the difference in initial inoculum dose, with 3×10^4 pfu/ml of virus recovered from the animals that received the lower dose (100 PFU), and 3×10^5 pfu/ml of virus recovered from the animals that received a higher dose (500 PFU). A considerable increase in virus recovered from the lungs when compared to the viral challenge dose given to animals demonstrates the ability of PVM to successfully replicate in Balb/c mice.

Figure 4.2.3 Viral titers in the lungs of Balb/c mice inoculated with 100 PFU or 500 PFU determined by modified plaque assay of the lung homogenates on day six post infection. Each value represents the average +/- one standard deviation (SD) of the mean for three mice per group. Statistical significance was determined by unpaired Student t-test (* = $p < 0.02$).

Figure 4.2.3



4.2.4 Macroscopic and Microscopic Pulmonary Lesions in Balb/c mice

Examination of macroscopic pulmonary changes revealed an absence of pulmonary lesions in control mice that were intranasally inoculated with diluent only. Analogous to what was observed for clinical signs and viral titers, the number of lung lesions and the percentage of lung tissue involved in lesions were dependent on the initial dose of virus the animals received at the time of inoculation. In animals that received 500 PFU of PVM at the time of challenge, approximately 80% of lung tissue had pulmonary lesions, compared to ~30% in the group challenged with 100 PFU (Figure 4.2.4a). A slight discoloration and necrotic appearance was observed in all challenged groups, but the 100 PFU group showed multifocal rather than confluent areas of necrotizing lesions that were readily seen in the group challenged with 500 PFU.

Tissue sections from lungs of control and test animals were examined, and characteristic sections of microscopic lesions are depicted in Figure 4.2.4b. Histopathology observations corresponded with clinical signs, and the lesion patterns appeared to be similar among groups but as previously seen, the extent of pulmonary damage and percent lung involvement appeared to depend on the initial inoculum dose. There was no apparent difference in the extent of pulmonary damage between mice from the same treatment group. As shown in Figure 4.2.4b, an appreciable difference can be seen when the normal lung architecture of a control mouse is compared to the histopathology of a mouse inoculated with 500 PFU of PVM. Apparent limited type II cell proliferation edema was present, with multifocal regions of alveolitis, bronchiolitis, and in some cases, interstitial pneumonia. Visible necrotizing areas were present with noticeable neutrophilic and lymphocytic infiltration, and hemorrhaging.

Figure 4.2.4 – Representative macroscopic and microscopic observations in the lung tissue of PVM infected Balb/c mice. Figure 4.2.4 a) Macroscopic pulmonary differences between control mice and mice inoculated on day 0 with 100 or 500 PFU of PVM strain 15. Figure 4.2.4 b) Microscopic observations in a representative section of lung tissue acquired on day six post inoculation. Panel A) a section of H+E stained lung tissue from a control animal. Panels B, C and D) a section of H+E stained lung tissue from an animal inoculated with 500 PFU. Original magnification 10X (panel A and B), 20X (panel C) and 40X (panel D). Letters inside panels A, B, C, and D in Figure 4.2.4b represent: a – Alveoli, b – Bronchiole, n – Neutrophil, v – Vein).

Figure 4.2.4a Lung Macroscopic Pathology Observations

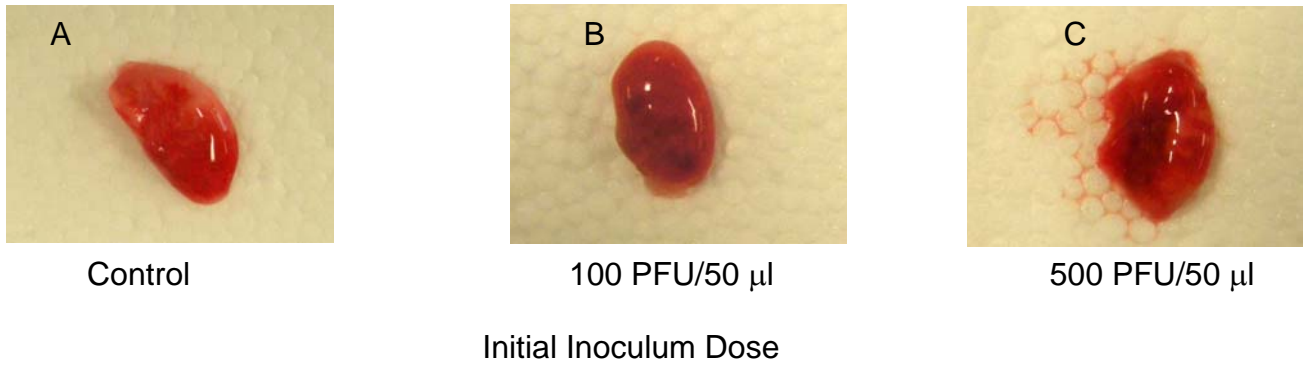
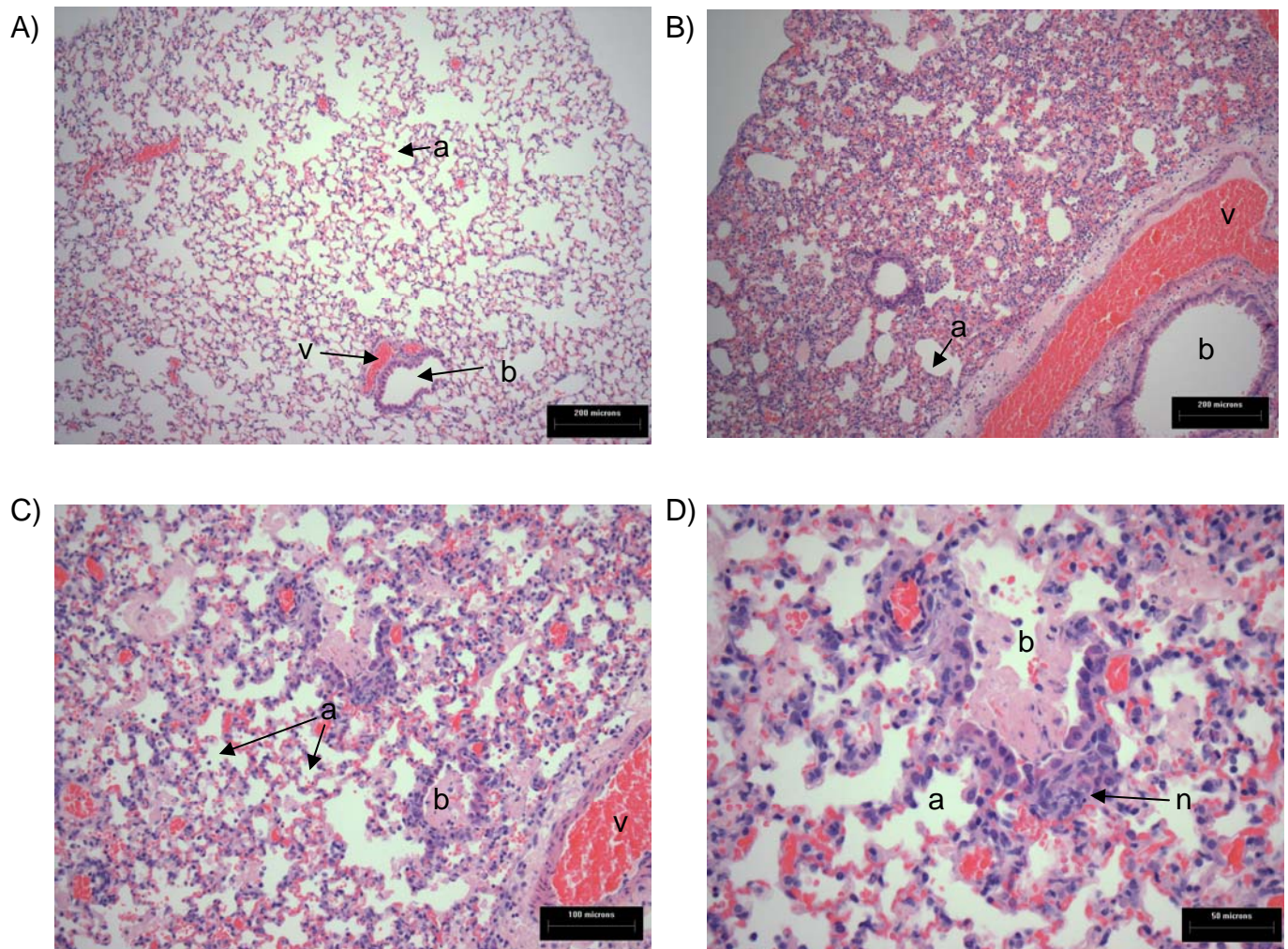


Figure 4.2.4b Histopathological Observations



4.3 Establishment of an Intranasal Pneumonia Virus of Mice Challenge Model in C57/Bl Mice

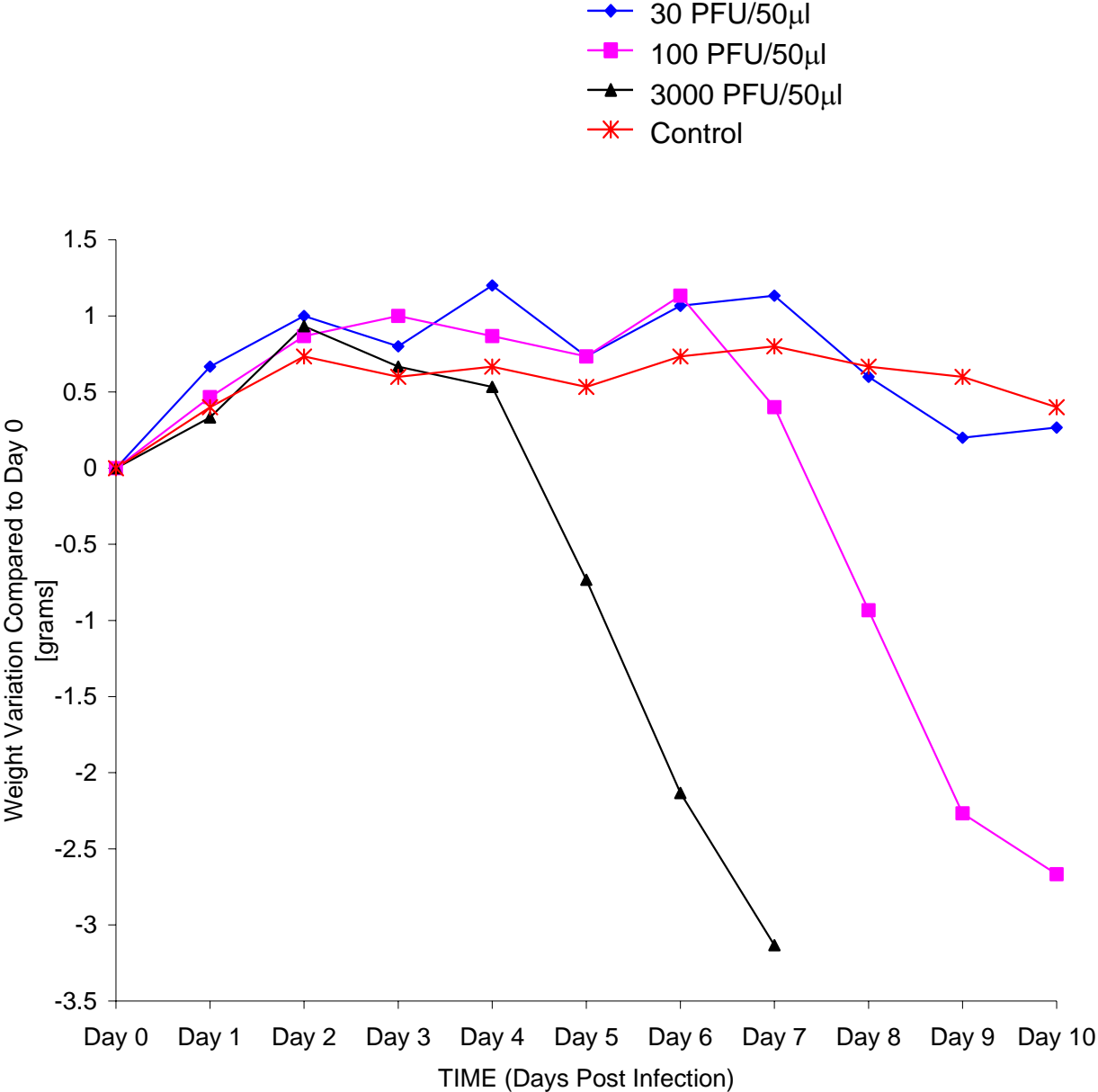
In order to establish an intranasal PVM challenge model in C57/Bl mice, we used standard methods for evaluation of the infectious process, including clinical evaluation of infected animals based on weight measurement and clinical signs, assessment of macroscopic and microscopic lung pathology, and evaluation of virus load in the lungs.

4.3.1 Body Weight Loss

C57/Bl mice were intranasally inoculated on day 0 with 0, 30, 100, or 3000 PFU of PVM strain 15 in a 30 μ l inoculum volume. Control animals were inoculated with the same volume of diluent. Clinical symptoms and body weight loss were monitored for 10 days post infection. Figure 4.3.1 shows the weight variations compared to day 0 for four experimental groups. Animals in the control group maintained their weight throughout the experiment. Mice inoculated with 30 PFU also maintained their body weight. Rapid weight loss from four days post infection was present in the group inoculated with 3000 PFU; these animals had lost ~ 27% of their body weight by day seven post infection. Mice inoculated with 100 PFU showed delayed body weight loss that started on day seven, and reached 19% by day 10 post infection.

Figure 4.3.1- Body weight changes compared to day 0 in C57/Bl mice (n=3), inoculated with 0, 30, 100 or 3000 PFU of PVM strain 15. Each point represents the average body weight change for three mice per group compared to preinoculation control values. The average preinoculation weight was 19 grams.

Figure 4.3.1



4.3.2 Clinical Illness and Survival

Clinical signs including physical appearance, unprovoked behavior and response to external stimulation were monitored in the same manner as for Balb/c animals. As shown in Figure 4.3.2, control mice and animals inoculated with 30 PFU remained asymptomatic throughout the experiment. Animals inoculated with 100 PFU or 3000 PFU first showed clinical signs on day six or seven post inoculation, respectively. However, the changes in general appearance of animals inoculated with 100 PFU or 3000 PFU were less dramatic than those seen in Balb/c mice. Animals were less alert than control animals, but still quite mobile. Absence of hair coat grooming was apparent, but the piloerection was prominent only in the neck areas. As late as 10 days post inoculation, animals inoculated with 100 PFU showed only minor changes in their response to external stimuli (Panel C), that were limited to minor signs of depression. Furthermore, less than 5% increase in the respiratory rate was observed in animals that received a 3000 PFU dose, whereas no effects were observed in animals that received a 100 PFU dose. On day seven after inoculation all animals from the 3000 PFU group were euthanized due to the illness, whereas the survival rate for the other animals was 100% at 10 days post inoculation.

4.3.3 Viral Titers in the Lungs

In order to quantitate virus recovered from lungs of control and PVM-infected C57/Bl mice, the same procedure used for Balb/c mice was employed. As shown in Figure 4.3.3, viral titers were significantly different between the groups of mice inoculated with 3000 PFU and 100 PFU. As previously demonstrated in the Balb/c model, the amount of virus recovered from the

lung tissue reflected the difference in the initial inoculum dose, with $\sim 5 \times 10^2$ pfu/ml of virus recovered from the animals that received the lower dose (100 PFU) and $\sim 2 \times 10^4$ PFU /ml of virus recovered from the animals that received the higher dose (3000 PFU). Considering the extremely small viral load the animals received on day 0, PVM can successfully replicate in C57/Bl mice, but it is obvious that the presence of a “critical initial load” is necessary for disease establishment.

Figure 4.3.2 - Scoring of clinical signs for C57/Bl mice from day five to day 10 day post PVM infection. Three categories of clinical signs were monitored: physical appearance, unprovoked behavior and the response to external stimulation. The scoring system was as follows : Panel A (physical appearance) 0 - normal, 1 - lack of grooming, 2 - rough coat, nasal/ocular discharge, 3 - very rough coat, abnormal posture, enlarged pupils. Panel B (unprovoked behavior) 0 - normal, 1 - minor changes, 2 - abnormal; reduced mobility, decreased alertness, inactive. Panel C (behavioral response to external stimuli) 0 - normal, 1 - minor depression/exaggeration of response, 2 - moderately abnormal response, 3 - comatose. For all categories of clinical signs a score of 4 represents a dead animal.

Figure 4.3.2

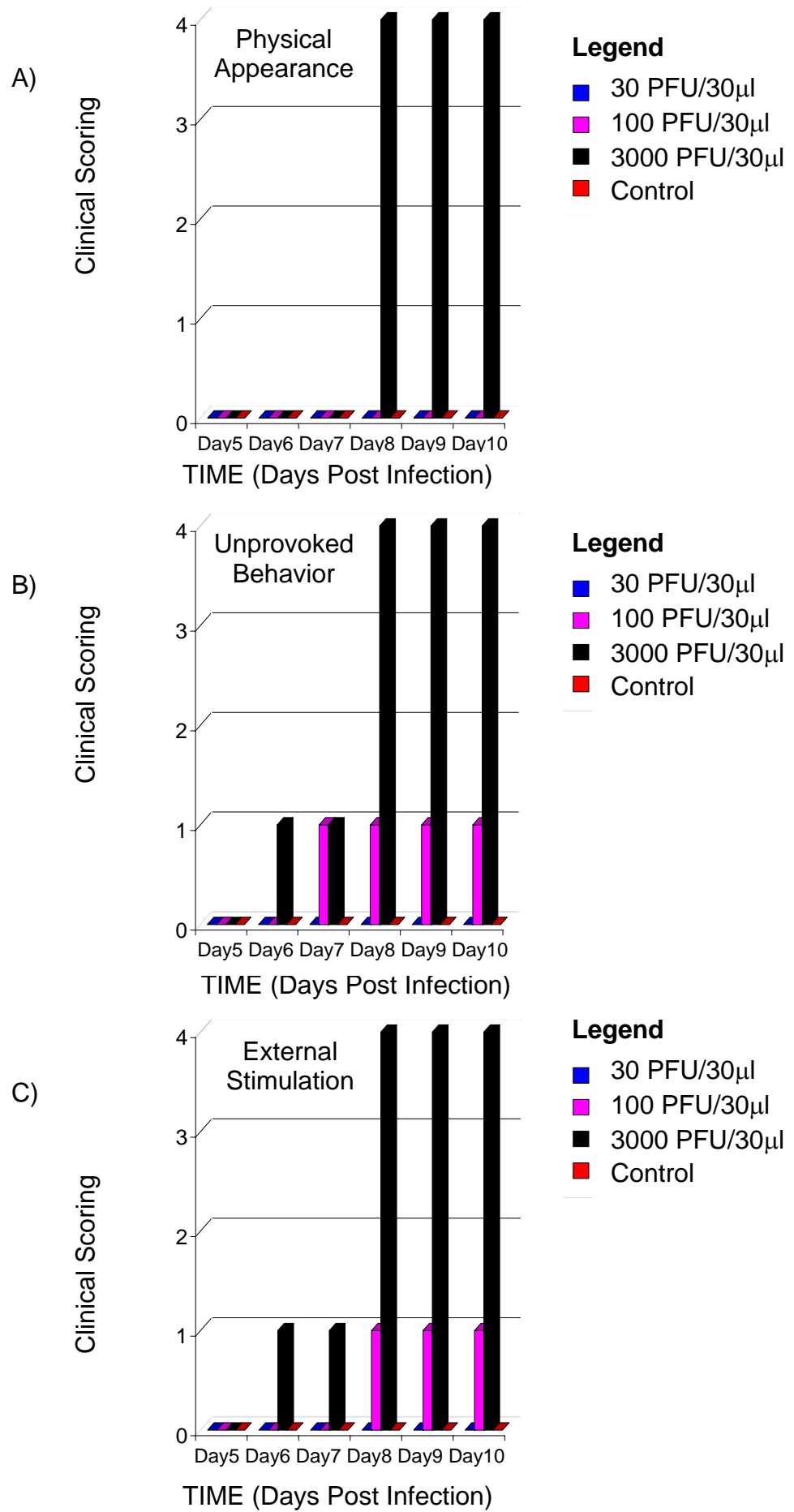
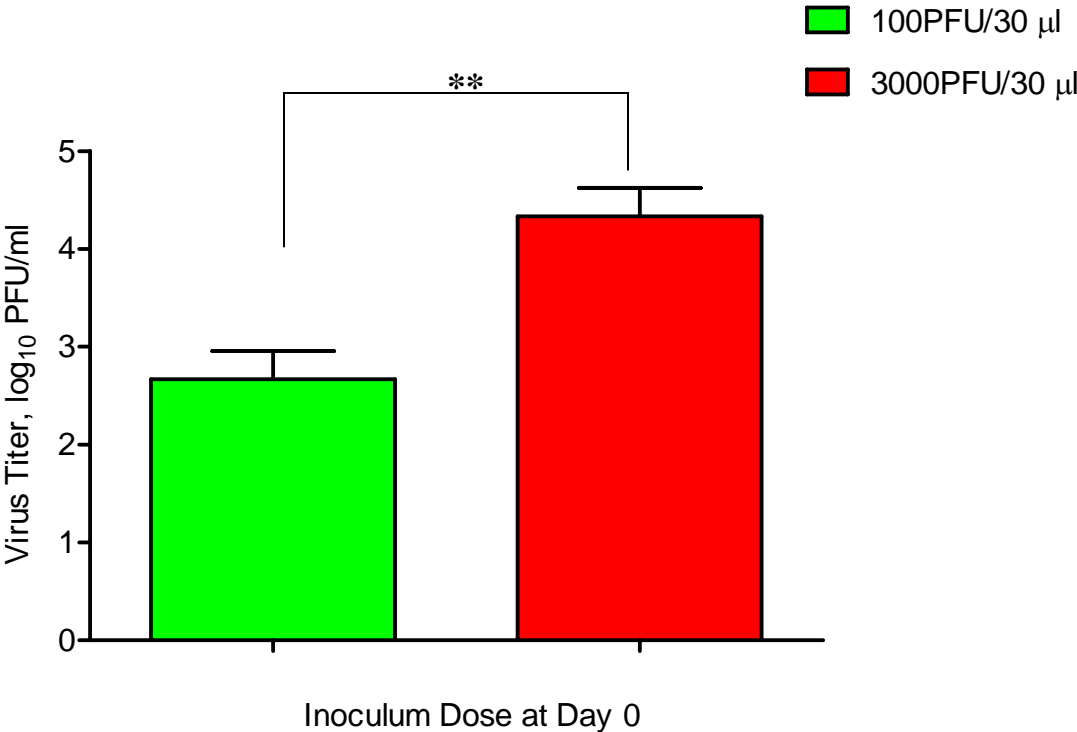


Figure 4.3.3 Viral titers in the lungs of C57/Bl mice inoculated with 100 PFU or 3000 PFU determined by modified plaque assay of the lung homogenates on day seven post infection. Each value represents the average +/- one standard deviation (SD) of the mean for three mice per group. Statistical significance was determined by paired Student t-test (** = $p < 0.01$).

Figure 4.3.3



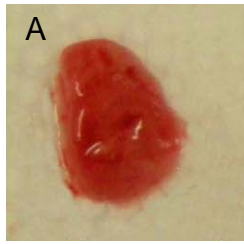
4.3.4 Macroscopic and Microscopic Pulmonary Lesions in C57/Bl mice

Examination of macroscopic pulmonary changes revealed an absence of pulmonary lesions in control mice inoculated with diluent only as well as in mice challenged with 30 PFU of PVM on day 0. Similar to what was observed for clinical signs and viral titers, the number of lung lesions and the percentage of lung tissue involved in lesions were directly dependant on the initial dose of virus the animals received at the time of inoculation. In the animals that received 3000 PFU of PVM, approximately 50% of the lung tissue showed an involvement in pulmonary lesions, characterized by grayish and dark-red areas (Figure 4.3.4a). In the group challenged with 100 PFU, considerably less lung tissue showed signs of pathology. In this group multifocal areas of reddish discoloration were observed in ~15% of the lung tissue area.

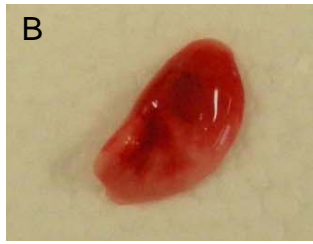
Tissue sections from lungs of control and test animals were examined and characteristic sections of microscopic pulmonary lesions are depicted in Figure 4.3.4b. Histopathology observations showed lesion patterns that were similar to those in Balb/c mice. As seen in Figure 4.3.4b, PVM-infected animals showed signs of inflammation compared to the normal lung structure of control mice. Limited type II cell proliferation, with alveolitis and areas of multifocal bronchiolitis, were found. Areas of visible neutrophil, macrophage and lymphocyte infiltration were easily identified. The degree of pulmonary damage and percentage of lung tissue engaged appeared to be dissimilar among test groups and correlated to the initial inoculum doses, with animals that received high doses exhibiting more severe lung tissue involvement.

Figure 4.3.4 – Representative macroscopic and microscopic observations in the lung tissue of PVM infected C57/Bl mice. 4.3.4a) Macroscopic pulmonary differences between control mice and mice inoculated on day 0 with 100 or 3000 PFU of PVM strain 15. 4.3.4b) Microscopic observations in a representative section of lung tissue acquired on day six post infection. Panels A and B) a section of H+E stained lung tissue from a control animal. Panels C and D) a section of H+E stained lung tissue from an animal inoculated with 3000 PFU. Original magnification 10X (panels A and C) and 20X (panels B and D). Letters inside panels A, B, C, and D in Figure 4.3.4b represent: a – Alveoli, b – Bronchiole, n – Neutrophil, v – Vein).

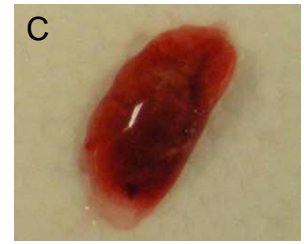
Figure 4.3.4a Lung Macroscopic Pathology Observations



Control



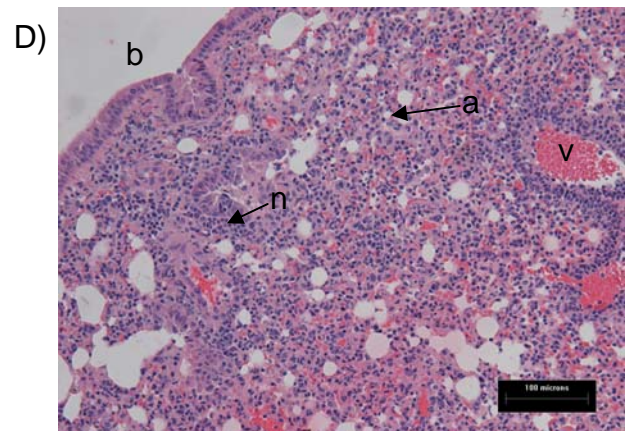
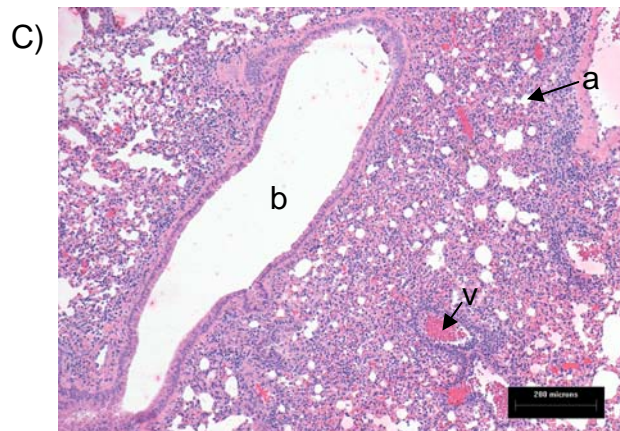
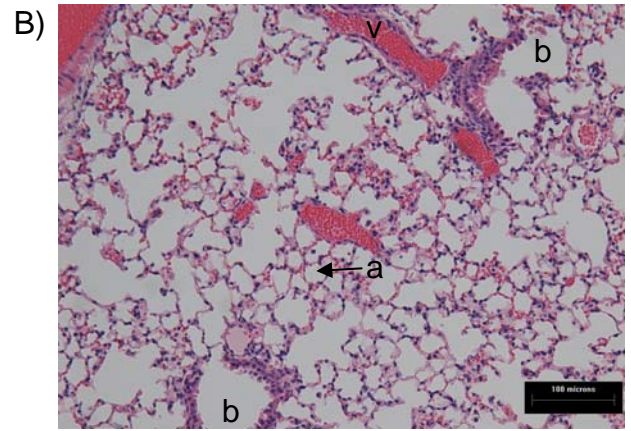
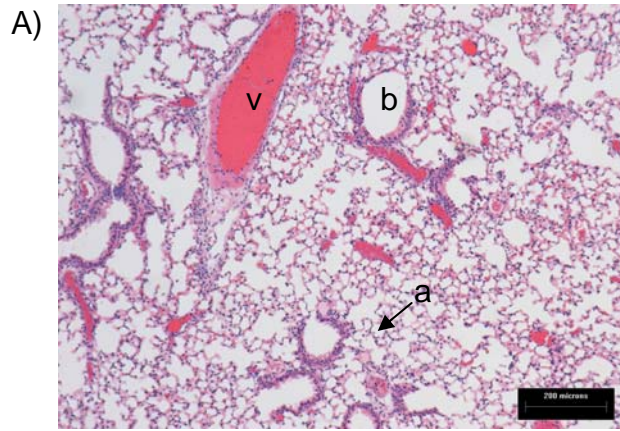
100 PFU/30 µl



3000 PFU/30 µl

Initial Inoculum Dose

Figure 4.3.4b Histopathological Observations



4.4 Comparative study of Pneumonia Virus of Mice infection of Balb/c and C57/Bl Mice

4.4.1 Influence of the volume of inoculum on Pneumonia Virus of Mice infection of Balb/c and C57/Bl mice

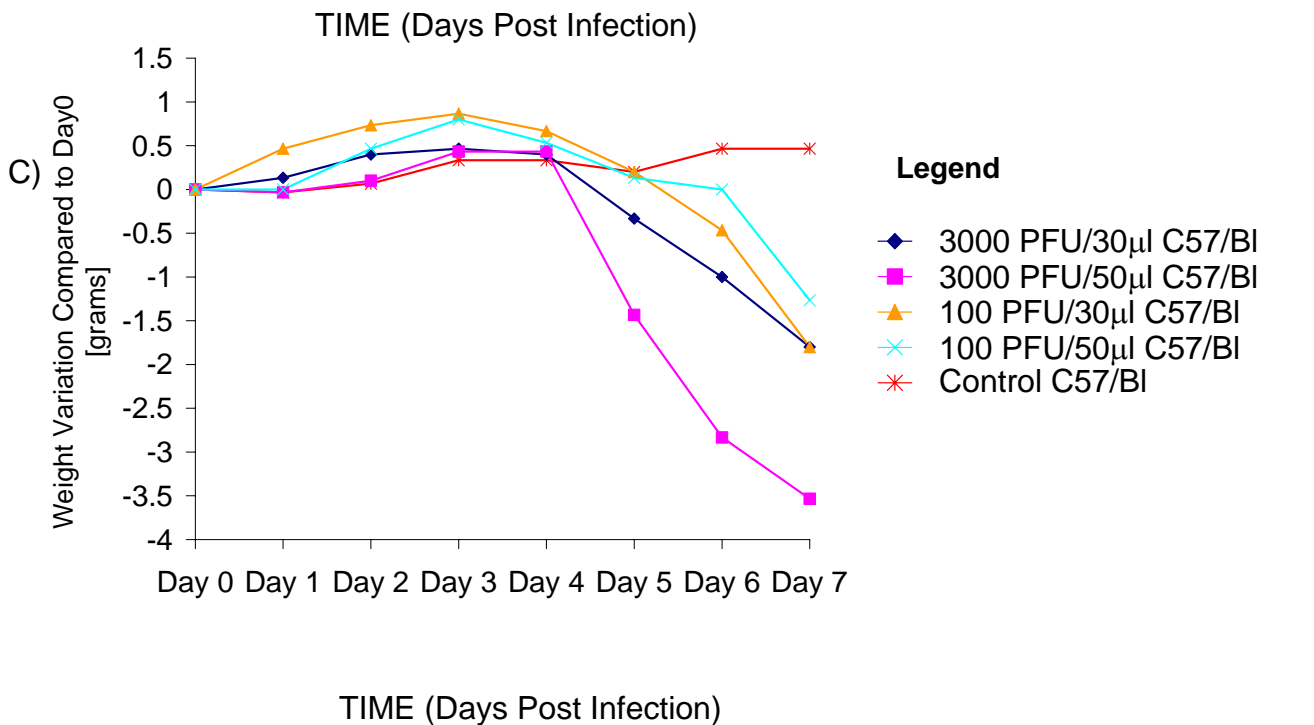
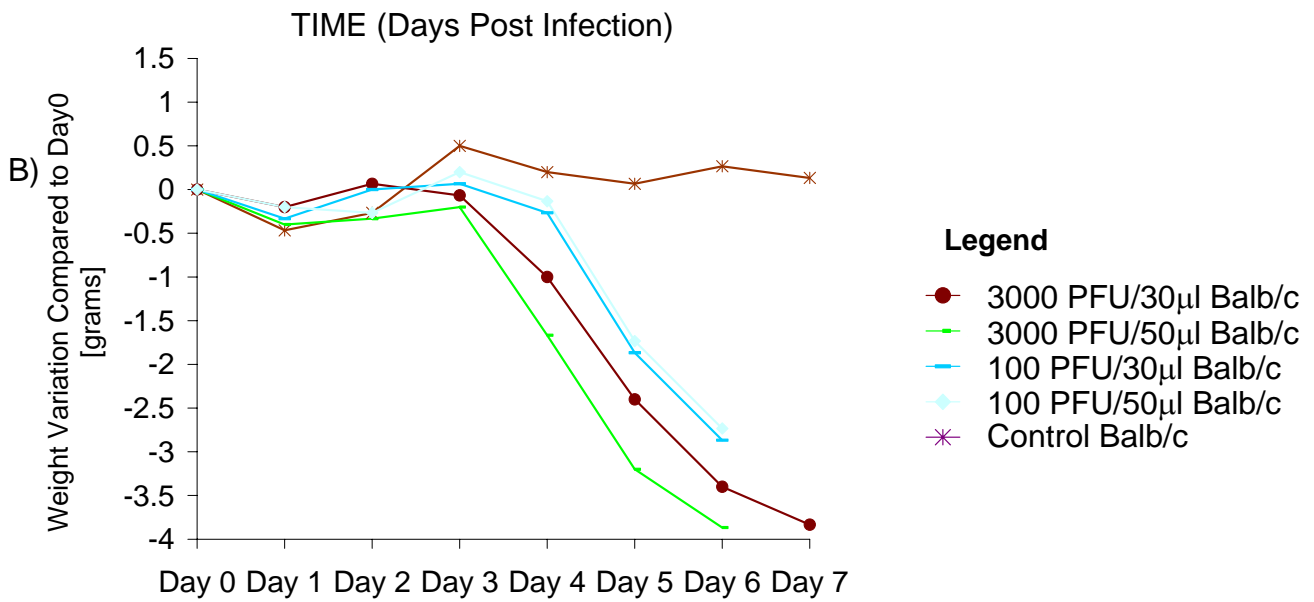
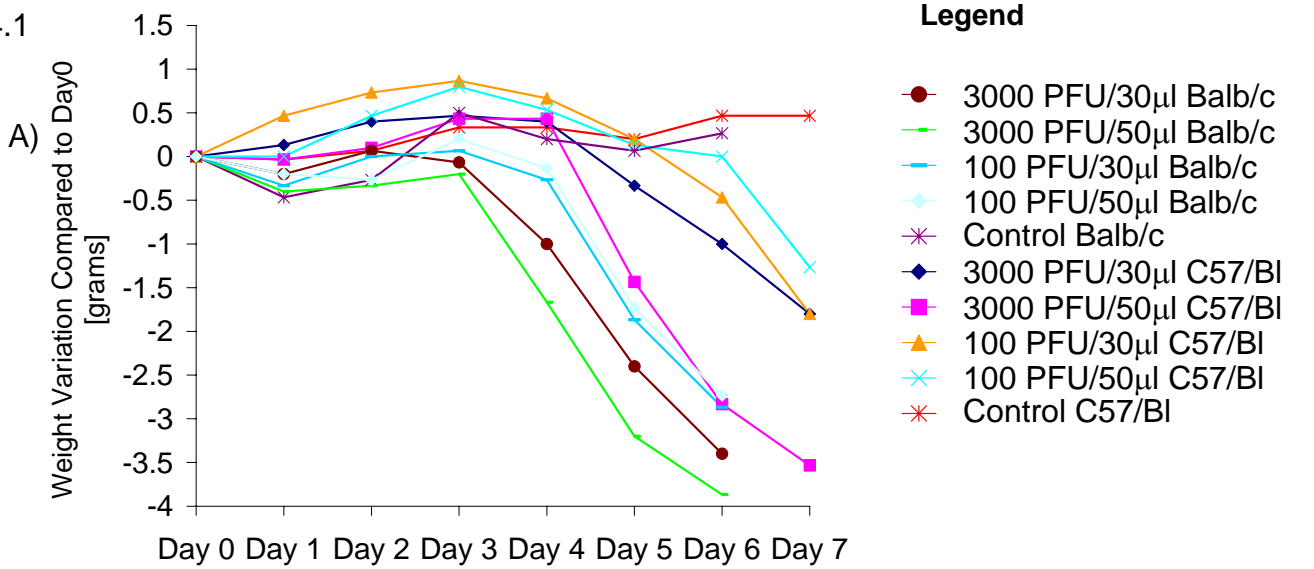
In view of the observed difference in susceptibility of Balb/c and C57/Bl mice to PVM, we wanted to confirm that the differences found in body weight loss, clinical signs and macroscopic and microscopic findings were present when the same initial volume of virus inoculum was used. For that purpose, a comparative study was performed in the two strains of mice. Mice were inoculated with high (3000 PFU) or low (100 PFU) doses of PVM in 30 μ l or 50 μ l inoculum volumes.

The difference in susceptibility to PVM infection between these two strains was confirmed. Weight variations for PVM infected Balb/c and C57/Bl mice are depicted in Figure 4.4.1. In Balb/c mice (Figure 4.4.1 B), the same pattern seen previously was present, with a decrease in body weight in mice inoculated with a high (3000 PFU) dose on day four post infection, whereas mice inoculated with a low (100 PFU) dose started to lose weight at five days post infection. Even though statistical analysis was not performed because group body weights were recorded, a clear dose-dependant pattern was present as seen previously. Furthermore, there was no apparent difference in body weight change between the groups inoculated with 30 μ l or 50 μ l inoculum volumes for the 100 PFU groups. A slight difference was observed in groups inoculated with 3000 PFU, with the mice inoculated with a 50 μ l volume showing larger loss in body weight compared to the ones inoculated with the same viral load but a 30 μ l inoculum volume.

Panel C of Figure 4.4.1 shows body weight changes compared to day 0 for the C57/Bl strain. Yet again, a delayed onset of disease in this strain was present and was characterized by loss of body weight in both the 3000 PFU groups at five days post infection, and on day seven post infection for animals in the 100 PFU groups. It also appeared that animals inoculated with 3000 PFU in a 50 μ l volume experienced more dramatic weight loss, ~20%, than the ones inoculated with the same viral load but in a 30 μ l volume. At day seven these animals lost ~13% of their body weight.

Figure 4.4.1- Body weight changes compared to day 0 in PVM-infected Balb/c and C57/Bl mice. Five mice per group were inoculated with 100 or 3000 PFU of PVM strain 15 in either a 30 μ l or 50 μ l inoculum volume. Each point represents average body weight change for five animals per group compared to preinoculation control values. A) Body weight changes compared to day 0 in PVM strain 15 infected Balb/c and C57/Bl mice. B) Body weight changes compared to day 0 in PVM infected Balb/c mice. C) Body weight changes compared to day 0 in PVM infected C57/Bl mice.

Figure 4.4.1



4.4.2 Clinical Illness and Survival

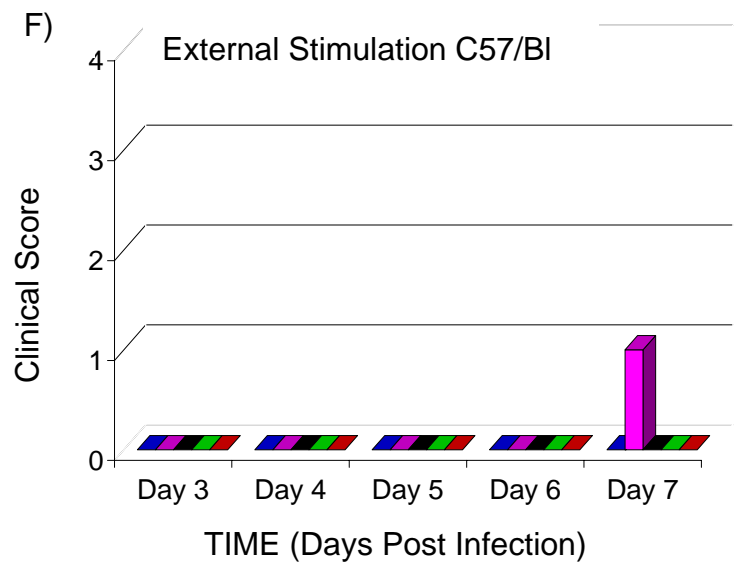
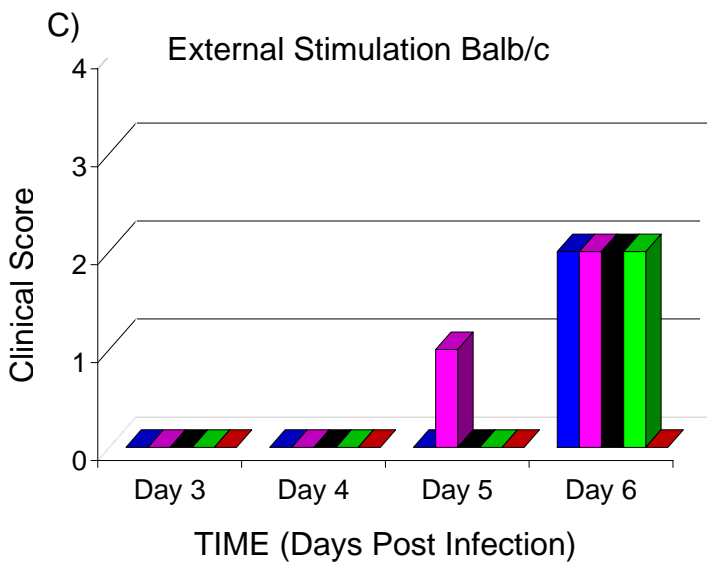
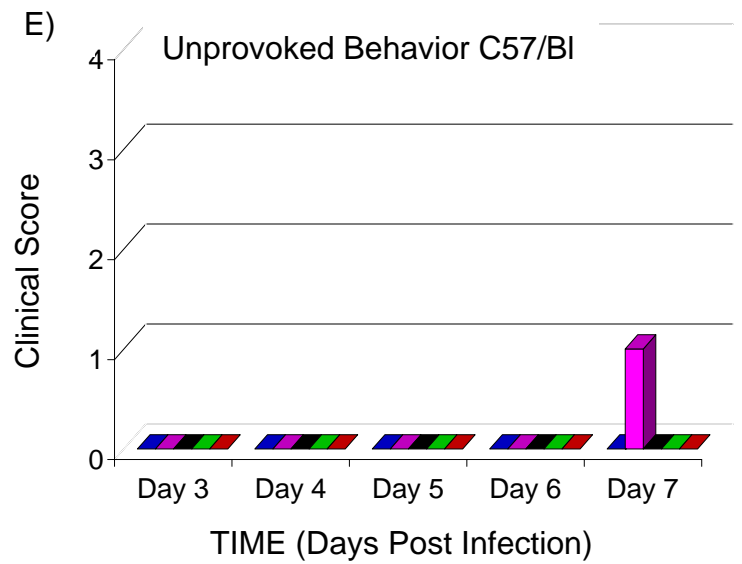
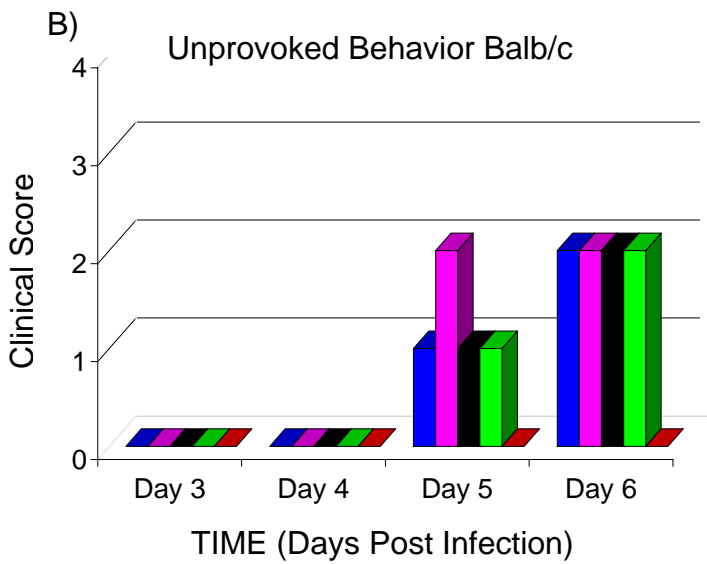
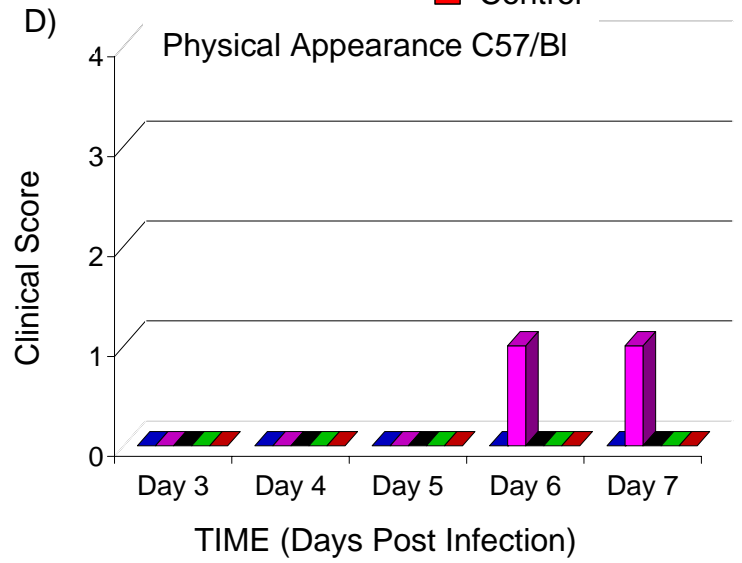
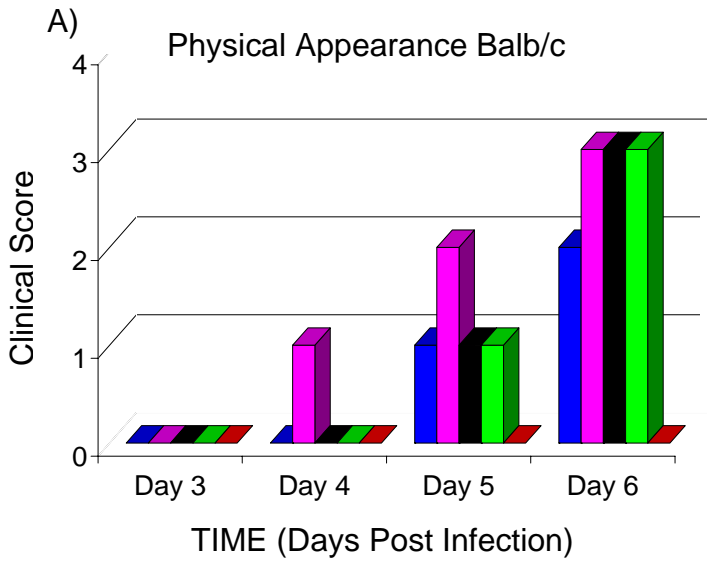
The clinical signs, shown in Figure 4.4.2, illustrate the difference in susceptibility of Balb/c and C57/Bl mice to PVM infection. As early as four days post infection, Balb/c mice inoculated with 3000 PFU in a 50 μ l volume showed absence of grooming (Panel A). Five DPI, all groups, except the control group, exhibited changes in both physical appearance and unprovoked behavior, as shown in panels A and B respectively. The extent of clinical illness appeared to be dose-dependant, with more severe manifestations in the groups inoculated with high viral load and larger inoculum volumes. Less obvious signs of clinical disease were observed in PVM-infected C57/Bl mice. As shown in panel D of Figure 4.4.2, the first signs of change in physical appearance were observed in mice inoculated with 3000 PFU in a 50 μ l volume at six DPI and these did not change until the animals were euthanized. Animals from the same group showed changes in unprovoked behavior and alteration in reaction to external stimulation at seven days post infection (panels E and F). All remaining C57/Bl groups, including the control group, remained asymptomatic throughout the experiment. Animals in all groups survived throughout the experiment.

Figure 4.4.2 – Scoring of clinical signs of Balb/c and C57/Bl mice for six and seven days post PVM infection, respectively. Three categories of clinical signs were monitored: physical appearance, unprovoked behavior and the response to external stimulation. Scoring system was as follows : Panels A and D (physical appearance) 0 - normal, 1 - lack of grooming, 2 - rough coat, nasal/ocular discharge, 3- very rough coat, abnormal posture, enlarged pupils. Panels B and E (unprovoked behavior) 0 - normal, 1 - minor changes, 2 - abnormal; reduced mobility, decreased alertness, inactive. Panels C and F (behavioral response to external stimuli) 0 - normal, 1 - minor depression/ exaggeration of response, 2 - moderately abnormal response, 3 - comatose. For all categories of clinical signs a score of 4 represents a dead animal.

Figure 4.4.2

LEGEND

- 3000 PFU/30 μ l
- 3000 PFU/50 μ l
- 100 PFU/30 μ l
- 100 PFU/50 μ l
- Control



4.4.3 Viral Titers in the Lungs

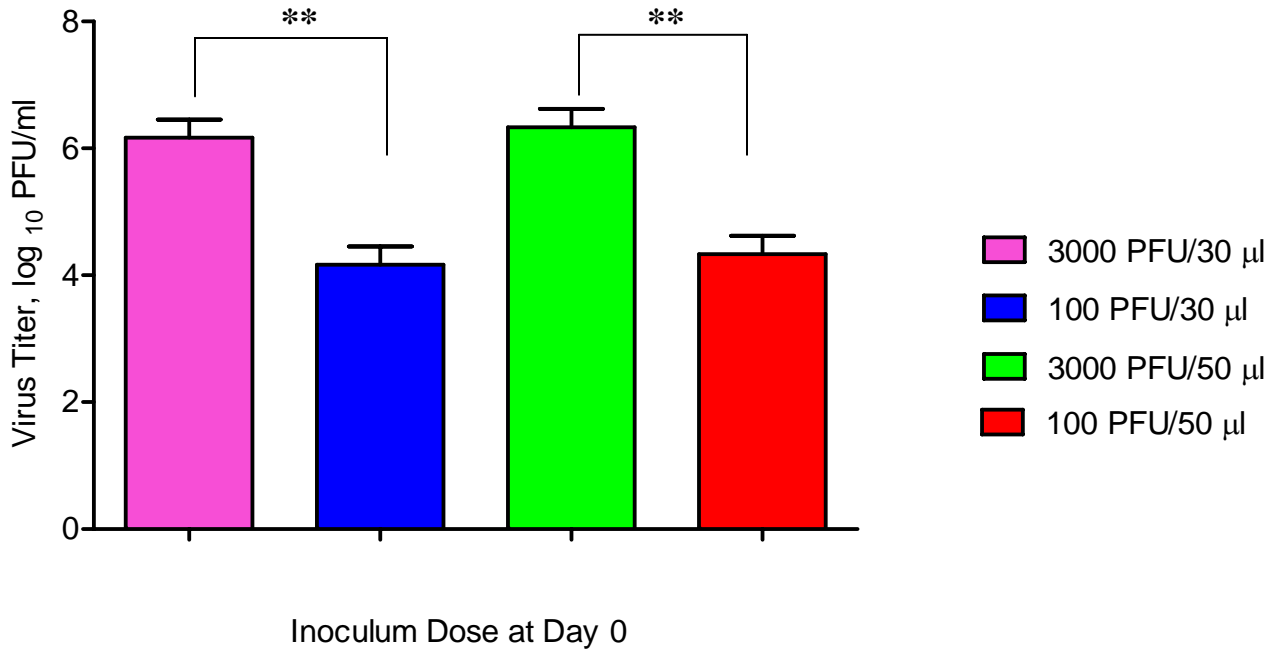
A modified plaque assay was used to quantitate viral titers from lung homogenates of Balb/c and C57/Bl mice inoculated at time 0 with 100 or 3000 PFU in 30 μ l or 50 μ l inoculum volumes. Figure 4.4.3 shows the viral titer at six days post infection for Balb/c mice and seven days post infection for C57/Bl mice. As shown in Figure 4.4.3, panel A, viral titers recovered from the lung tissue of Balb/c mice showed significant differences between animals that received a high or low viral load. This difference was present regardless of the viral inoculum volume. However, no significant difference was found between virus recovered from animals that received the same viral dose but were inoculated with different inoculum volumes. Figure 4.4.3, panel B, depicts results for C57/Bl mice. Similar to Balb/c mice, C57/Bl mice inoculated with 3000 PFU showed significantly higher viral titers than the ones inoculated with 100 PFU. A more significant difference was found between groups that were inoculated with a 50 μ l inoculum volume. There was no difference between the viral titers of the animals that received the same viral dose but were inoculated with different inoculum volumes.

Figure 4.4.4 shows significant differences between Balb/c and C57/Bl mice that received a 100 PFU (panel A) or 3000 PFU (panel B) inoculum dose in a 30 μ l or 50 μ l volume. In both cases the viral titers in Balb/c mice were significantly higher than the titers in C57/Bl mice. For both Balb/c and C57/Bl mice there was no significant difference between groups that received the same inoculum dose but were inoculated with different volumes.

Figure 4.4.3 Virus recovered from PVM challenged Balb/c and C57/Bl mice. A) Viral titers of Balb/c mice and B) Viral titers of C57/Bl mice. The mice were inoculated with 100 PFU or 3000 PFU of PVM strain 15 in a 30 μ l or 50 μ l inoculum volume. The titers of the lung homogenates were determined by modified plaque assay at six days post infection for Balb/c and seven days post infection for C57/Bl mice. Each value represents the average \pm one standard deviation (SD) of the mean for five mice per group. For Balb/c animals, the statistical significance was determined by unpaired Student t-test (** = $p < 0.002$), whereas for C57/Bl animals the statistical significance was determined by paired Student t-test (* $p < 0.03$, ** $p < 0.006$).

Figure 4.4.3

A)



B)

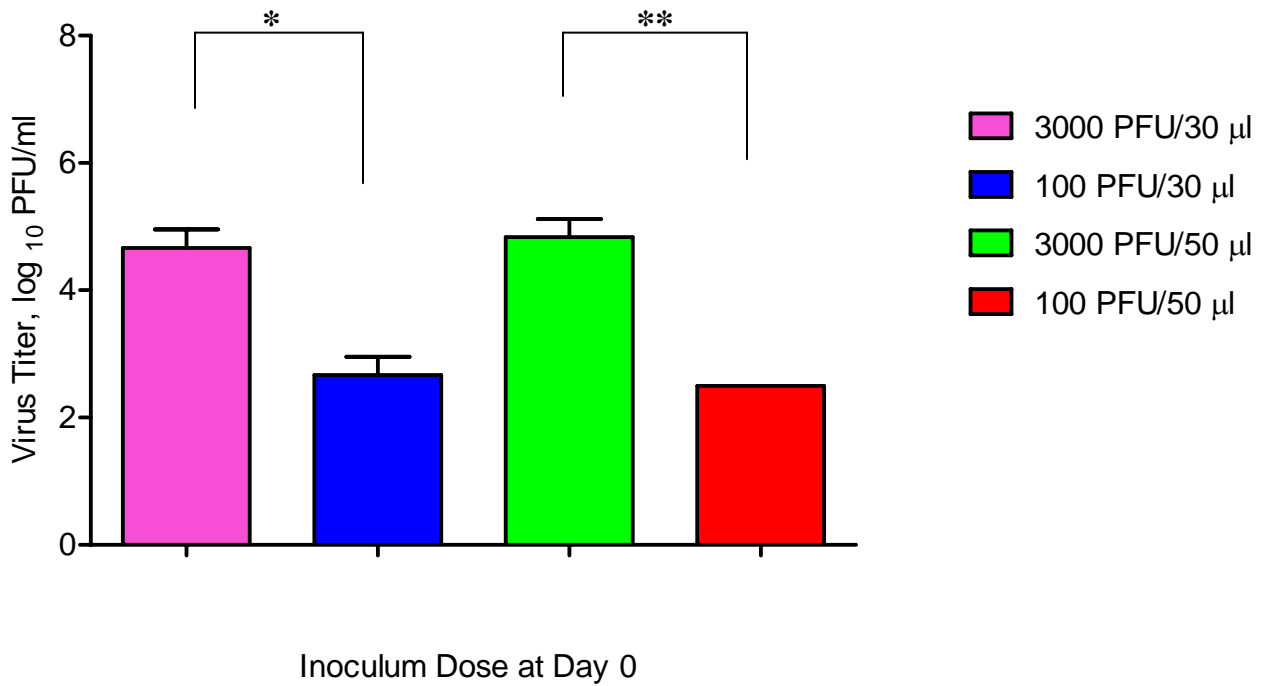
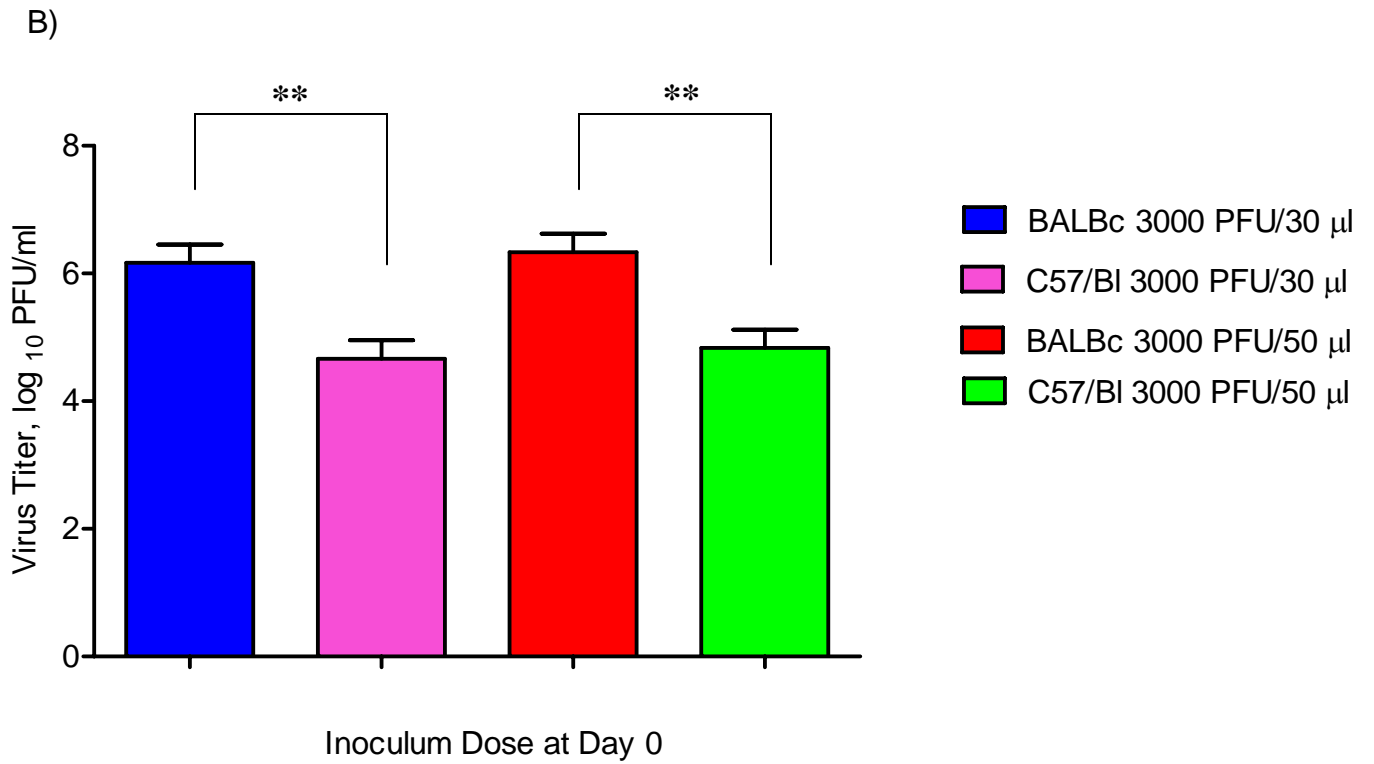
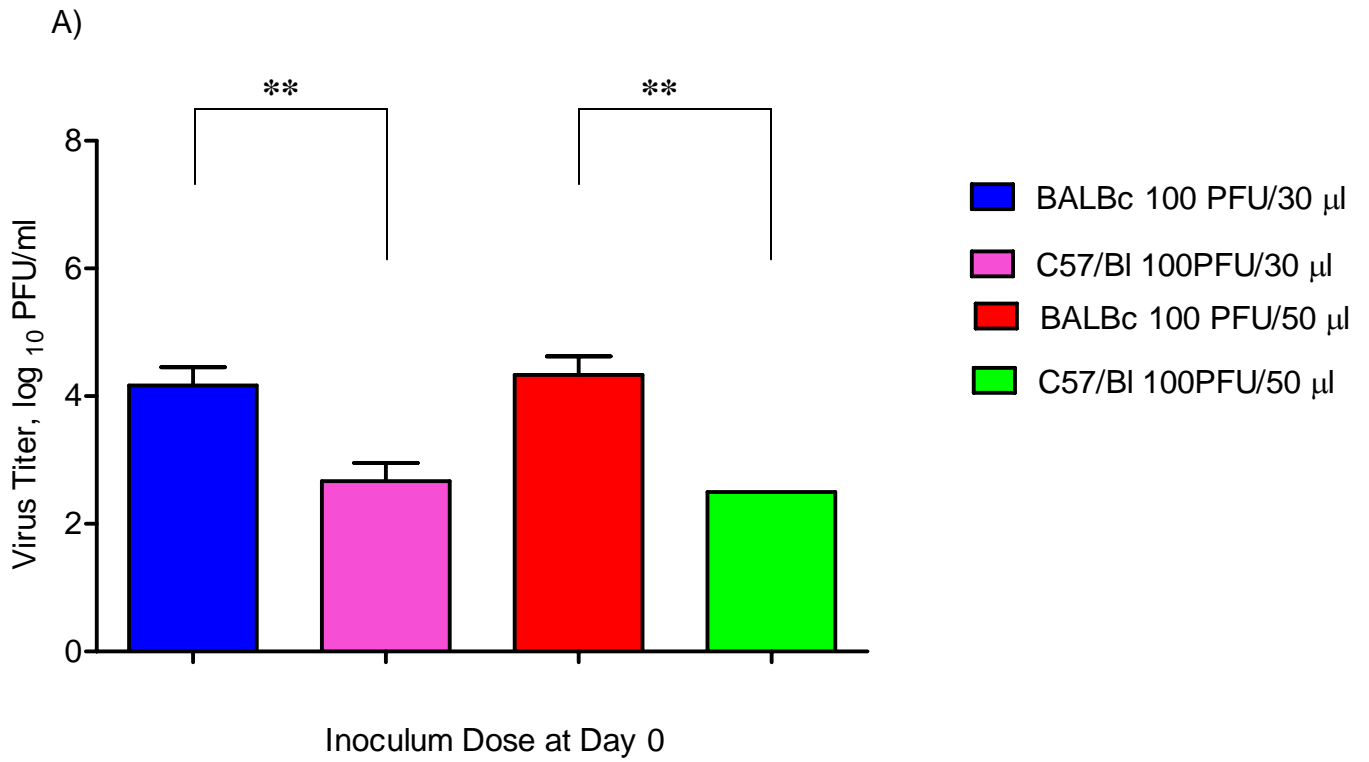


Figure 4.4.4 Comparison of viral titers between Balb/c and C57/Bl mice. A) Comparison of viral titers between Balb/c and C57/Bl mice inoculated with 100 PFU in a 30 μ l or 50 μ l inoculum volume. Each value represents the average \pm one standard deviation (SD) of the mean for five mice per group. For the 30 μ l inoculum volume, the statistical significance was determined by unpaired Student t-test (** = $p < 0.004$), and for the 50 μ l inoculum volume, the statistical significance was determined by paired Student t-test (** $p < 0.009$). B) Comparison of viral titers between Balb/c and C57/Bl mice inoculated with 3000 PFU in a 30 μ l or 50 μ l inoculum volume. Each value represents the average \pm one standard deviation (SD) of the mean for five mice per group. For the 30 μ l inoculum volume, the statistical significance was determined by unpaired Student t-test (** = $p < 0.004$), and for the 50 μ l inoculum volume, the statistical significance was determined by unpaired Student t-test (** $p < 0.004$).

Figure 4.4.4



4.5 In Vitro BM-DCs studies

Intrigued by the difference in susceptibility/resistance patterns to PVM infection between Balb/c and C57/Bl strain of mice, we wanted to examine the impact of a PVM infection on the phenotype and function of BM-DCs derived from the two strains. Two sets of *in vitro* experiments were done; one with Balb/c- and the other with C57/Bl-derived BM-DCs. Briefly, immature DCs at day five were cultured for 24 hours with PVM (MOI 5) or UV-PVM (MOI 5) and several functional and phenotypical assays were completed. Appropriate controls including medium only, BHK-21 cells and LPS (1µg/ml) were included in all experiments.

4.5.1. Confirmation of infection of BM-DCs with Pneumonia Virus of Mice by Western blot

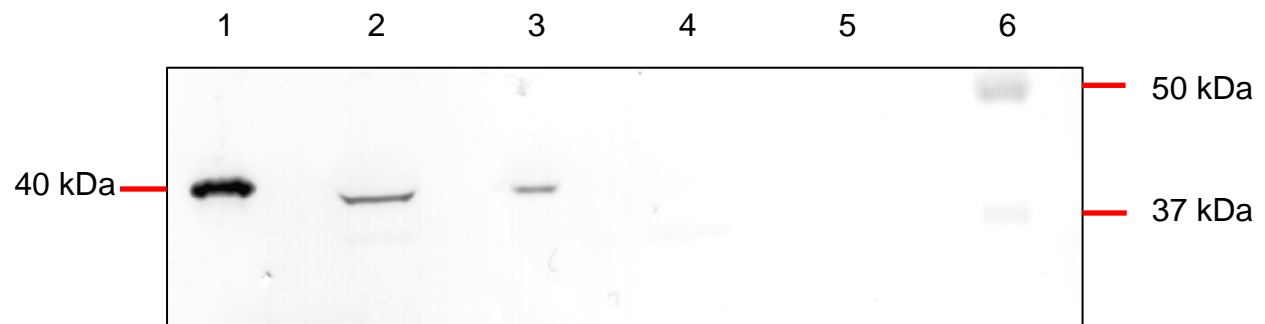
Before the evaluation of the effect of PVM infection on BM-DCs, we first wanted to confirm the ability of PVM to infect BM-DCs. Figure 4.5.1 shows the Western blot results for Balb/c (Panel A) and C57/Bl (Panel B) mice. Following 24 hours of incubation with PVM or UV-PVM, BM-DCs were examined for PVM N protein expression. PVM from ATCC stock 5×10^5 TCID₅₀ was used as a positive control. As shown in Figure 4.5.1 both Balb/c- and C57/Bl-derived BM-DCs cultured with PVM showed the presence of a protein with an apparent molecular weight size of ~40 kDa which corresponded to the size of PVM N protein (Panels A and B respectively). However, this band was absent in the BM-DCs cultured with UV-inactivated PVM. Since 24 hours post infection Western blot results from UV-PVM-treated BM-DCs did not show the presence of PVM-specific N protein, we concluded that progeny virus

could be the only source of N protein in PVM treated BM-DCs; indicating the ability of PVM to infect and replicate in BM-DCs.

Figure 4.5.1 The presence of PVM N protein in BM-DCs cultured for 24 hours with PVM or UV-inactivated PVM. Polyclonal rabbit PVM α -N antibody was used to confirm the expression of viral protein in A) Balb/c-derived BM-DCs cultured for 24 hours with PVM or UV-inactivated PVM and B) C57/Bl-derived BM-DCs cultured for 24 hours with PVM or UV-inactivated PVM. PVM from ATCC (2.4×10^3 PFU) was used as a positive control.

Figure 4.5.1 Western Blot

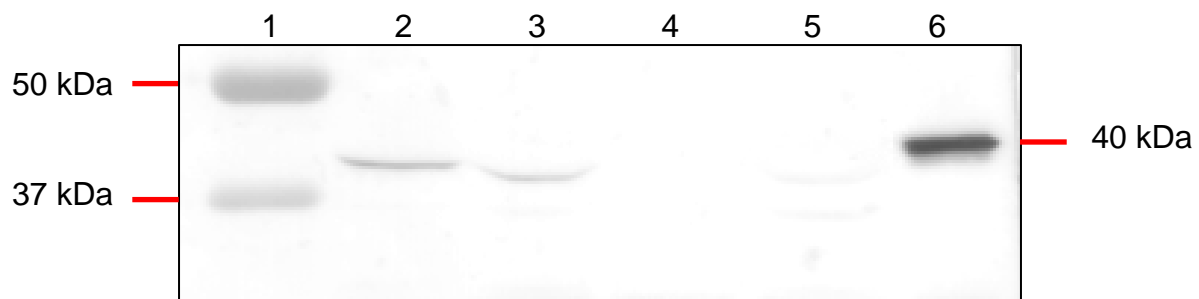
A) Balb/c



Legend

- 1 - ATTC PVM
- 2 - 20 μ l PVM-infected DC
- 3 - 7 μ l PVM-infected DC
- 4 - 20 μ l UV-inactivated PVM-infected DC
- 5 - 7 μ l UV-inactivated PVM-infected DC
- 6 - Protein standards

B) C57/Bl



Legend

- 1 - Protein standards
- 2 - 20 μ l PVM-infected DC
- 3 - 10 μ l PVM-infected DC
- 4 - 10 μ l UV-inactivated PVM-infected DC
- 5 - 20 μ l UV-inactivated PVM-infected DC
- 6 - ATTC PVM

4.5.2. Phenotypical changes of Pneumonia Virus of Mice infected BM-DC's

To analyze whether PVM infection alters cell surface expression of markers involved in antigen presentation and T cell – DC interaction, immature BM-DCs cultured for 24 hours with PVM (MOI 5), UV-PVM (MOI 5), an equivalent amount of BHK-21 cells, LPS (1 μ g/ml) or medium only were analyzed for expression of several surface molecules. These included major histocompatibility complex (MHC II) and co-stimulatory molecule (CD40 and CD86) markers. Additionally, the cells were stained with a CD11c marker and the percentage of double-positive cells was used for analysis. Since there was a report that pro-B cells show a capacity to express BMDC-related CD11c marker when cultured with GM-CSF (26), the expression of the B lineage lymphocyte marker CD19 was also included in order to ensure that CD11c-positive BM-DCs were not contaminated with high numbers of B cells.

Figure 4.5.2.1 represents flow-cytometry results for the expression of MHC II and co-stimulatory markers in Balb/c (Panel A) or C57/Bl (Panel B) BM-DCs. As shown in Figure 4.5.2.1 (Panel A), there were no statistically significant differences in the expression of MHC II, CD40 or CD86 surface markers on PVM-infected DCs compared to UV-PVM and BHK-21 treated DCs. The LPS group, which served as the positive control, showed signs of DC maturation based on a significant increase in the expression of MHC II, CD40 and CD86 surface markers compared to the medium control group. In the case of BM-DC cultures derived from C57/Bl mice (Panel B), there was no statistically significant difference in expression of MHC II, CD86 and CD40 DC maturation surface markers between the PVM, UV-PVM and BHK-21 groups. Similar to what was observed for Balb/c BM-DCs, C57/Bl-derived DCs treated with LPS showed signs of maturation. CD19 expression was negligible in both Balb/c and C57/Bl derived

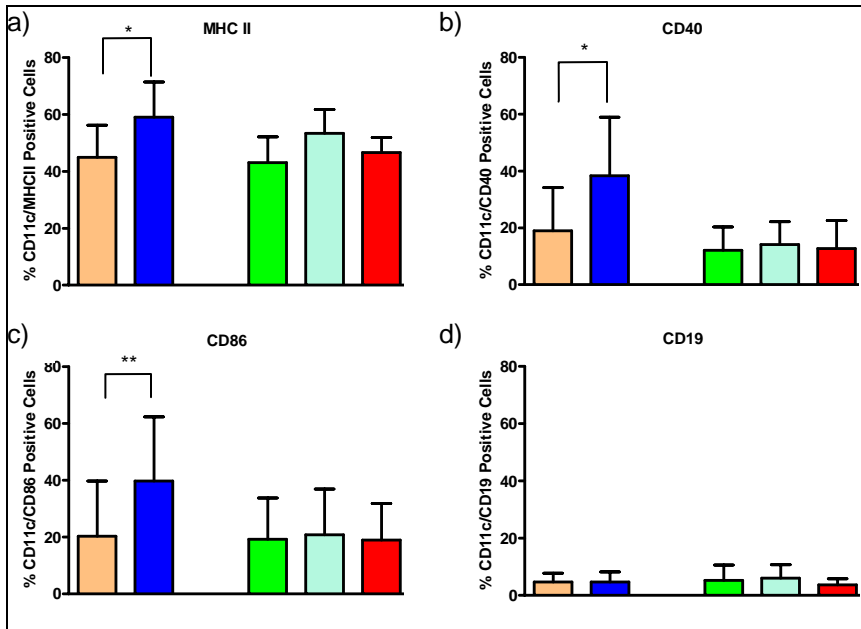
BM-DCs. Figure 4.5.2.2 represents dot-plot FACS results from one representative experiment out of three.

When compared, there was no difference in expression of MHC II, CD40, CD86 and CD19 surface markers between the BM-DCs generated from the two strains of mice (Figure 4.5.2.3). We also examined the mean fluorescent intensities for these markers, and no difference was found in expression between the tested groups (data not shown). Based on these observations we concluded that, under these experimental conditions, PVM infection of BM-DCs did not change expression of markers associated with DC maturation.

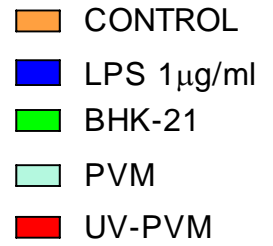
Figure 4.5.2.1 Phenotypic changes of PVM-infected BM-DCs, measured by the expression of costimulatory surface markers. Panel A) Balb/c- and B) C57/Bl- derived BM-DCs were cultured on day five with PVM (MOI 5), UV-inactivated PVM (MOI 5), LPS (1 μ g/ml), an equivalent amount of BHK-21 cells or medium. FACS analysis was performed 24 hours later. Cells were stained with CD11c PE-labeled specific antibodies, and FITC-labeled antibodies specific for MHC II, CD80, CD40 or CD19. Bars represent the percentage of double positive cells \pm one standard deviation (SD) of the mean from three independent experiments. Two types of statistical analysis were done. First, the difference between positive and negative control was evaluated using two-tailed student T test (* $p < 0.05$) (** $p < 0.01$). Significant differences between PVM, UV-PVM and BHK-21 groups were evaluated using one-way ANOVA.

Figure 4.5.2.1

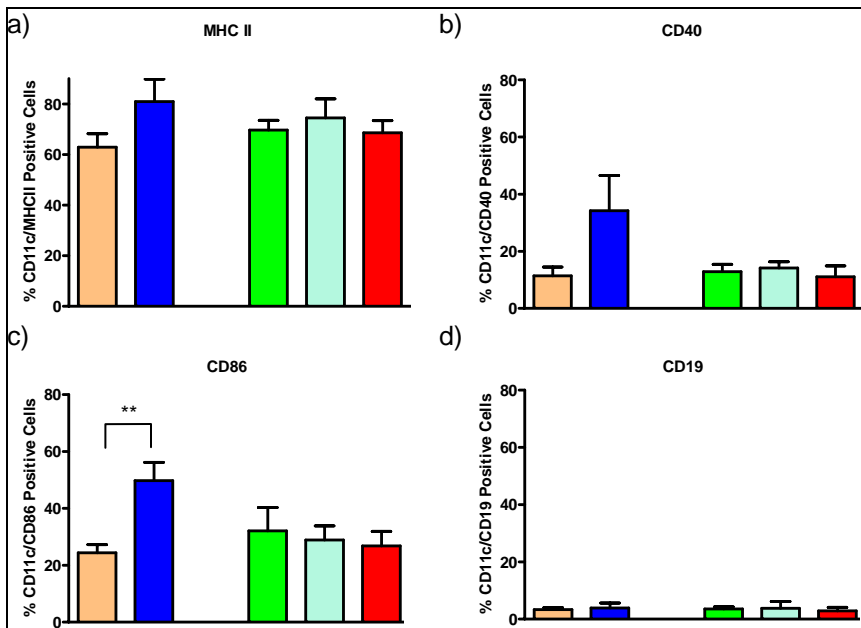
A) Balb/c



Legend



B) C57/Bl



Legend

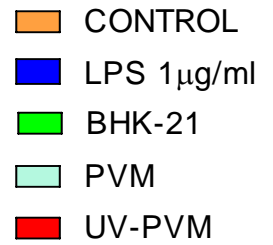
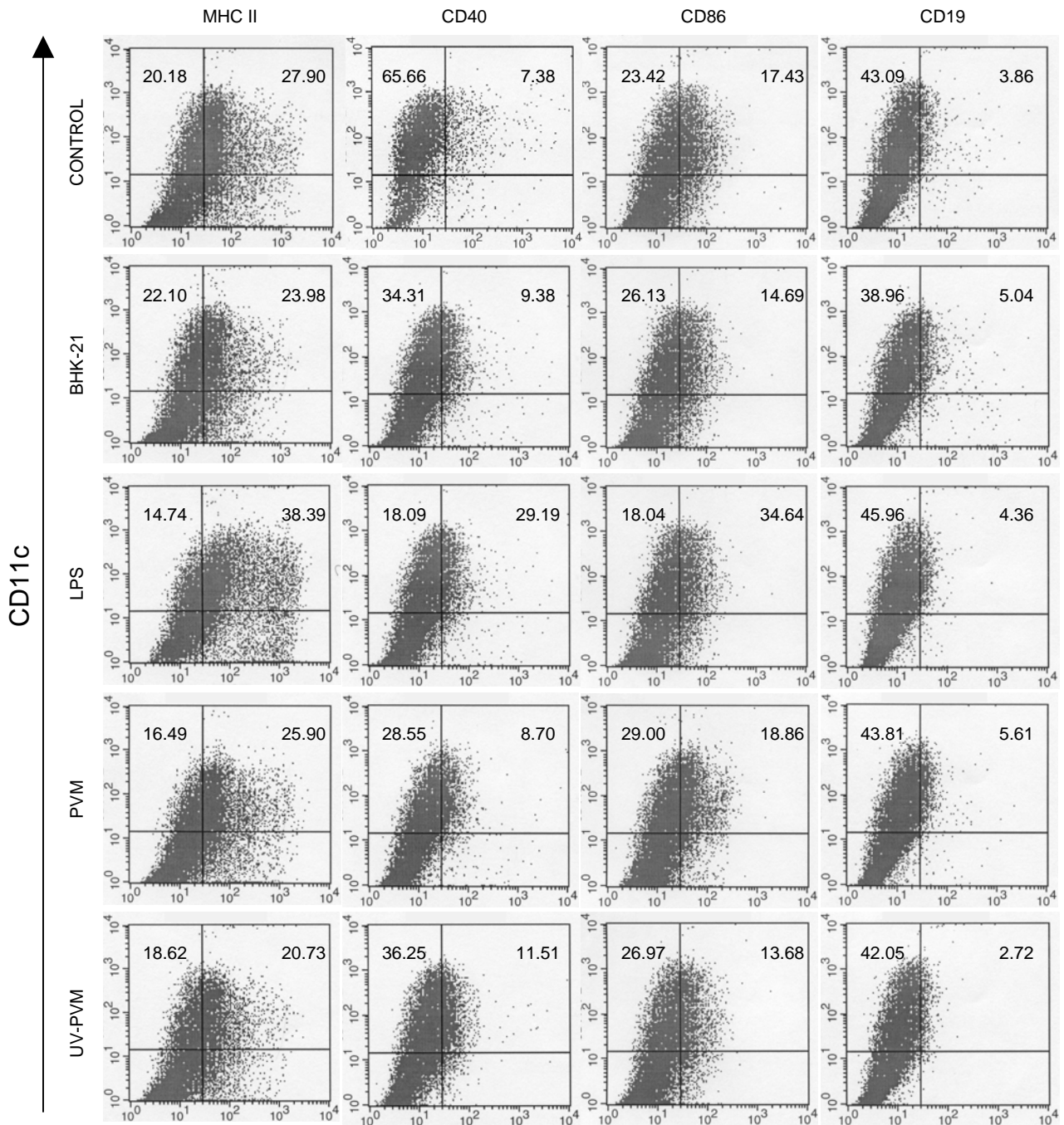


Figure 4.5.2.2 Phenotypic changes of PVM infected BM-DCs measured by the expression of costimulatory surface markers. A) Balb/c- and B) C57/Bl-derived BM-DCs were cultured on day five with PVM (MOI 5), UV-inactivated PVM (MOI 5), LPS (1µg/ml), an equivalent amount of BHK-21 cells or medium. FACS analysis was performed 24 hours later. Cells were stained with CD11c PE-labeled specific antibodies, and FITC-labeled antibodies specific for MHC II, CD80, CD40 or CD19. Numbers within the dot plots represent the percentages of positive cells within the quadrants.

Figure 4.5.2.2

A) Balb/c



B) C57/BI

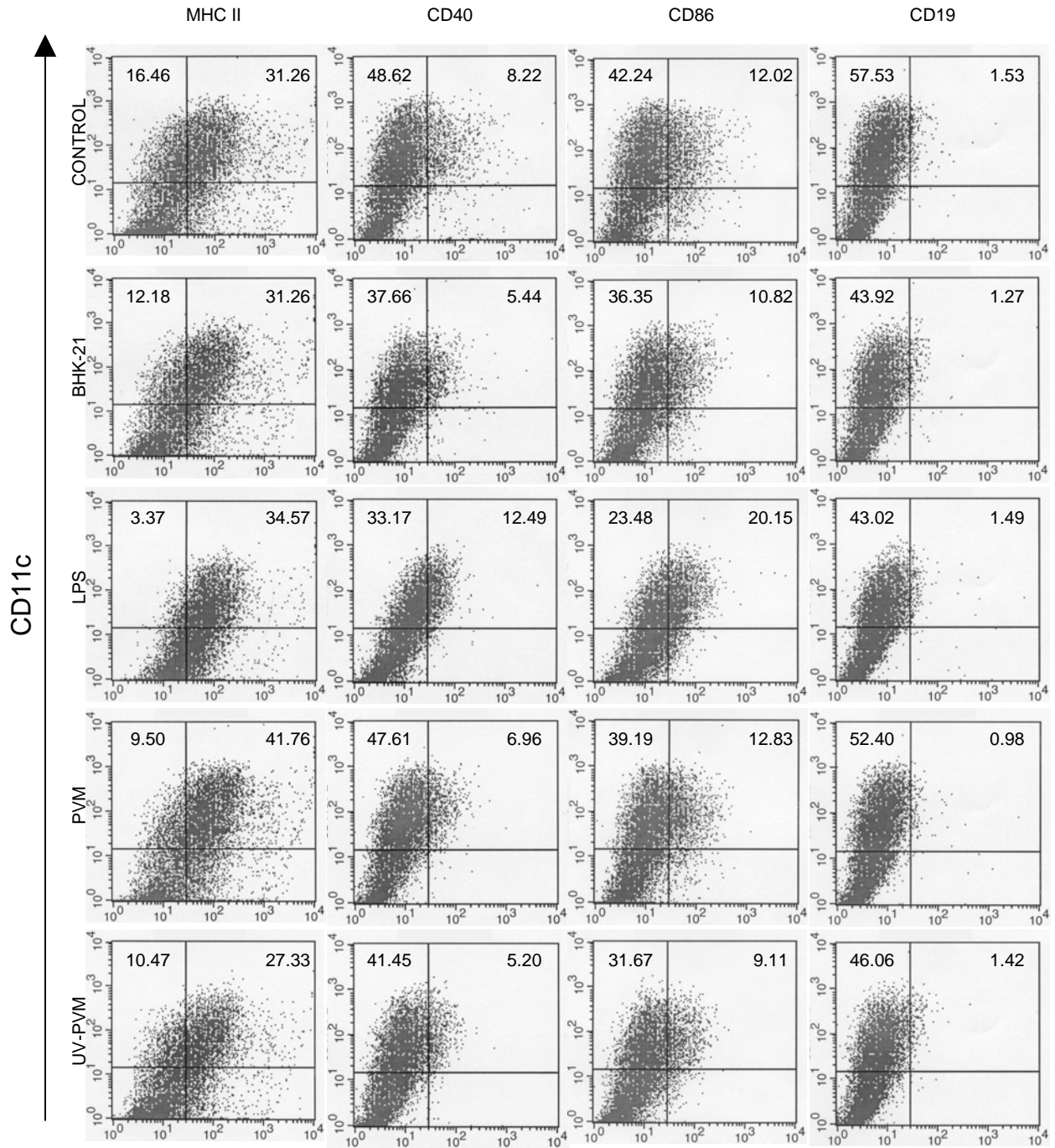
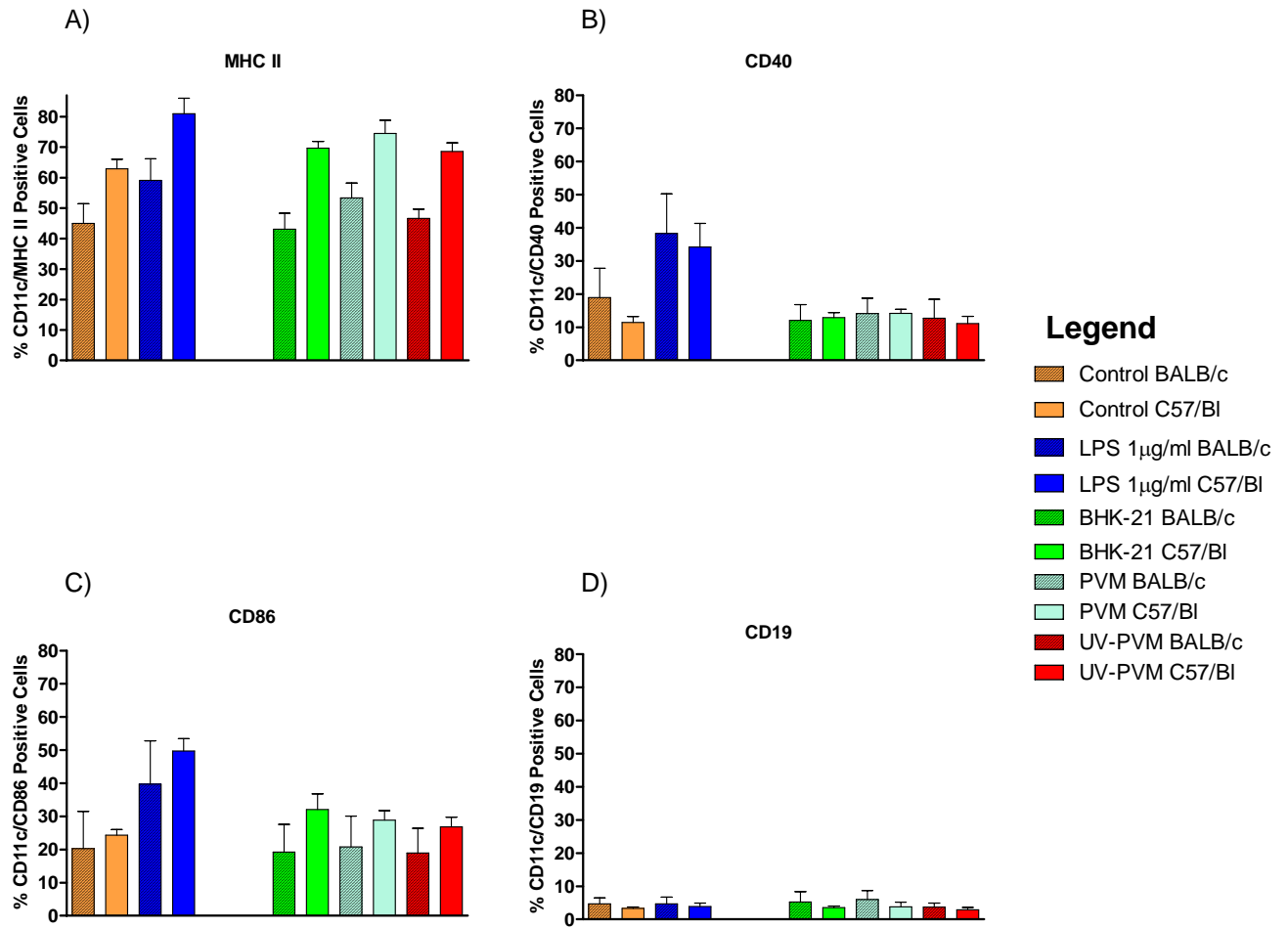


Figure 4.5.2.3 Comparison of the expression of costimulatory surface markers between Balb/c- and C57/Bl-derived BM-DCs cultured for 24 hours with PVM (MOI 5), UV-inactivated PVM (MOI 5), LPS (1µg/ml), equivalent amounts of BHK-21 cells or medium. Bars represent the percentage of double positive cells +/- one standard deviation (SD) of the mean from three independent experiments.

Figure 4.5.2.3



4.5.3. Functional changes of Pneumonia Virus of Mice infected BM-DC's

4.5.3.1. Endocytosis

Immature DCs capture antigen efficiently and then lose this capacity upon maturation. To evaluate how PVM infection influences the capacity of DCs to take up soluble antigens, we decided to test the ability of our differently treated BM-DCs to take up FITC-Dextran from the medium.

Immature BM-DCs derived from Balb/c and C57/Bl were cultured for 24 hours with PVM (MOI 5), UV-PVM (MOI 5), an equivalent amount of BHK-21 cells, LPS (1 μ g/ml) or medium only. After 24 hours, cells were cultured with 1 μ g/ml of FITC-Dextran incubated for 30 minutes on ice or at 37 $^{\circ}$ C, and analysed by Flow-cytometry (Figure 4.5.3.1.1). Balb/c-derived BM-DCs cultured with PVM, UV-PVM or BHK-21 showed no statistically significant decrease in their ability to take up FITC-Dextran (Panel A). In contrast, a significant decrease in the ability to take up FITC-Dextran was found in the LPS group compared to the medium control group. Figure 4.5.3.1.1 (Panel B) depicts the observation for the C57/Bl-derived BM-DCs. In the case of C57/Bl-derived BM-DCs, the LPS group also showed a significant decrease in FITC-Dextran uptake compared to the medium control group. In contrast, statistically significant differences between BM-DCs cultured with PVM, UV-PVM or BHK-21 were not found. We also analyzed MFI values for these experimental groups, and a similar trend between groups was found (data not shown).

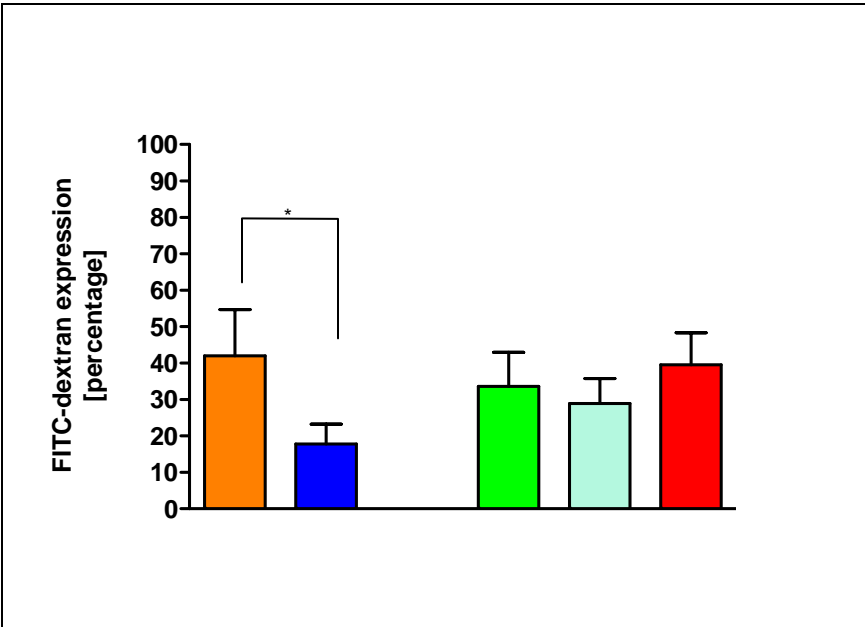
Furthermore, a comparison of the capacity of the individual experimental groups to take up FITC-Dextran from culture medium between the two mouse strains also failed to show any significant differences (Figure 4.5.3.1.2).

Overall, these results suggest that PVM infection of BM-DCs tended to induce a difference in endocytosis, which could be perceived as a sign of change in functional capacity of BM-DCs associated with maturation; however, the extent of these changes were not significant. Thus, we were not able to demonstrate that productive PVM infection of BM-DCs has a biologically significant impact on the capacity of BM-DCs to take up soluble antigens.

Figure 4.5.3.1.1 Uptake of FITC-labeled dextran from medium by BM-DCs. A) Balb/c- and B) C57/Bl-derived BM-DCs were cultured on day five with PVM (MOI 5), UV-inactivated PVM (MOI 5), LPS (1 μ g/ml), an equivalent amount of BHK-21 cells or medium. Cells cultured for 24 hours were subsequently cultured with FITC-dextran for 30 minutes and the percentage of cells having successfully taken up FITC-dextran was determined by FACS analysis. Bars represent the percentage of double positive cells \pm one standard deviation (SD) of the mean from three independent experiments. Two types of statistical analysis were done. First, the difference between positive and negative control was evaluated using a two-tailed student T test (* $p < 0.05$). Significant differences between PVM, UV-PVM and BHK-21 groups were evaluated using a one-way ANOVA.

Figure 4.5.3.1.1

A) BALB/c



B) C57/BI

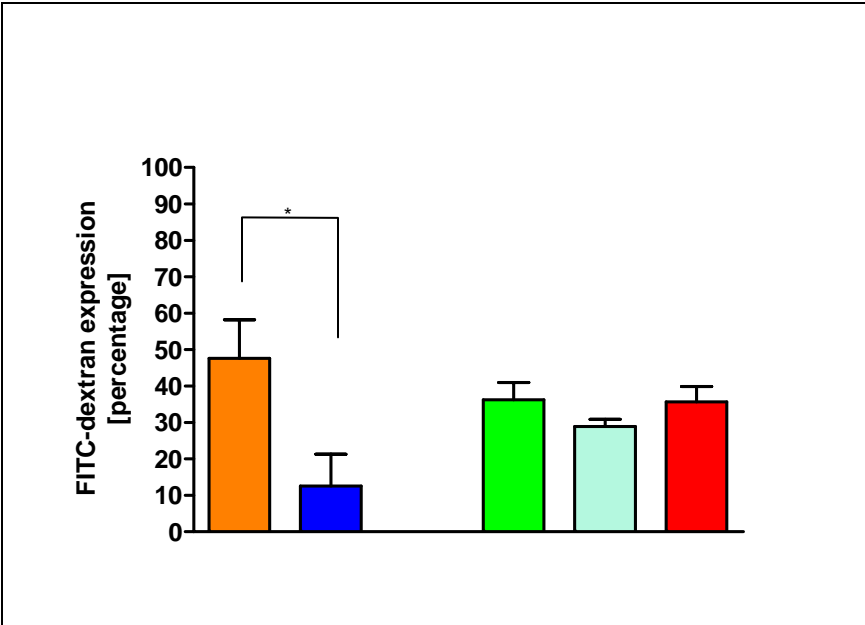


Figure 4.5.3.1.2 Comparison of the uptake of FITC-labeled dextran from medium by BM-DCs between Balb/c and C57/Bl mice. BM-DCs were cultured for 24 hours with PVM (MOI 5), UV-inactivated PVM (MOI 5), LPS (1 μ g/ml), an equivalent amount of BHK-21 cells or medium. Cells cultured for 24 hours were subsequently cultured with FITC-dextran for 30 minutes and the percentage of cells having successfully taken up FITC-dextran was determined by FACS analysis. Bars represent the percentage of double positive cells +/- one standard deviation (SD) of the mean from three independent experiments.

Figure 4.5.3.1.2

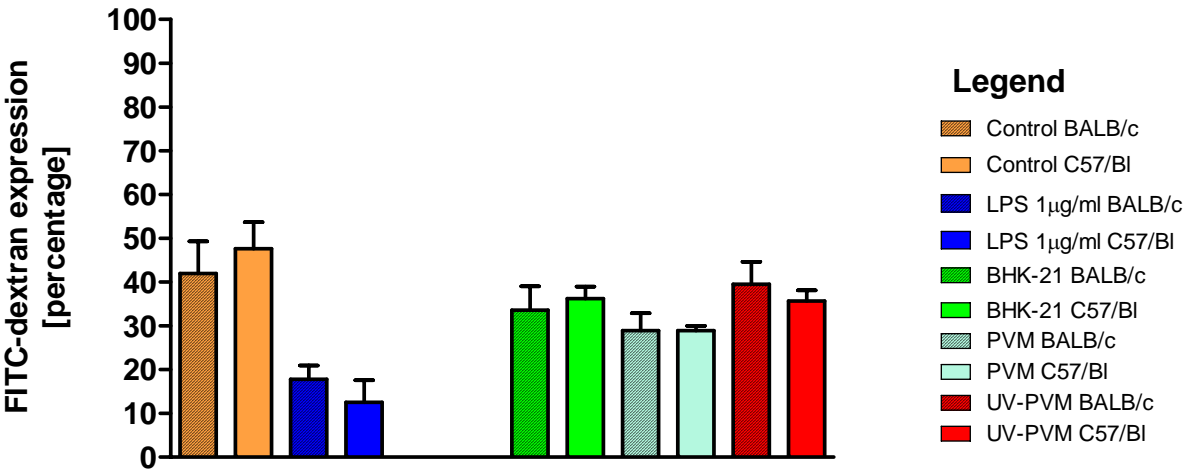
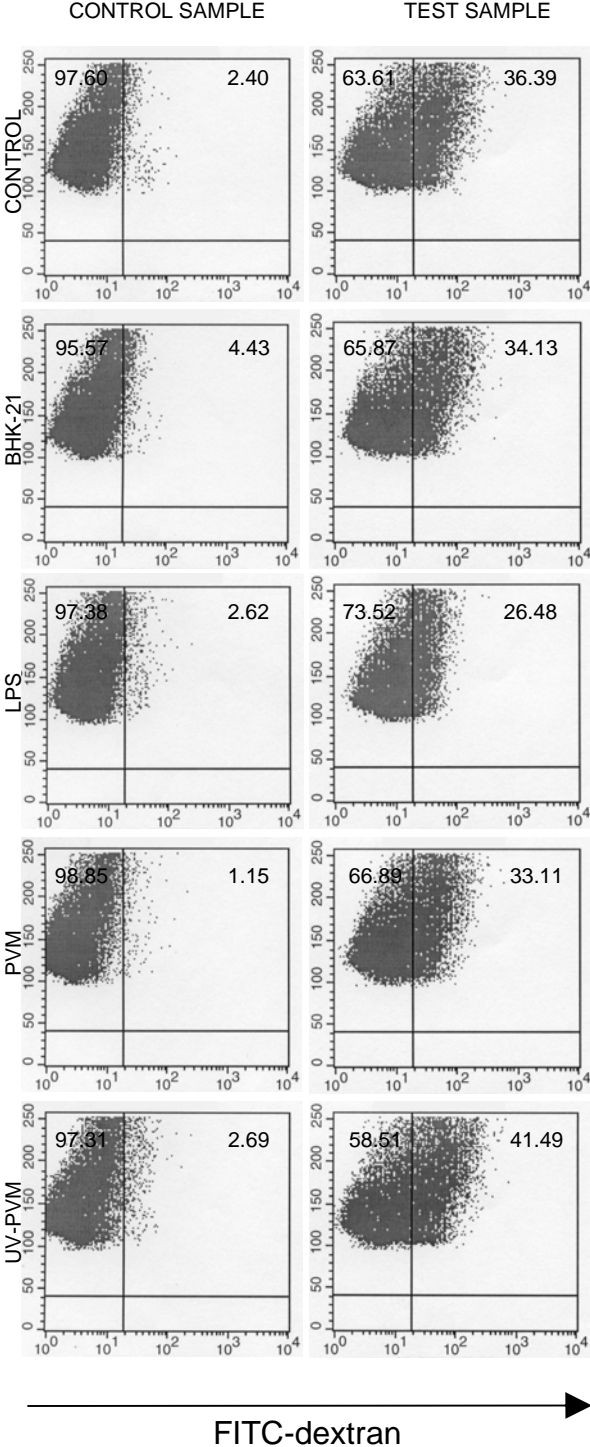


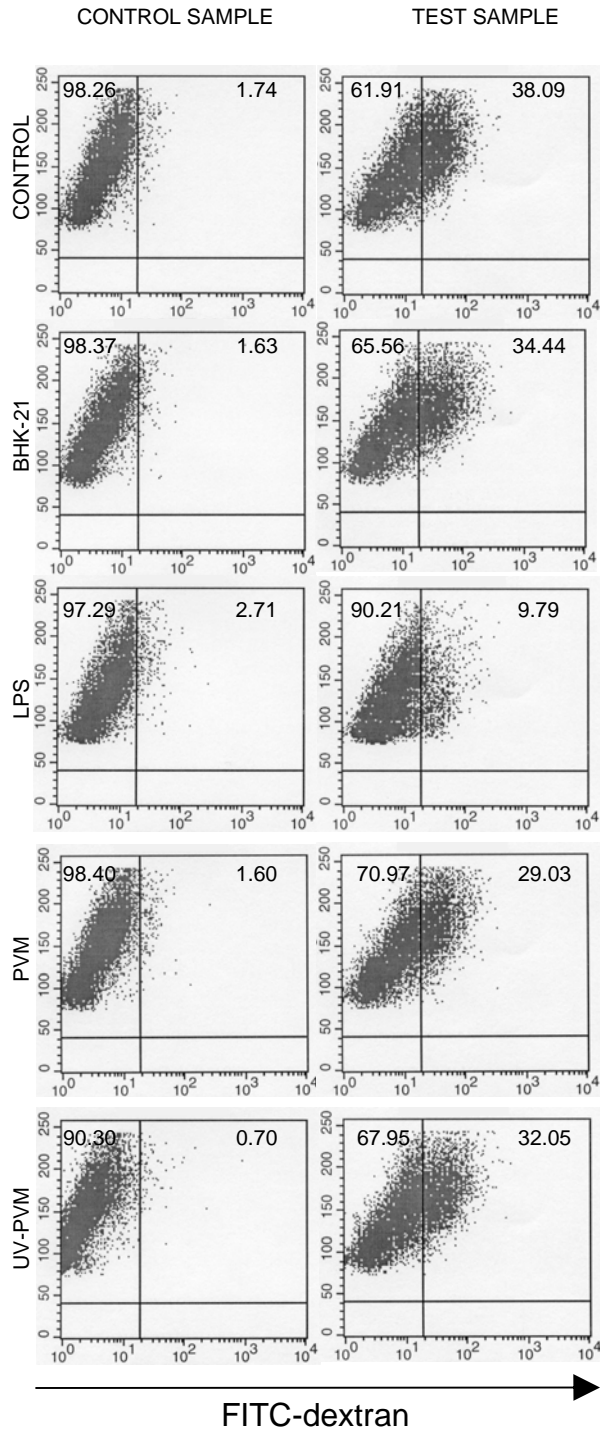
Figure 4.5.3.1.3 Influence on the uptake of FITC-labeled dextran from medium by BM-DCs. A) Balb/c- and B) C57/Bl-derived BM-DCs were cultured on day five with PVM (MOI 5), UV-inactivated PVM (MOI 5), LPS (1µg/ml), an equivalent amount of BHK-21 cells or medium. Cells cultured for 24 hours were subsequently cultured with FITC-dextran for 30 minutes either on ice (Control sample) or at 37⁰ C (Test sample). The percentage of cells having successfully taken up FITC-dextran was determined by FACS analysis. Numbers within the dot plots represent the percentages of positive cells within the quadrants.

Figure 4.5.3.1.3

A) Balb/c



B) C57/BI



4.5.3.2 Mixed Lymphocyte reaction

DCs increase their antigen presentation capabilities upon maturation due to up-regulation of MHC class I and II and co-stimulatory molecules on their surface. Thus, their ability to stimulate allogeneic lymphocytes reflects their state of maturity.

Figure 4.5.3.2.1 shows C57/Bl T cell proliferation induced by Balb/c derived BM-DCs exposed to various treatments. Panels A and B depict representative findings at days three and five post infection. A clear dose-dependant reduction in T cell proliferation is seen both at day three and day five, with more pronounced differences at day five.

Since the DC : T cell ratio of 1:10 proved to be the most suitable ratio for comparison between treatment groups, we used this result for further analysis. Panels C and D in Figure 4.5.3.2.1 show significant differences in T cell proliferation induced by different DC treatments. On day three (Panel C), no significant differences in the extent of T cell proliferation between PVM, UV-PVM and BHK-21 groups were found. Similarly, there was no significant increase in T cell proliferation in the LPS-treated group, which served as our positive control, compared to the medium control group at this time point. However, on day five (Panel D), there was a statistically significant decrease in the extent of T cell proliferation in the PVM group compared to the BHK-21 group. Unfortunately, the PVM-treated group did not show a significant decrease in T cell proliferation compared to the UV-PVM group.

In the case of C57/Bl-derived BM-DCs (Figure 4.5.3.2.2) the same dose-dependant decrease in T cell proliferation could be seen both on day three and day five (Panels A and B respectively). With regards to the DC : T cell ratio of 1: 10, somewhat different results compared to those found for Balb/c-derived BM-DCs were found. On day three, there was no significant

difference in T cell proliferation between PVM, UV-PVM and BHK-21 treated groups. Additionally, there was no significant difference in the level of T cell proliferation when LPS-treated and medium control groups were compared. On day five (Panel D), even though the LPS-treated group appeared to show an increase in T cell proliferation compared to other treatment groups, no biologically significant differences were demonstrated.

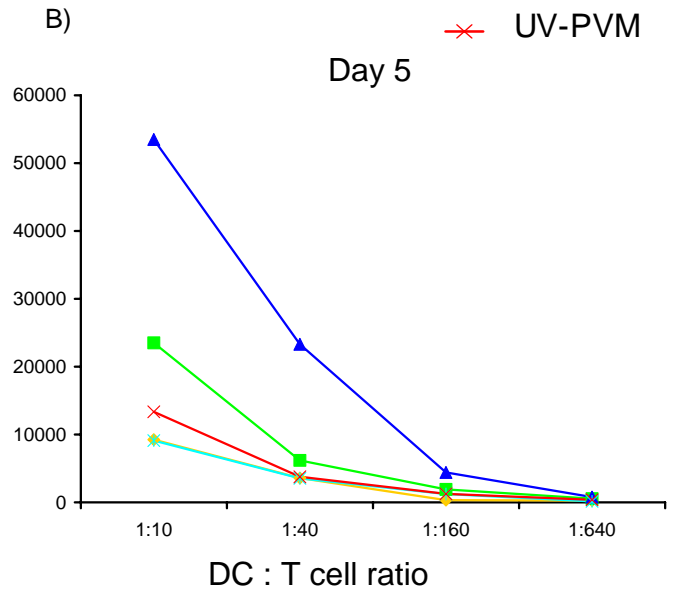
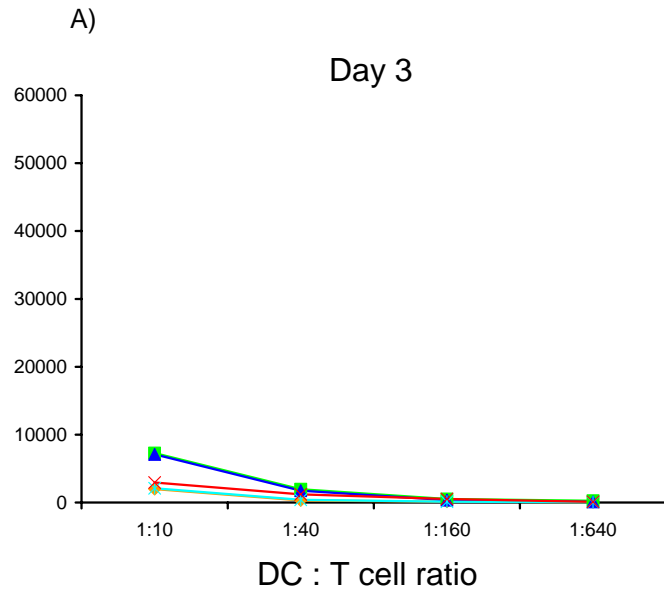
When compared, the ability of Balb/c- and C57/Bl-derived BM-DC's to induce naïve T cell proliferation on day three did not show any significant differences in any of the test groups (Figure 4.5.3.2.3).

Figure 4.5.3.2.1 Induction of naïve T cell proliferation by Balb/c BM-DCs subjected to different treatments. Allogeneic MLR was performed by culturing different numbers of irradiated BM-DCs from Balb/c mice (stimulatory cells) with a constant number (2×10^5 /well) of C57/Bl derived T cells (responding cells). Eighteen hours before harvesting, cells were pulsed with [methyl- ^3H] thymidine. Panels A and B - uptake of [methyl- ^3H] thymidine (c.p.m.) on days three and five. Panels C and D - Representative results for [methyl- ^3H] thymidine (c.p.m.) uptake on days three and five, derived from three independent experiments. Two types of statistical analysis were done. First, the difference between positive and negative control was evaluated using a two-tailed student T test (* $p < 0.05$). Significant differences between PVM, UV-PVM and BHK-21 groups were evaluated using one-way ANOVA (* $p < 0.03$).

Figure 4.5.3.2.1

Legend

- Control
- BHK-21
- ▲— LPS 1 μ g/ml
- *— PVM
- ×— UV-PVM



Legend

- Control
- LPS 1 μ g/ml
- BHK-21
- PVM
- UV-PVM

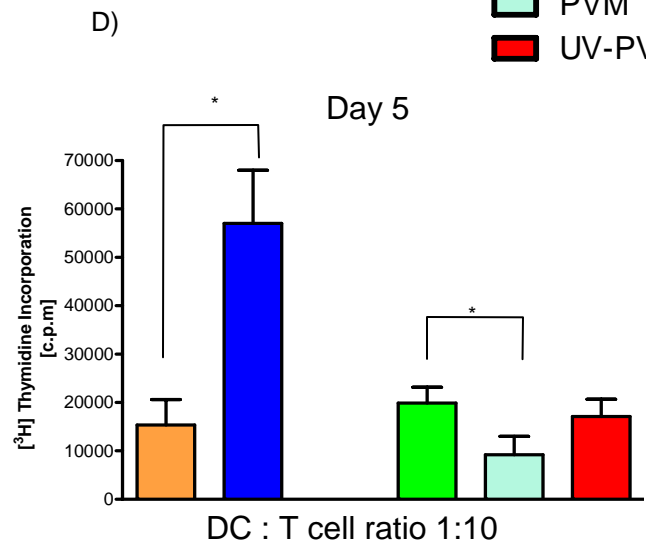
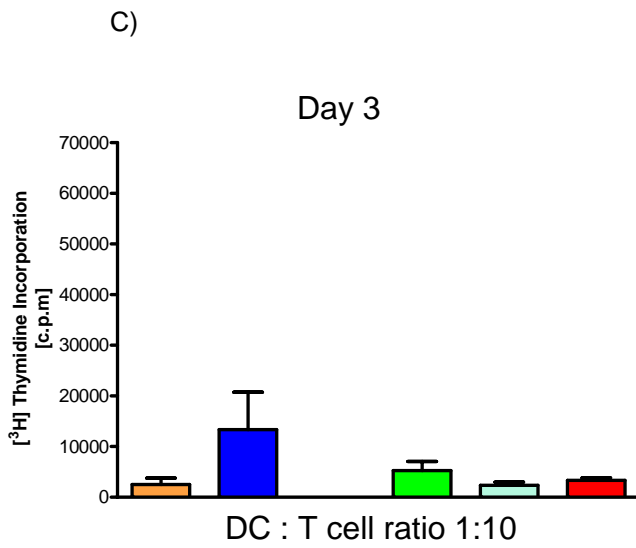


Figure 4.5.3.2.2 Induction of naïve T cell proliferation by C57/Bl BM-DCs subjected to different treatments. Allogeneic MLR was performed by culturing different numbers of irradiated BM-DCs from Balb/c mice as a stimulatory cells and constant number (2×10^5 /well) of Balb/c derived T cells as a responding cells. Eighteen hours before harvesting, cells were pulsed with [methyl- ^3H] thymidine. Panels A and B - uptake of [methyl- ^3H] thymidine (c.p.m.) on days three and five. Panels C and D - Representative results for [methyl- ^3H] thymidine (c.p.m.) uptake on days three and five, derived from three independent experiments. Two types of statistical analysis were done. First, the difference between positive and negative control was evaluated using a two-tailed student T test. Significant differences between PVM, UV-PVM and BHK-21 groups were evaluated using one-way ANOVA.

Figure 4.5.3.2.2

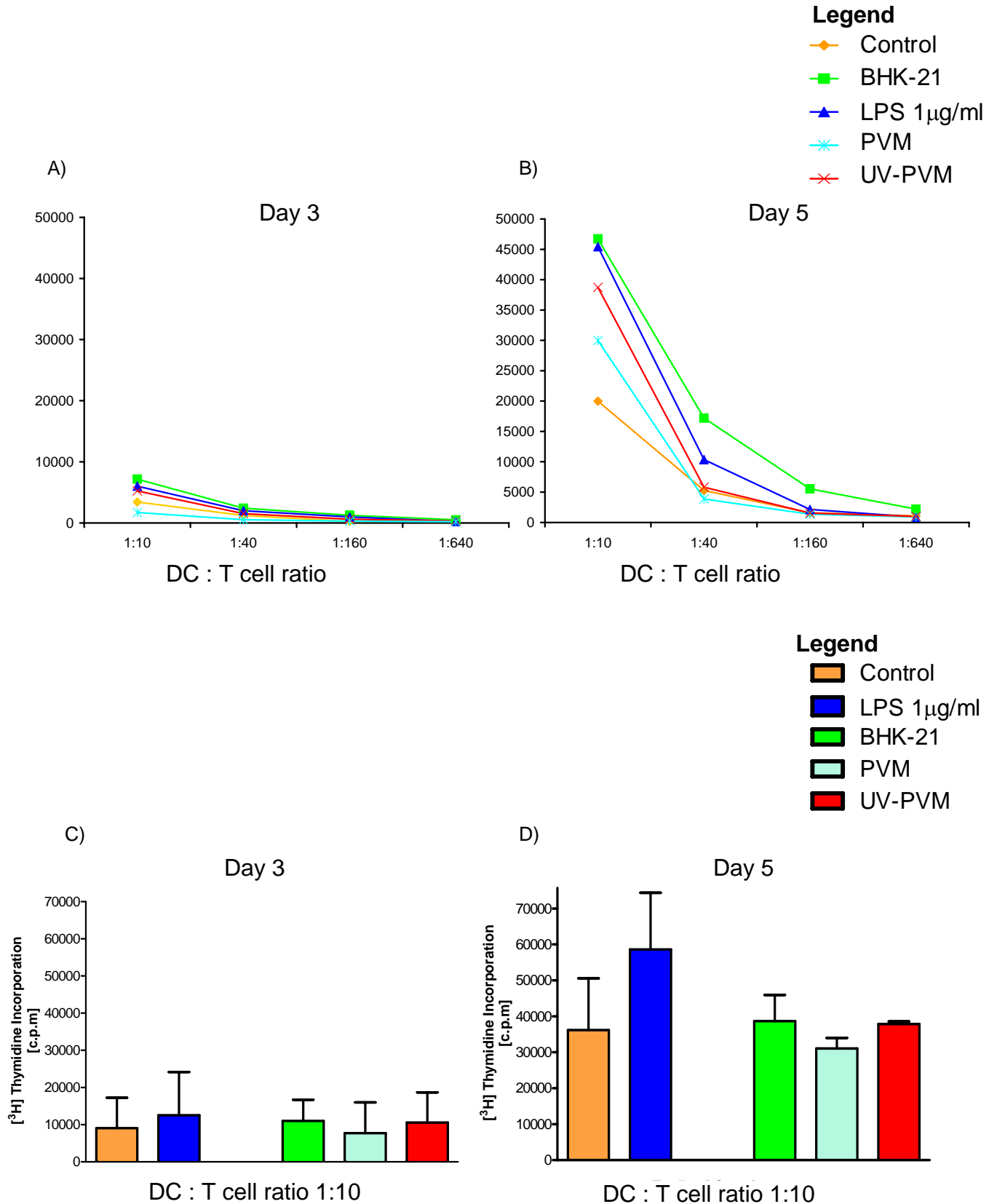
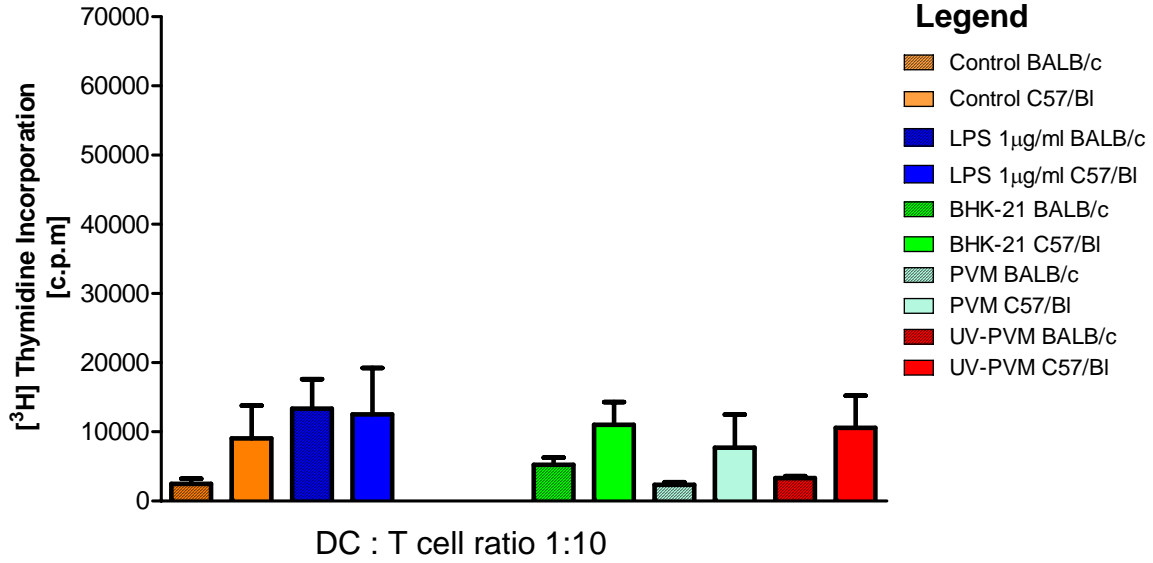


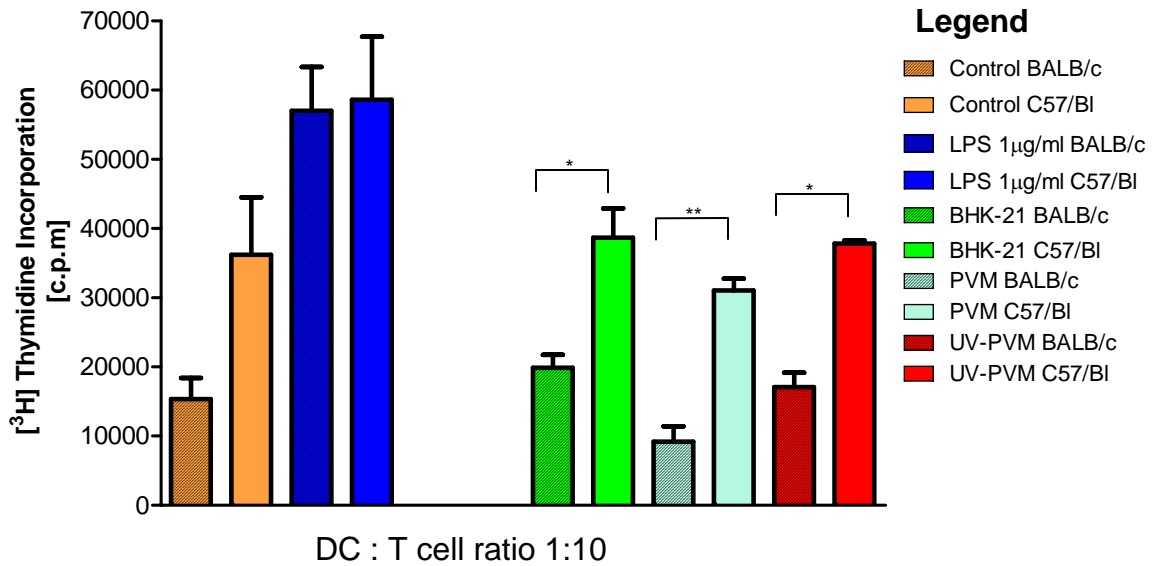
Figure 4.5.3.2.3 Comparison of the ability to induce naïve T cell proliferation in allogeneic MLR in Balb/c and C57/Bl BM-DCs subjected to different treatments. Uptake of [methyl-³H] thymidine (c.p.m.) was determined on day three (panel A) and day five (panel B). Cultures were prepared as previously described. Bars represent the [methyl-³H] thymidine (c.p.m.) uptake on day three and day five, +/- one standard deviation (SD) of the mean from three independent experiments. Significant differences between groups are as indicated (* p< 0.05), (** p< 0.01).

Figure 4.5.3.2.3

A) DAY 3



B) DAY 5



4.5.3.3 IL-12 p70 production by Pneumonia Virus of Mice infected BM-DCs

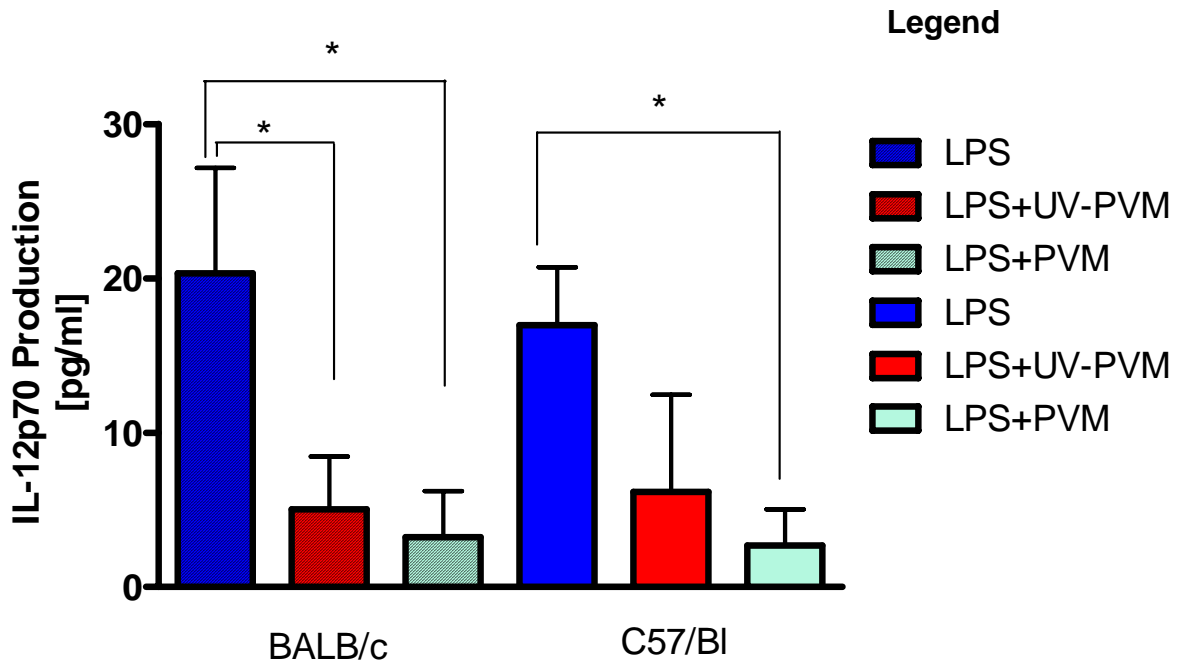
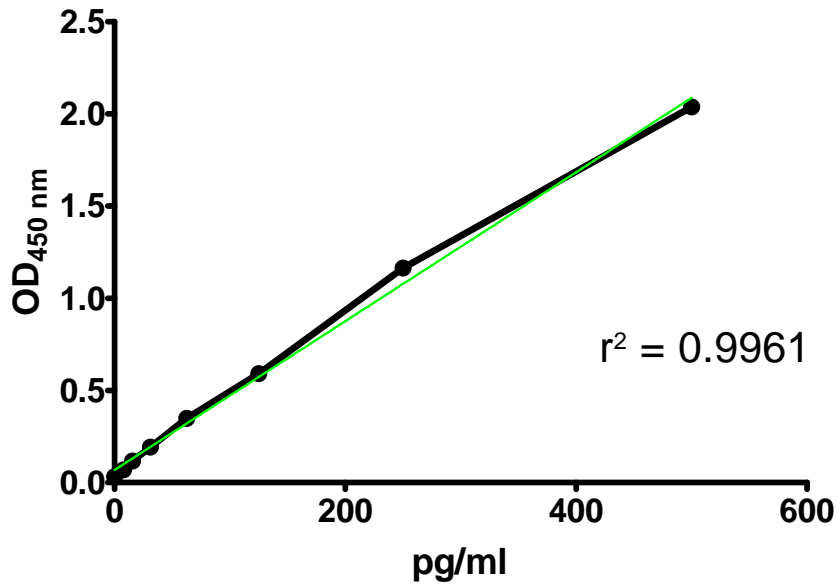
After uptake of an antigen in peripheral sites and migration toward the T cell areas in draining lymph nodes, mature DCs initially release IL-12 and induce the generation of effector T cells with a Th1 phenotype (167, 236). Since the Th1-type response is usually seen in viral infections and helps in the control and clearance of the virus, we wanted to take a closer look at the production of pivotal cytokines in a Th1-type response. Based on previously reported results for RSV-infected DCs, we anticipated that the amount of IL-12p70 might be too low to detect by presently available ELISA kits. We were also aware that LPS is a strong inducer of IL-12 production (94, 271). For these reasons, we cultured immature BM-DCs derived from two mouse strains with LPS (1 μ g/ml) only or in combination with PVM (MOI 5), or UV-PVM (MOI 5). Following a 24 hour incubation period, supernatants were collected and examined for the presence of IL-12p70 by ELISA. Figure 4.5.3.3 represents the expression of IL-12p70 in the Balb/c- and C57/Bl-derived DCs.

It was observed that even though the co-culturing of LPS-treated DCs with PVM or UV-PVM resulted in a significant decrease of IL-12p70 production compared to the LPS group ($p < 0.01$), no significant differences were found between the groups co-cultured with PVM or UV-PVM. When compared, IL-12p70 production by Balb/c- and C57/Bl-derived BM-DCs also did not show any significant differences between the test groups. In our preliminary studies we also tested the quantity of IL-12p70 production by BHK-21 treated BM-DCs. Our results did not show any significant difference between IL-12p70 production by BHK-21- and PVM-treated BM-DCs. Our findings exclude the involvement of IL-12p70 cytokine in the different functional responses of the PVM-infected BM-DCs between Balb/c and C57/Bl mice.

Figure 4.5.3.3 IL-12p70 production by Balb/c and C57/Bl BM-DCs subjected to different treatments. Balb/c- and C57/Bl-derived DCs were cultured on day five with PVM (MOI 5), UV-inactivated PVM (MOI 5), LPS (1µg/ml), an equivalent amount of BHK-21 cells or medium. After 24 hours, supernatants were collected and cytokine production was measured using standard ELISA assays. Bars represent the amount of IL-12p70 (pg/ml) production +/- one standard deviation (SD) of the mean from three independent experiments. Two types of statistical analysis were done. Significant differences between LPS, LPS+PVM, LPS+UV-PVM treated groups were evaluated using a one-way ANOVA (** p<0.01). Significant differences between different treatments of Balb/c- and C57/Bl-derived BM-DCs were evaluated using a two-tailed student T test.

Figure 4.5.3.3

Standard Curve



5.0 Discussion

5.1 Virus propagation and quantitation

Respiratory syncytial virus is the most common cause of lower respiratory tract disease including bronchiolitis and pneumonia in infants and young children (187). RSV has also been indicated as an important cause of severe lower respiratory tract infections in the immunocompromised and elderly (81, 129). Since immunity to RSV is short – lived, reinfection is frequent throughout life in all age groups, and the necessity for the development of safe and effective vaccines against RSV may be beneficial, especially in immune compromised individuals. Regardless of the enormous body of work that has been generated over the years, a clear understanding of all the mechanisms involved in the pathogenesis of severe RSV infections is still absent. In general, based on the research up to this point, it is clear that severe RSV infections develop as a result of a rather complex interplay between viral and host factors.

In an effort to scrutinize the contribution of factors involved in the pathogenesis of RSV, several animal models were used including mice, cotton rats, cattle and primates (74, 227, 257, 307). Unfortunately, none of these models successfully replicated all the clinical findings seen in humans infected with RSV, and their usefulness depended on the type of problem studied. In recent years, Cook *et al.* established the PVM infection model for severe RSV infection in the mouse (60). This mouse model replicated features of severe RSV disease in humans to a greater extent than the previously most often used mouse model. Most importantly, PVM is an innate rodent Pneumovirus pathogen and an initial inoculum size as low as 30 PFU was sufficient for establishment of an infection in its natural host.

Since Cook *et al.*, as well as other investigators used PVM strain J3666 in their work (60), our objective was to establish an *in vivo* animal model for RSV disease with the PVM strain available at ATCC: strain 15. Furthermore, being aware of the possible influence of the host genetic factors on the establishment and progression of disease, we also wanted to explore differences in the resistance/susceptibility patterns to PVM strain 15 in Balb/c and C57/Bl mice.

Since PVM is a highly thermolabile virus, inconsistent information regarding the optimal temperature for growth of PVM strain 15 was found in the literature. While some investigators reported propagation at 37 °C as most favorable (124), others argued that propagation of PVM at that temperature would lead to viral attenuation and loss of infectivity, and reported optimal propagation at 33 °C (291). Following viral propagation in BHK-21 cells at both 33 °C and 37 °C we have found that virus propagated at both temperatures showed similar replicative abilities *in vivo*. We also observed more prominent clinical signs in mice inoculated with PVM propagated at 37 °C. Slightly superior performance of a virus grown at 37 °C could be explained by the simple fact that the normal murine body temperature is also ~37 °C (195). Being already accommodated to this temperature during the propagation in BHK-21 cells, once inside the mouse lungs, virus replication did not have to be delayed due to the virus adjustment to the temperature of the host. In contrast, the somewhat delayed clinical disease in mice inoculated with PVM propagated at 33 °C was probably caused by the less effective initial replication of the virus in mouse lungs.

The next challenge encountered was the unavailability of an accurate method for PVM quantitation. As early as 1970, scientists in this field were struggling to find a reliable method to quantitate this virus (263). This problem has repeatedly been reported, and scientists in this field

tried to overcome this obstacle by implementation of standardized protocols for the use of quantitative reverse transcriptase PCR (qRT-PCR) assays (86).

In our work, we found that while BHK-21 cells used for standard plaque assays grow extremely fast even at the lower temperature and in nutritionally less favorable conditions, PVM-induced plaques develop slowly and show relatively indistinct borders. Thus, we modified the standard plaque assay method and used polyclonal antibody specific for PVM N protein as primary and FITC-labeled goat α -rabbit IgG as secondary antibodies in order to visualize viral plaques. This method showed reliable and most importantly reproducible results. It is also less time consuming and less expensive than quantitative reverse transcriptase PCR assays.

5.2 Susceptibility / resistance patterns to Pneumonia Virus of Mice infection in Balb/c and C57/Bl mice

It is a well established belief that a relationship exists between augmentation of disease caused by RSV and the type of T cell response mounted upon infection. Furthermore, studies performed with FI-RSV vaccines revealed that a Th2 type response was associated with more severe manifestations of RSV infection (155). Different susceptibility/resistance patterns to a pathogen exist for different mouse strains. In the case of Balb/c and C57/Bl mice, these patterns are well characterized for several pathogens including *Leishmania major* and adenovirus type 1 (113, 168, 260). Given that Balb/c and C57/Bl mice are the prototypic Th2 and Th1 responding strains, respectively, we anticipated that susceptibility to PVM infection and progression of disease in these two strains might be dissimilar. Since these possible differences should be taken

into account when interpreting the results from an animal model study, we wanted to establish and characterize PVM strain 15 infection in both of these strains.

To examine susceptibility of Balb/c mice to infection with PVM, eight week- old female Balb/c mice were intranasally inoculated with various doses of PVM in a 50 μ l inoculum. In this way we wanted to eliminate any differences between test groups related to sex, somatic growth or viral preparation. Our results demonstrated that Balb/c mice showed a high susceptibility to PVM infection even when only 30 PFU of PVM was used for inoculation. Two distinct patterns of body weight loss were observed. Groups that were inoculated with a high initial viral load showed first signs of body weight loss after three days post infection and lost \sim 15% of their preinoculation weight by day six post infection. In contrast, groups that received a low inoculum dose showed delayed weight loss that started on day four or five after infection, depending on the initial viral load, and lost \sim 10% of their preinoculation weight by day seven post infection. Changes in clinical signs were also similar among these two groups and showed a dose dependence. Macroscopic and microscopic pulmonary changes in all groups were comparable to those reported for PVM strain J3666-infected mice. The only difference was the absence of infiltration of eosinophils, which was reported elsewhere for Balb/c PVM J3666-infected mice (9, 76). This discrepancy in histological observations is probably due to the use of a more aggressive PVM strain by other groups. Most importantly, our histopathological observations, with the presence of inflammatory edema and multifocal regions of alveolitis, bronchiolitis and in some instances interstitial pneumonia, closely mimicked those in RSV-infected humans (79). Viral titers were significantly different between the groups, with higher viral titers recovered from the lungs of animals inoculated with a higher initial dose of virus. Furthermore, recovery of $\sim 3 \times 10^4$ PFU/ml from the mice inoculated with only 100 PFU/ml without a doubt confirmed an

excellent ability of PVM to replicate in Balb/c mouse lungs. This extremely useful feature of the PVM animal model is better appreciated when compared with RSV infection of mice which can be achieved only when the initial inoculum dose reaches 10^6 to 10^7 PFU while lung viral titers never reach the levels of the initial inoculum.

A somewhat different “picture” was present in our studies with C57/Bl mice. Our results clearly demonstrated that C57/Bl mice are also susceptible to PVM infection, but to a lesser degree than Balb/c mice. With regard to body weights, mice from the group inoculated with a high (3000 PFU/30 μ l) viral inoculum showed a decrease in body weight on day five post infection, which is late when compared to Balb/c mice inoculated with that same dose. Furthermore, C57/Bl mice in the 100 PFU/30 μ l group showed body weight loss on day seven post infection, which represents a three-day delay compared to Balb/c mice inoculated with the same dose. Interestingly, while Balb/c mice that received a 30 PFU/30 μ l inoculum showed body weight loss on day five post infection, which by day seven reached 10% of their weight, C57/Bl mice inoculated with the same dose did not show any decrease in weight throughout the ten day observation period. Furthermore, delayed and reduced clinical signs in C57/Bl mice compared to Balb/c mice were observed. Clinical signs recorded for C57/Bl mice confirmed the dose-dependent nature of the changes in physical appearance, as well as unprovoked and external stimulation behavior.

We also confirmed that the observed differences in the susceptibility to PVM infection between Balb/c and C57/Bl mice were due to strain differences and not inoculation volume used for these two studies. Our comparative study clearly showed that regardless of the initial inoculum volume, clear differences in susceptibility between these two strains existed. The same strain- and dose-dependent pattern of body weight loss was repeatedly observed, with Balb/c

mice showing loss in body weight at four or five days post infection, while C57/Bl mice inoculated with same viral load and inoculum size as Balb/c mice showed delayed weight loss which occurred on days five or seven post infection, depending on initial inoculum dose. Furthermore, C57/Bl mice inoculated with 30 PFU/50 μ l did not show any changes in body weight. Clinical observations for these two strains of mice also showed distinct differences. While PVM-infected Balb/c mice in all tested groups showed changes in physical appearance and unprovoked behavior by day five post infection, the PVM-infected C57/Bl mice, with the exception of the ones in the 3000 PFU/50 μ l group, stayed asymptomatic throughout the experiment.

In addition, viral titers from homogenized lung tissue were significantly different between Balb/c and C57/Bl infected mice. Viral titers of PVM-infected Balb/c mice were always significantly higher than the titers of C57/Bl mice, regardless of the initial inoculum dose or the volume of inoculation. We have also confirmed that the viral titers in the lungs of mice inoculated with the same initial viral dose but different inoculum volumes were not significantly different.

We anticipated that in order for full-blown infection to take place, PVM would need to replicate in the host lungs until a “critical” viral load point was reached. Once the “critical” viral load point was reached, indistinguishable disease sequelae and lung pathology between the test groups and mouse strains was repeatedly observed. We also expected that reduced susceptibility to PVM infection of C57/Bl mice stems either from some intrinsic genetic factors that allowed C57/Bl mice to exhibit greater resistance to the initial infection and prevent robust virus replication, or from the presence of some unidentified local lung tissue factors that were capable of keeping viral replication under control, thus postponing intensification of the disease.

In light of these observations, the need for additional more in-depth studies is apparent. Further characterization of PVM infection in these and other strains, including quantitation of immune response factors, would without doubt help to identify relevant biomarkers involved in this mechanism.

5.3 Phenotypical and functional changes in BM-DCs upon Pneumonia Virus of Mice infection

In view of the fact that our *in vivo* studies demonstrated differential susceptibility and resistance patterns to PVM infection in Balb/c and C57/Bl mice, we wanted to further examine factors that might be responsible for this phenomenon. As previously discussed, the different susceptibility patterns to PVM infection observed in *in vivo* studies strongly indicated innate immune response involvement. Natural killer (NK) cells and DCs represent central innate immune cells that contribute to viral clearance. This contribution is accomplished either via direct antimicrobial action or indirectly by cytokine secretion and modulation of the adaptive immune response. Numerous studies revealed the central role DCs play in the development of tolerance, memory and Th1/Th2 polarization (37, 72, 220).

With regard to Pneumovirus infections, it was demonstrated that mice infected with RSV show a constant increase in numbers of mature DCs (24). It was also shown that RSV infections are more severe in infants. Animal studies demonstrated a post-natal delay in the development of the class II MHC positive DC population in the respiratory tract compared to older animals (246). Thus we wanted to examine more closely the DC phenotypes and possible changes in their functions following PVM infection.

We hypothesized that PVM infection of DCs would change their phenotypic characteristics and thus contribute to functional alterations that inevitably lead to inappropriate T cell activation and disease augmentation. We used PVM-infected BM-DCs derived from Balb/c and C57/Bl mice and evaluated their phenotypic and functional differences 24 hours post-infection.

BM-DCs cultured with PVM for 24 hours failed to show any significant increase in the expression of the costimulatory and MHC II DC markers associated with maturation. In another study, murine myeloid BM-DCs cultured for 48 hours with RSV (MOI 10) showed an increase in costimulatory marker expression that corresponded to a mature DC phenotype (31). Inconsistency between our results and those reported by this group could reflect differences in experimental design. Even though we were successful in the production of PVM stock having a titer of 10^6 PFU, which was higher than usually reported for PVM grown in culture, low viral titers limited our ability to more efficiently infect DCs.

In peripheral sites DCs serve as sentinel cells that take up and process antigens. Subsequently, DCs travel via efferent lymphatics toward the draining lymph nodes, where they present the antigens to T cells. DCs recognize and mediate uptake of pathogens that expresses pathogen-associated molecular patterns via pattern recognition receptors expressed on the surface of the DCs. Apart from this receptor-mediated mechanism, immature DCs also have the unique ability of constitutively taking up large quantities of fluid from their environment. This process is mediated by aquaporins; water channels the expression of which is irreversibly down-regulated following DC maturation (210).

Hence, we wanted to examine changes in the ability of DCs to take up soluble antigens from their environment following infection with PVM. Even though we were not able to

demonstrate statistically significant differences between PVM-infected DCs and controls, both Balb/c- and C57/Bl-derived PVM-infected BM-DCs showed a consistent decrease in FITC-labeled dextran uptake. As reported by de Graaff *et al.*, 48 hours post RSV infection less than 25% of human monocyte-derived DCs showed signs of infection (70). Thus, our results might reflect phenotypic and functional changes of only a small part of the DC population under examination. The observed changes might be an indication that a small percentage of the BM-DC population that was successfully infected with PVM underwent the maturation process, which inevitably shut down non receptor-mediated uptake of FITC-dextran. Since the decrease of FITC-dextran uptake by PVM-infected BM-DC was not significantly lower than in control groups, we were not able to conclude with certainty that active infection of BM-DC with PVM significantly influences the function of DCs. Studying a purified PVM-infected DC population, selected by one of the currently available methods such as cell sorting, might be a good way to overcome this problem, and permit us to closely examine changes inflicted by PVM in the population of interest.

In the last decade it has become increasingly clear that DCs play a pivotal role in regulating primary immune responses, equally by inducing T cell proliferation and by directing the type of effector T cells (Th1, Th2, cytotoxic, or regulatory T cell). Modification of the host immune response by several RSV proteins is well documented (33, 255, 256, 292-294). It was also shown that species-specific inhibition of T cell proliferation by RSV F protein can occur. Therefore, we wanted to examine the impact of PVM infection on the ability of DCs to induce naïve T cell proliferation in their natural host.

T cell proliferation studies with RSV-infected DCs showed contradictory results. Boogaard *et al.* reported up-regulation of costimulatory maturation markers on murine myeloid

DCs co-cultured with OVA and RSV along with enhanced OVA-specific T cell proliferation (31). In contrast, de Graaff *et al.* also reported up-regulation of maturation markers, but the ability of RSV-infected-monocyte-derived human DCs to induce T cell proliferation was decreased (3, 5). A separate *in vitro* study also showed reduced T cell proliferation when human monocytes were co-cultured with RSV and LPS compared to LPS only (111).

Our results showed a negligible impact of infection of BM-DCs with PVM on the extent of T cell proliferation. Even though T cell proliferation was observed on days three and five after infection, a significant decrease in T cell proliferation in the group stimulated with PVM-infected DCs compared to the BHK-21 control group was found only on day five for Balb/c mice. However, T cell proliferation for the same mouse strain and time point did not show a significant difference between PVM and UV-PVM control groups. Thus, we were not able to conclude with confidence that DCs have a biologically significant impact on T cell proliferation during a productive PVM infection.

Since a Th1-type response is usually seen in viral infection and helps in the control and clearance of the virus, we also wanted to take a closer look at the production of IL-12p70, a pivotal cytokine in the differentiation to a Th1-type response. In our preliminary studies, all groups with the exception of the LPS-treated group, showed IL-12p70 levels that were below the detection limit. Hence we chose to measure the effect of PVM on IL-12p70 production by DCs co-cultured with LPS. Our results showed a significant inhibitory effect of PVM on LPS-induced IL-12p70 production, but the same effect was also seen in UV-PVM and BHK-21 controls. Since a common factor between our tested groups was the presence of BHK-21 cells, we are inclined to believe that the demonstrated inhibitory effect might be induced by BHK-21 cells. BHK-21 cells are fibroblast cells that under certain conditions produce TNF- α the

inhibitory effect of which on IL-12 production is well documented (176). Furthermore, since the differences in IL-12p70 inhibition between the two strains were not significant, we were not able to correlate differential susceptibility to PVM infection between the two strains to differences in IL-12 production.

6.0 General Discussion and Conclusions

Respiratory syncytial virus infection is the most common cause of hospitalization of infants and young children around the world due to LRT complications, such as bronchiolitis and pneumonia. Recently, in an effort to better understand the factors involved in the pathogenesis of RSV infections, scientists turned their attention toward a new, more appropriate mouse model. Another virus in the Pneumovirus family, Pneumonia virus of mice, showed an excellent potential of becoming a more suitable model for RSV disease studies than previously used murine RSV models. PVM-infected mice exhibited similar clinical signs to those found in RSV-infected infants and, most importantly, this model allowed studies of Pneumovirus infection in its natural host.

Even though published work pertaining to PVM is still scarce, most of the research groups that are currently working with PVM use mouse-passaged strain J3666 in their work. In contrast, we wanted to establish a PVM animal model in two mouse strains using an ATCC available strain, strain 15. In our work, we established a method for propagating PVM strain 15 in a hamster fibroblast cell line, BHK-21. We also established a modified plaque assay for PVM quantization. During the establishment of animal models in Balb/c and C57/Bl mice, our work shed light on an interesting difference in the susceptibility/resistance patterns to PVM infection

in these two strains. Based on the results from our *in vivo* studies we have concluded that strain-dependant susceptibility to PVM infection exists; with Balb/c strain showing more susceptible pattern. Because a correlation between host genetic background and susceptibility to more severe RSV disease exists, our findings open new opportunities for research in this field.

As a first step toward identifying factors responsible for the difference in susceptibility to PVM infection between the two mouse strains, we also looked at the impact of PVM infection on phenotypic and functional changes of BM-DCs *in vitro*. We have concluded that, under our experimental conditions, PVM-infected BM-DCs failed to demonstrate biologically significant differences in their phenotypic or functional profiles compared to control groups. Thus, we were not able to confirm our hypothesis. Perhaps our approach may have been too simple to provide us with definite answers to such complex questions. Further complicating matters are the contradictory findings reported by other research groups that have worked with RSV.

Furthermore, it is well documented that even though all DCs originate from the same bone marrow precursors, mucosal DCs possess unique site-specific phenotypic and functional characteristics that inevitably coordinate the type of response mounted. Therefore, if one wants to examine DC phenotypes and functions in the context of respiratory viral infections, studying lung DCs instead of BM-DCs would perhaps be a more suitable approach.

In addition, recent studies indicated an important role for mucosal epithelial cells in the process of self, non-self discrimination. Apparently, mucosal DCs are incapable of mounting a Th1-type immune response to pathogenic bacteria without additional cytokine and chemokine signals derived from infected mucosal epithelial cells (244). This was also indicated as the reason why *in vitro* activation of mucosal DCs with strong TLR agonists always fail to induce

IL-12 or TNF production (2, 131, 252). Therefore, the importance of examining DCs *in vivo* in the context of their environment is of paramount importance.

Furthermore, our *in vivo* findings clearly suggested the involvement of innate immune factors in the different responses to PVM infection. As previously indicated, DCs and NK cells are the most important innate cells directly regulating innate immunity, and indirectly mediating establishment of an appropriate acquired immune response. In recent years, it has become clear that DCs and NK cells interact and mutually regulate each other during the early phase of an innate immune response (96). In addition, when considering the cross-talk between these two types of cells, it was shown that DCs induce NK cell proliferation and IFN- γ production, while NK cells induce increases in maturation marker expression and IL-12 cytokine secretion (8).

We also strongly believe that in the future, research of mucosal DCs *in vitro* should without doubt include more sophisticated models, including mucosal epithelial cells in culture. Only this kind of *in vitro* setting would more closely mimic the complex interactions found *in vivo*, and take into account the multifaceted interactions between key innate immunity players at the mucosal sites following Pneumovirus infections.

7.0 References

1. **Aherne, W., T. Bird, S. D. Court, P. S. Gardner, and J. McQuillin.** 1970. Pathological changes in virus infections of the lower respiratory tract in children. *J Clin Pathol* **23**:7-18.
2. **Akbari, O., R. H. DeKruyff, and D. T. Umetsu.** 2001. Pulmonary dendritic cells producing IL-10 mediate tolerance induced by respiratory exposure to antigen. *Nat Immunol* **2**:725-31.
3. **Alwan, W. H., W. J. Kozlowska, and P. J. Openshaw.** 1994. Distinct types of lung disease caused by functional subsets of antiviral T cells. *J Exp Med* **179**:81-9.
4. **Alwan, W. H., F. M. Record, and P. J. Openshaw.** 1992. CD4+ T cells clear virus but augment disease in mice infected with respiratory syncytial virus. Comparison with the effects of CD8+ T cells. *Clin Exp Immunol* **88**:527-36.
5. **American Academy of Pediatrics (AAP).** 2003. Respiratory syncytial virus, p. 523-528, 2003 red book: Report of the Committee on Infectious Diseases, 26th ed. AAP, Elk Grove Village, IL.
6. **American Academy of Pediatrics (AAP), A. W. S., American Academy of Pediatrics, 141 Northwest Point Blvd., Elk Grove Village. World Wide Web (URL: <http://www.aap.org/advocacy/releases/rsv.htm>).** last database update: **March 03,2008**, posting date. RSV: A SERIOUS THREAT TO INFANTS AND CHILDREN [Online.]
7. **Anderson, L. J., J. C. Hierholzer, C. Tsou, R. M. Hendry, B. F. Fernie, Y. Stone, and K. McIntosh.** 1985. Antigenic characterization of respiratory syncytial virus strains with monoclonal antibodies. *J Infect Dis* **151**:626-33.
8. **Andrews, D. M., A. A. Scalzo, W. M. Yokoyama, M. J. Smyth, and M. A. Degli-Esposti.** 2003. Functional interactions between dendritic cells and NK cells during viral infection. *Nat Immunol* **4**:175-81.
9. **Anh, D. B., P. Faisca, and D. J. Desmecht.** 2006. Differential resistance/susceptibility patterns to pneumovirus infection among inbred mouse strains. *Am J Physiol Lung Cell Mol Physiol* **291**:L426-35.
10. **Aoyagi, M., N. Shimojo, K. Sekine, T. Nishimuta, and Y. Kohno.** 2003. Respiratory syncytial virus infection suppresses IFN-gamma production of gammadelta T cells. *Clin Exp Immunol* **131**:312-7.
11. **Ardavin, C., L. Wu, C. L. Li, and K. Shortman.** 1993. Thymic dendritic cells and T cells develop simultaneously in the thymus from a common precursor population. *Nature* **362**:761-3.
12. **Arnold, R., B. Humbert, H. Werchau, H. Gallati, and W. Konig.** 1994. Interleukin-8, interleukin-6, and soluble tumour necrosis factor receptor type I release from a human pulmonary epithelial cell line (A549) exposed to respiratory syncytial virus. *Immunology* **82**:126-33.
13. **Arnold, R., and W. Konig.** 1996. ICAM-1 expression and low-molecular-weight G-protein activation of human bronchial epithelial cells (A549) infected with RSV. *J Leukoc Biol* **60**:766-71.
14. **Aspinall, R., S. M. Henson, and J. Pido-Lopez.** 2003. My T's gone cold, I'm wondering why. *Nat Immunol* **4**:203-5.

15. **Asselin-Paturel, C., G. Brizard, J. J. Pin, F. Briere, and G. Trinchieri.** 2003. Mouse strain differences in plasmacytoid dendritic cell frequency and function revealed by a novel monoclonal antibody. *J Immunol* **171**:6466-77.
16. **Awomoyi, A. A., P. Rallabhandi, T. I. Pollin, E. Lorenz, M. B. Sztein, M. S. Boukhvalova, V. G. Hemming, J. C. Blanco, and S. N. Vogel.** 2007. Association of TLR4 polymorphisms with symptomatic respiratory syncytial virus infection in high-risk infants and young children. *J Immunol* **179**:3171-7.
17. **Bangham, C. R., and B. A. Askonas.** 1986. Murine cytotoxic T cells specific to respiratory syncytial virus recognize different antigenic subtypes of the virus. *J Gen Virol* **67 (Pt 4)**:623-9.
18. **Bangham, C. R., P. J. Openshaw, L. A. Ball, A. M. King, G. W. Wertz, and B. A. Askonas.** 1986. Human and murine cytotoxic T cells specific to respiratory syncytial virus recognize the viral nucleoprotein (N), but not the major glycoprotein (G), expressed by vaccinia virus recombinants. *J Immunol* **137**:3973-7.
19. **Barnard, D. L., C. L. Hill, T. Gage, J. E. Matheson, J. H. Huffman, R. W. Sidwell, M. I. Otto, and R. F. Schinazi.** 1997. Potent inhibition of respiratory syncytial virus by polyoxometalates of several structural classes. *Antiviral Res* **34**:27-37.
20. **Bartz, H., O. Turkel, S. Hoffjan, T. Rothoelt, A. Gonschorek, and U. Schauer.** 2003. Respiratory syncytial virus decreases the capacity of myeloid dendritic cells to induce interferon-gamma in naive T cells. *Immunology* **109**:49-57.
21. **Beem, M., R. Egerer, and J. Anderson.** 1964. Respiratory Syncytial Virus Neutralizing Antibodies in Persons Residing in Chicago, Illinois. *Pediatrics* **34**:761-70.
22. **Belshe, R. B., L. S. Richardson, W. T. London, D. L. Sly, J. H. Lorfeld, E. Camargo, D. A. Prevar, and R. M. Chanock.** 1977. Experimental respiratory syncytial virus infection of four species of primates. *J Med Virol* **1**:157-62.
23. **Bendelja, K., A. Gagro, A. Bace, R. Lokar-Kolbas, V. Krsulovic-Hresic, V. Drazenovic, G. Mlinaric-Galinovic, and S. Rabatic.** 2000. Predominant type-2 response in infants with respiratory syncytial virus (RSV) infection demonstrated by cytokine flow cytometry. *Clin Exp Immunol* **121**:332-8.
24. **Beyer, M., H. Bartz, K. Horner, S. Doths, C. Koerner-Rettberg, and J. Schwarze.** 2004. Sustained increases in numbers of pulmonary dendritic cells after respiratory syncytial virus infection. *J Allergy Clin Immunol* **113**:127-33.
25. **Bitko, V., A. Velazquez, L. Yang, Y. C. Yang, and S. Barik.** 1997. Transcriptional induction of multiple cytokines by human respiratory syncytial virus requires activation of NF-kappa B and is inhibited by sodium salicylate and aspirin. *Virology* **232**:369-78.
26. **Bjorck, P., and P. W. Kincade.** 1998. CD19+ pro-B cells can give rise to dendritic cells in vitro. *J Immunol* **161**:5795-9.
27. **Blanco, J. C., L. Pletneva, M. Boukhvalova, J. Y. Richardson, K. A. Harris, and G. A. Prince.** 2004. The cotton rat: an underutilized animal model for human infectious diseases can now be exploited using specific reagents to cytokines, chemokines, and interferons. *J Interferon Cytokine Res* **24**:21-8.
28. **Bonville, C. A., A. J. Easton, H. F. Rosenberg, and J. B. Domachowske.** 2003. Altered pathogenesis of severe pneumovirus infection in response to combined antiviral and specific immunomodulatory agents. *J Virol* **77**:1237-44.

29. **Bonville, C. A., P. A. Mehta, L. R. Krilov, H. F. Rosenberg, and J. B. Domachowske.** 2001. Epithelial cells infected with respiratory syncytial virus are resistant to the anti-inflammatory effects of hydrocortisone. *Cell Immunol* **213**:134-40.
30. **Bonville, C. A., H. F. Rosenberg, and J. B. Domachowske.** 1999. Macrophage inflammatory protein-1alpha and RANTES are present in nasal secretions during ongoing upper respiratory tract infection. *Pediatr Allergy Immunol* **10**:39-44.
31. **Boogaard, I., M. van Oosten, L. S. van Rijt, F. Muskens, T. G. Kimman, B. N. Lambrecht, and A. M. Buisman.** 2007. Respiratory syncytial virus differentially activates murine myeloid and plasmacytoid dendritic cells. *Immunology* **122**:65-72.
32. **Borkowski, T. A., J. J. Letterio, A. G. Farr, and M. C. Udey.** 1996. A role for endogenous transforming growth factor beta 1 in Langerhans cell biology: the skin of transforming growth factor beta 1 null mice is devoid of epidermal Langerhans cells. *J Exp Med* **184**:2417-22.
33. **Bossert, B., and K. K. Conzelmann.** 2002. Respiratory syncytial virus (RSV) nonstructural (NS) proteins as host range determinants: a chimeric bovine RSV with NS genes from human RSV is attenuated in interferon-competent bovine cells. *J Virol* **76**:4287-93.
34. **Bramley, A. M., T. Z. Vitalis, B. R. Wiggs, and R. G. Hegele.** 1999. Effects of respiratory syncytial virus persistence on airway responsiveness and inflammation in guinea-pigs. *Eur Respir J* **14**:1061-7.
35. **Brandenburg, A. H., A. Kleinjan, B. van Het Land, H. A. Moll, H. H. Timmerman, R. L. de Swart, H. J. Neijens, W. Fokkens, and A. D. Osterhaus.** 2000. Type 1-like immune response is found in children with respiratory syncytial virus infection regardless of clinical severity. *J Med Virol* **62**:267-77.
36. **Brandenburg, A. H., H. J. Neijens, and A. D. Osterhaus.** 2001. Pathogenesis of RSV lower respiratory tract infection: implications for vaccine development. *Vaccine* **19**:2769-82.
37. **Brossart, P., S. Wirths, G. Stuhler, V. L. Reichardt, L. Kanz, and W. Brugger.** 2000. Induction of cytotoxic T-lymphocyte responses in vivo after vaccinations with peptide-pulsed dendritic cells. *Blood* **96**:3102-8.
38. **Bukreyev, A., S. S. Whitehead, B. R. Murphy, and P. L. Collins.** 1997. Recombinant respiratory syncytial virus from which the entire SH gene has been deleted grows efficiently in cell culture and exhibits site-specific attenuation in the respiratory tract of the mouse. *J Virol* **71**:8973-82.
39. **Burnette, W. N.** 1981. "Western blotting": electrophoretic transfer of proteins from sodium dodecyl sulfate--polyacrylamide gels to unmodified nitrocellulose and radiographic detection with antibody and radioiodinated protein A. *Anal Biochem* **112**:195-203.
40. **Byrd, L. G., and G. A. Prince.** 1997. Animal models of respiratory syncytial virus infection. *Clin Infect Dis* **25**:1363-8.
41. **Cane, P. A., D. A. Matthews, and C. R. Pringle.** 1991. Identification of variable domains of the attachment (G) protein of subgroup A respiratory syncytial viruses. *J Gen Virol* **72 (Pt 9)**:2091-6.
42. **Cannon, M. J., P. J. Openshaw, and B. A. Askonas.** 1988. Cytotoxic T cells clear virus but augment lung pathology in mice infected with respiratory syncytial virus. *J Exp Med* **168**:1163-8.

43. **Cannon, M. J., E. J. Stott, G. Taylor, and B. A. Askonas.** 1987. Clearance of persistent respiratory syncytial virus infections in immunodeficient mice following transfer of primed T cells. *Immunology* **62**:133-8.
44. **Caux, C., B. Vanbervliet, C. Massacrier, C. Dezutter-Dambuyant, B. de Saint-Vis, C. Jacquet, K. Yoneda, S. Imamura, D. Schmitt, and J. Banchereau.** 1996. CD34+ hematopoietic progenitors from human cord blood differentiate along two independent dendritic cell pathways in response to GM-CSF+TNF alpha. *J Exp Med* **184**:695-706.
45. **Cella, M., A. Engering, V. Pinet, J. Pieters, and A. Lanzavecchia.** 1997. Inflammatory stimuli induce accumulation of MHC class II complexes on dendritic cells. *Nature* **388**:782-7.
46. **Cella, M., D. Scheidegger, K. Palmer-Lehmann, P. Lane, A. Lanzavecchia, and G. Alber.** 1996. Ligation of CD40 on dendritic cells triggers production of high levels of interleukin-12 and enhances T cell stimulatory capacity: T-T help via APC activation. *J Exp Med* **184**:747-52.
47. **Champlin, R. E., and E. Whimbey.** 2001. Community respiratory virus infections in bone marrow transplant recipients: the M.D. Anderson Cancer Center experience. *Biol Blood Marrow Transplant* **7 Suppl**:8S-10S.
48. **Chandwani, S., W. Borkowsky, K. Krasinski, R. Lawrence, and R. Welliver.** 1990. Respiratory syncytial virus infection in human immunodeficiency virus-infected children. *J Pediatr* **117**:251-4.
49. **Chanock, R., and L. Finberg.** 1957. Recovery from infants with respiratory illness of a virus related to chimpanzee coryza agent (CCA). II. Epidemiologic aspects of infection in infants and young children. *Am J Hyg* **66**:291-300.
50. **Chanock, R., B. Roizman, and R. Myers.** 1957. Recovery from infants with respiratory illness of a virus related to chimpanzee coryza agent (CCA). I. Isolation, properties and characterization. *Am J Hyg* **66**:281-90.
51. **Chanock, R. M., A. Z. Kapikian, and R. H. Parrot.** 1968. Possible role of immunologic factors in pathogenesis of RS virus lower respiratory tract disease. *Perspect. Virol.* **6**:125-139.
52. **Chanock, R. M., A. Z. Kapikian, J. Mills, H. W. Kim, and R. H. Parrott.** 1970. Influence of immunological factors in respiratory syncytial virus disease. *Arch Environ Health* **21**:347-55.
53. **Chiba, Y., Y. Higashidate, K. Suga, K. Honjo, H. Tsutsumi, and P. L. Ogra.** 1989. Development of cell-mediated cytotoxic immunity to respiratory syncytial virus in human infants following naturally acquired infection. *J Med Virol* **28**:133-9.
54. **Choi, E. H., H. J. Lee, T. Yoo, and S. J. Chanock.** 2002. A common haplotype of interleukin-4 gene IL4 is associated with severe respiratory syncytial virus disease in Korean children. *J Infect Dis* **186**:1207-11.
55. **Coates, H. V., and R. M. Chanock.** 1962. Experimental infection with respiratory syncytial virus in several species of animals. *Am J Hyg* **76**:302-12.
56. **Collins, P. L., and B. S. Graham.** 2007. Viral and host factors in human respiratory syncytial virus pathogenesis. *J Virol.*
57. **Collins, P. L., R. H. Purcell, W. T. London, L. A. Lawrence, R. M. Chanock, and B. R. Murphy.** 1990. Evaluation in chimpanzees of vaccinia virus recombinants that express the surface glycoproteins of human respiratory syncytial virus. *Vaccine* **8**:164-8.

58. **Connors, M., N. A. Giese, A. B. Kulkarni, C. Y. Firestone, H. C. Morse, 3rd, and B. R. Murphy.** 1994. Enhanced pulmonary histopathology induced by respiratory syncytial virus (RSV) challenge of formalin-inactivated RSV-immunized BALB/c mice is abrogated by depletion of interleukin-4 (IL-4) and IL-10. *J Virol* **68**:5321-5.
59. **Connors, M., A. B. Kulkarni, C. Y. Firestone, K. L. Holmes, H. C. Morse, 3rd, A. V. Sotnikov, and B. R. Murphy.** 1992. Pulmonary histopathology induced by respiratory syncytial virus (RSV) challenge of formalin-inactivated RSV-immunized BALB/c mice is abrogated by depletion of CD4+ T cells. *J Virol* **66**:7444-51.
60. **Cook, P. M., R. P. Eglin, and A. J. Easton.** 1998. Pathogenesis of pneumovirus infections in mice: detection of pneumonia virus of mice and human respiratory syncytial virus mRNA in lungs of infected mice by in situ hybridization. *J Gen Virol* **79** (Pt 10):2411-7.
61. **Correale, P., G. Campoccia, K. Y. Tsang, L. Micheli, M. G. Cusi, M. Sabatino, G. Bruni, S. Sestini, R. Petrioli, D. Pozzessere, S. Marsili, G. Fanetti, G. Giorgi, and G. Francini.** 2001. Recruitment of dendritic cells and enhanced antigen-specific immune reactivity in cancer patients treated with hr-GM-CSF (Molgramostim) and hr-IL-2. results from a phase Ib clinical trial. *Eur J Cancer* **37**:892-902.
62. **Cowton, V. M., D. R. McGivern, and R. Fearn.** 2006. Unravelling the complexities of respiratory syncytial virus RNA synthesis. *J Gen Virol* **87**:1805-21.
63. **Crowe, J. E., Jr., P. T. Bui, A. R. Davis, R. M. Chanock, and B. R. Murphy.** 1994. A further attenuated derivative of a cold-passaged temperature-sensitive mutant of human respiratory syncytial virus retains immunogenicity and protective efficacy against wild-type challenge in seronegative chimpanzees. *Vaccine* **12**:783-90.
64. **Crowe, J. E., Jr., P. T. Bui, C. Y. Firestone, M. Connors, W. R. Elkins, R. M. Chanock, and B. R. Murphy.** 1996. Live subgroup B respiratory syncytial virus vaccines that are attenuated, genetically stable, and immunogenic in rodents and nonhuman primates. *J Infect Dis* **173**:829-39.
65. **Crowe, J. E., Jr., P. T. Bui, G. R. Siber, W. R. Elkins, R. M. Chanock, and B. R. Murphy.** 1995. Cold-passaged, temperature-sensitive mutants of human respiratory syncytial virus (RSV) are highly attenuated, immunogenic, and protective in seronegative chimpanzees, even when RSV antibodies are infused shortly before immunization. *Vaccine* **13**:847-55.
66. **Crowe, J. E., Jr., P. L. Collins, W. T. London, R. M. Chanock, and B. R. Murphy.** 1993. A comparison in chimpanzees of the immunogenicity and efficacy of live attenuated respiratory syncytial virus (RSV) temperature-sensitive mutant vaccines and vaccinia virus recombinants that express the surface glycoproteins of RSV. *Vaccine* **11**:1395-404.
67. **Culley, F. J., A. M. Pennycook, J. S. Tregoning, T. Hussell, and P. J. Openshaw.** 2006. Differential Chemokine Expression following Respiratory Virus Infection Reflects Th1- or Th2-Biased Immunopathology. *J Virol* **80**:4521-7.
68. **Culley, F. J., J. Pollott, and P. J. Openshaw.** 2002. Age at first viral infection determines the pattern of T cell-mediated disease during reinfection in adulthood. *J Exp Med* **196**:1381-6.
69. **Darville, T., and T. Yamauchi.** 1998. Respiratory syncytial virus. *Pediatr Rev* **19**:55-61.
70. **de Graaff, P. M., E. C. de Jong, T. M. van Capel, M. E. van Dijk, P. J. Roholl, J. Boes, W. Luytjes, J. L. Kimpen, and G. M. van Bleek.** 2005. Respiratory syncytial

- virus infection of monocyte-derived dendritic cells decreases their capacity to activate CD4 T cells. *J Immunol* **175**:5904-11.
71. **de Heer, H. J., H. Hammad, M. Kool, and B. N. Lambrecht.** 2005. Dendritic cell subsets and immune regulation in the lung. *Semin Immunol* **17**:295-303.
 72. **De Smedt, T., B. Pajak, E. Muraille, L. Lespagnard, E. Heinen, P. De Baetselier, J. Urbain, O. Leo, and M. Moser.** 1996. Regulation of dendritic cell numbers and maturation by lipopolysaccharide in vivo. *J Exp Med* **184**:1413-24.
 73. **De Smedt, T., M. Van Mechelen, G. De Becker, J. Urbain, O. Leo, and M. Moser.** 1997. Effect of interleukin-10 on dendritic cell maturation and function. *Eur J Immunol* **27**:1229-35.
 74. **De Swart, R. L., T. Kuiken, H. H. Timmerman, G. van Amerongen, B. G. Van Den Hoogen, H. W. Vos, H. J. Neijens, A. C. Andeweg, and A. D. Osterhaus.** 2002. Immunization of macaques with formalin-inactivated respiratory syncytial virus (RSV) induces interleukin-13-associated hypersensitivity to subsequent RSV infection. *J Virol* **76**:11561-9.
 75. **Dickens, L. E., P. L. Collins, and G. W. Wertz.** 1984. Transcriptional mapping of human respiratory syncytial virus. *J Virol* **52**:364-9.
 76. **Domachowske, J. B., C. A. Bonville, K. D. Dyer, A. J. Easton, and H. F. Rosenberg.** 2000. Pulmonary eosinophilia and production of MIP-1alpha are prominent responses to infection with pneumonia virus of mice. *Cell Immunol* **200**:98-104.
 77. **Domachowske, J. B., C. A. Bonville, A. J. Easton, and H. F. Rosenberg.** 2002. Differential expression of proinflammatory cytokine genes in vivo in response to pathogenic and nonpathogenic pneumovirus infections. *J Infect Dis* **186**:8-14.
 78. **Domachowske, J. B., C. A. Bonville, J. L. Gao, P. M. Murphy, A. J. Easton, and H. F. Rosenberg.** 2000. MIP-1alpha is produced but it does not control pulmonary inflammation in response to respiratory syncytial virus infection in mice. *Cell Immunol* **206**:1-6.
 79. **Domachowske, J. B., C. A. Bonville, and H. F. Rosenberg.** 2001. Gene expression in epithelial cells in response to pneumovirus infection. *Respir Res* **2**:225-33.
 80. **Domachowske, J. B., and H. F. Rosenberg.** 1999. Respiratory syncytial virus infection: immune response, immunopathogenesis, and treatment. *Clin Microbiol Rev* **12**:298-309.
 81. **Dowell, S. F., L. J. Anderson, H. E. Gary, Jr., D. D. Erdman, J. F. Plouffe, T. M. File, Jr., B. J. Marston, and R. F. Breiman.** 1996. Respiratory syncytial virus is an important cause of community-acquired lower respiratory infection among hospitalized adults. *J Infect Dis* **174**:456-62.
 82. **Dreizin, R. S., L. O. Vyshnevetskaia, E. E. Bagdamian, O. D. Iankevich, and L. B. Tarasova.** 1971. [Experimental RS virus infection of cotton rats. A viral and immunofluorescent study]. *Vopr Virusol* **16**:670-6.
 83. **Dyer, K. D., I. M. Schellens, C. A. Bonville, B. V. Martin, J. B. Domachowske, and H. F. Rosenberg.** 2007. Efficient replication of pneumonia virus of mice (PVM) in a mouse macrophage cell line. *Virol J* **4**:48.
 84. **Eaton, M. D., and W. van Herick.** 1944. Demonstration in cotton rats and rabbits of a latent virus related to pneumonia virus of mice. *Proceedings of the Society for Experimental Biology and Medicine* **54**:89-92.

85. **Elias, J. A., T. Zheng, O. Einarsson, M. Landry, T. Trow, N. Rebert, and J. Panuska.** 1994. Epithelial interleukin-11. Regulation by cytokines, respiratory syncytial virus, and retinoic acid. *J Biol Chem* **269**:22261-8.
86. **Ellis, J. A., B. V. Martin, C. Waldner, K. D. Dyer, J. B. Domachowske, and H. F. Rosenberg.** 2007. Mucosal inoculation with an attenuated mouse pneumovirus strain protects against virulent challenge in wild type and interferon-gamma receptor deficient mice. *Vaccine* **25**:1085-95.
87. **Everard, M. L., A. Swarbrick, M. Wraitham, J. McIntyre, C. Dunkley, P. D. James, H. F. Sewell, and A. D. Milner.** 1994. Analysis of cells obtained by bronchial lavage of infants with respiratory syncytial virus infection. *Arch Dis Child* **71**:428-32.
88. **Falsey, A. R., C. K. Cunningham, W. H. Barker, R. W. Kouides, J. B. Yuen, M. Menegus, L. B. Weiner, C. A. Bonville, and R. F. Betts.** 1995. Respiratory syncytial virus and influenza A infections in the hospitalized elderly. *J Infect Dis* **172**:389-94.
89. **Falsey, A. R., M. A. Formica, P. A. Hennessey, M. M. Criddle, W. M. Sullender, and E. E. Walsh.** 2006. Detection of respiratory syncytial virus in adults with chronic obstructive pulmonary disease. *Am J Respir Crit Care Med* **173**:639-43.
90. **Falsey, A. R., P. A. Hennessey, M. A. Formica, C. Cox, and E. E. Walsh.** 2005. Respiratory syncytial virus infection in elderly and high-risk adults. *N Engl J Med* **352**:1749-59.
91. **Falsey, A. R., R. M. McCann, W. J. Hall, M. A. Tanner, M. M. Criddle, M. A. Formica, C. S. Irvine, J. E. Kolassa, W. H. Barker, and J. J. Treanor.** 1995. Acute respiratory tract infection in daycare centers for older persons. *J Am Geriatr Soc* **43**:30-6.
92. **Falsey, A. R., and E. E. Walsh.** 2000. Respiratory syncytial virus infection in adults. *Clin Microbiol Rev* **13**:371-84.
93. **Ferrarini, M., E. Ferrero, L. Dagna, A. Poggi, and M. R. Zocchi.** 2002. Human gammadelta T cells: a nonredundant system in the immune-surveillance against cancer. *Trends Immunol* **23**:14-8.
94. **Flesch, I. E., J. H. Hess, S. Huang, M. Aguet, J. Rothe, H. Bluethmann, and S. H. Kaufmann.** 1995. Early interleukin 12 production by macrophages in response to mycobacterial infection depends on interferon gamma and tumor necrosis factor alpha. *J Exp Med* **181**:1615-21.
95. **Garofalo, R., F. Mei, R. Espejo, G. Ye, H. Haeberle, S. Baron, P. L. Ogra, and V. E. Reyes.** 1996. Respiratory syncytial virus infection of human respiratory epithelial cells up-regulates class I MHC expression through the induction of IFN-beta and IL-1 alpha. *J Immunol* **157**:2506-13.
96. **Gerosa, F., B. Baldani-Guerra, C. Nisii, V. Marchesini, G. Carra, and G. Trinchieri.** 2002. Reciprocal activating interaction between natural killer cells and dendritic cells. *J Exp Med* **195**:327-33.
97. **Gershwin, L. J., E. S. Schelegle, R. A. Gunther, M. L. Anderson, A. R. Woolums, D. R. Larochelle, G. A. Boyle, K. E. Friebertshausen, and R. S. Singer.** 1998. A bovine model of vaccine enhanced respiratory syncytial virus pathophysiology. *Vaccine* **16**:1225-36.
98. **Ghildyal, R., C. Hartley, A. Varrasso, J. Meanger, D. R. Voelker, E. M. Anders, and J. Mills.** 1999. Surfactant protein A binds to the fusion glycoprotein of respiratory syncytial virus and neutralizes virion infectivity. *J Infect Dis* **180**:2009-13.

99. **Gillette, R., M. U. Gillette, and W. J. Davis.** 1980. Action-potential broadening and endogenously sustained bursting are substrates of command ability in a feeding neuron of Pleurobranchaea. *J Neurophysiol* **43**:669-85.
100. **Gimenez, H. B., H. M. Keir, and P. Cash.** 1987. Immunoblot analysis of the human antibody response to respiratory syncytial virus infection. *J Gen Virol* **68 (Pt 5)**:1267-75.
101. **Glezen, W. P., A. Paredes, J. E. Allison, L. H. Taber, and A. L. Frank.** 1981. Risk of respiratory syncytial virus infection for infants from low-income families in relationship to age, sex, ethnic group, and maternal antibody level. *J Pediatr* **98**:708-15.
102. **Glezen, W. P., L. H. Taber, A. L. Frank, and J. A. Kasel.** 1986. Risk of primary infection and reinfection with respiratory syncytial virus. *Am J Dis Child* **140**:543-6.
103. **Goetghebuer, T., K. Isles, C. Moore, A. Thomson, D. Kwiatkowski, and J. Hull.** 2004. Genetic predisposition to wheeze following respiratory syncytial virus bronchiolitis. *Clin Exp Allergy* **34**:801-3.
104. **Goldmann, D. A.** 2000. Transmission of viral respiratory infections in the home. *Pediatr Infect Dis J* **19**:S97-102.
105. **Graham, B. S., L. A. Bunton, P. F. Wright, and D. T. Karzon.** 1991. Role of T lymphocyte subsets in the pathogenesis of primary infection and rechallenge with respiratory syncytial virus in mice. *J Clin Invest* **88**:1026-33.
106. **Graham, B. S., M. D. Perkins, P. F. Wright, and D. T. Karzon.** 1988. Primary respiratory syncytial virus infection in mice. *J Med Virol* **26**:153-62.
107. **Groh, V., A. Steinle, S. Bauer, and T. Spies.** 1998. Recognition of stress-induced MHC molecules by intestinal epithelial gammadelta T cells. *Science* **279**:1737-40.
108. **Groothuis, J. R., K. M. Gutierrez, and B. A. Lauer.** 1988. Respiratory syncytial virus infection in children with bronchopulmonary dysplasia. *Pediatrics* **82**:199-203.
109. **Groothuis, J. R., S. J. King, D. A. Hogerman, P. R. Paradiso, and E. A. Simoes.** 1998. Safety and immunogenicity of a purified F protein respiratory syncytial virus (PFV-2) vaccine in seropositive children with bronchopulmonary dysplasia. *J Infect Dis* **177**:467-9.
110. **Groothuis, J. R., E. A. Simoes, M. J. Levin, C. B. Hall, C. E. Long, W. J. Rodriguez, J. Arrobio, H. C. Meissner, D. R. Fulton, R. C. Welliver, and et al.** 1993. Prophylactic administration of respiratory syncytial virus immune globulin to high-risk infants and young children. The Respiratory Syncytial Virus Immune Globulin Study Group. *N Engl J Med* **329**:1524-30.
111. **Guerrero-Plata, A., A. Casola, G. Suarez, X. Yu, L. Spetch, M. E. Peeples, and R. P. Garofalo.** 2006. Differential response of dendritic cells to human metapneumovirus and respiratory syncytial virus. *Am J Respir Cell Mol Biol* **34**:320-9.
112. **Guerrero-Plata, A., E. Ortega, and B. Gomez.** 2001. Persistence of respiratory syncytial virus in macrophages alters phagocytosis and pro-inflammatory cytokine production. *Viral Immunol* **14**:19-30.
113. **Guida, J. D., G. Fejer, L. A. Pirofski, C. F. Brosnan, and M. S. Horwitz.** 1995. Mouse adenovirus type 1 causes a fatal hemorrhagic encephalomyelitis in adult C57BL/6 but not BALB/c mice. *J Virol* **69**:7674-81.
114. **Hacking, D., J. C. Knight, K. Rockett, H. Brown, J. Frampton, D. P. Kwiatkowski, J. Hull, and I. A. Udalova.** 2004. Increased in vivo transcription of an IL-8 haplotype associated with respiratory syncytial virus disease-susceptibility. *Genes Immun* **5**:274-82.

115. **Haerberle, H. A., A. Casola, Z. Gatalica, S. Petronella, H. J. Dieterich, P. B. Ernst, A. R. Brasier, and R. P. Garofalo.** 2004. IkappaB kinase is a critical regulator of chemokine expression and lung inflammation in respiratory syncytial virus infection. *J Virol* **78**:2232-41.
116. **Haerberle, H. A., W. A. Kuziel, H. J. Dieterich, A. Casola, Z. Gatalica, and R. P. Garofalo.** 2001. Inducible expression of inflammatory chemokines in respiratory syncytial virus-infected mice: role of MIP-1alpha in lung pathology. *J Virol* **75**:878-90.
117. **Hall, C. B.** 1998. Respiratory syncytial virus, p. 2084-2111. *In* R. D. Feigin, Cherry, J.D. (ed.), *Textbook of Pediatric Infectious Diseases*. W.B.Saunders, Philadelphia.
118. **Hall, C. B., C. E. Long, and K. C. Schnabel.** 2001. Respiratory syncytial virus infections in previously healthy working adults. *Clin Infect Dis* **33**:792-6.
119. **Hall, C. B., E. E. Walsh, C. E. Long, and K. C. Schnabel.** 1991. Immunity to and frequency of reinfection with respiratory syncytial virus. *J Infect Dis* **163**:693-8.
120. **Hall, W. J., C. B. Hall, and D. M. Speers.** 1978. Respiratory syncytial virus infection in adults: clinical, virologic, and serial pulmonary function studies. *Ann Intern Med* **88**:203-5.
121. **Hammad, H., V. C. de Vries, R. Maldonado-Lopez, M. Moser, C. Maliszewski, H. C. Hoogsteden, and B. N. Lambrecht.** 2004. Differential capacity of CD8+ alpha or CD8-alpha dendritic cell subsets to prime for eosinophilic airway inflammation in the T-helper type 2-prone milieu of the lung. *Clin Exp Allergy* **34**:1834-40.
122. **Handforth, J., J. S. Friedland, and M. Sharland.** 2000. Basic epidemiology and immunopathology of RSV in children. *Paediatr Respir Rev* **1**:210-4.
123. **Harrison, A. M., N. M. Boeing, J. B. Domachowske, M. R. Piedmonte, and R. K. Kanter.** 2001. Effect of RSV bronchiolitis practice guidelines on resource utilization. *Clin Pediatr (Phila)* **40**:489-95.
124. **Harter, D. H., and P. W. Choppin.** 1967. Studies on pneumonia virus of mice (PVM) in cell culture. I. Replication in baby hamster kidney cells and properties of the virus. *J Exp Med* **126**:251-66.
125. **Hemming, V. G., G. A. Prince, R. L. Horswood, W. J. London, B. R. Murphy, E. E. Walsh, G. W. Fischer, L. E. Weisman, P. A. Baron, and R. M. Chanock.** 1985. Studies of passive immunotherapy for infections of respiratory syncytial virus in the respiratory tract of a primate model. *J Infect Dis* **152**:1083-7.
126. **Henderson, F. W., A. M. Collier, W. A. Clyde, Jr., and F. W. Denny.** 1979. Respiratory-syncytial-virus infections, reinfections and immunity. A prospective, longitudinal study in young children. *N Engl J Med* **300**:530-4.
127. **Hendricks, D. A., K. McIntosh, and J. L. Patterson.** 1988. Further characterization of the soluble form of the G glycoprotein of respiratory syncytial virus. *J Virol* **62**:2228-33.
128. **Hendry, R. M., A. L. Talis, E. Godfrey, L. J. Anderson, B. F. Fernie, and K. McIntosh.** 1986. Concurrent circulation of antigenically distinct strains of respiratory syncytial virus during community outbreaks. *J Infect Dis* **153**:291-7.
129. **Hertz, M. I., J. A. Englund, D. Snover, P. B. Bitterman, and P. B. McGlave.** 1989. Respiratory syncytial virus-induced acute lung injury in adult patients with bone marrow transplants: a clinical approach and review of the literature. *Medicine (Baltimore)* **68**:269-81.

130. **Hildreth, S. W., Baggs, R. B., Eichberg, J. W., Johnson, C., Arumugham, R. G., Paradiso, P. R.** 1989. A parenterally administered subunit RSV vaccine: Safety studies in animals and adult humans. *Pediatric Research* **25**:180A.
131. **Hirotsu, T., P. Y. Lee, H. Kuwata, M. Yamamoto, M. Matsumoto, I. Kawase, S. Akira, and K. Takeda.** 2005. The nuclear IkappaB protein IkappaBNS selectively inhibits lipopolysaccharide-induced IL-6 production in macrophages of the colonic lamina propria. *J Immunol* **174**:3650-7.
132. **Ho, P. P., P. Fontoura, P. J. Ruiz, L. Steinman, and H. Garren.** 2003. An immunomodulatory GpG oligonucleotide for the treatment of autoimmunity via the innate and adaptive immune systems. *J Immunol* **171**:4920-6.
133. **Hoebee, B., L. Bont, E. Rietveld, M. van Oosten, H. M. Hodemaekers, N. J. Nagelkerke, H. J. Neijens, J. L. Kimpfen, and T. G. Kimman.** 2004. Influence of promoter variants of interleukin-10, interleukin-9, and tumor necrosis factor-alpha genes on respiratory syncytial virus bronchiolitis. *J Infect Dis* **189**:239-47.
134. **Holt, P. G., and P. A. Stumbles.** 2000. Regulation of immunologic homeostasis in peripheral tissues by dendritic cells: the respiratory tract as a paradigm. *J Allergy Clin Immunol* **105**:421-9.
135. **Hornsleth, A., B. Klug, M. Nir, J. Johansen, K. S. Hansen, L. S. Christensen, and L. B. Larsen.** 1998. Severity of respiratory syncytial virus disease related to type and genotype of virus and to cytokine values in nasopharyngeal secretions. *Pediatr Infect Dis J* **17**:1114-21.
136. **Horsfall, F. L., and E.C. Curnen** 1946. Studies on pneumonia virus of mice : II. Immunological evidence of latent infection with the virus in numerous mammalian species *The Journal of Experimental Medicine* **83**:43-64.
137. **Horsfall, F. L., and R.G. Hahn.** 1939. A Pneumonia virus of Swiss mice. *Proceedings of the Society for Experimental Biology and Medicine* **40**:684-686.
138. **Horsfall, F. L., and R.G. Hahn** 1940. A latent virus in normal mice capable of producing pneumonia in its natural host *The Journal of Experimental Medicine* **71**:391-408.
139. **Hruska, J. F., P. E. Morrow, S. C. Suffin, and R. G. Douglas, Jr.** 1982. In vivo inhibition of respiratory syncytial virus by ribavirin. *Antimicrob Agents Chemother* **21**:125-30.
140. **Hsu, K. H., M. D. Lubeck, A. R. Davis, R. A. Bhat, B. H. Selling, B. M. Bhat, S. Mizutani, B. R. Murphy, P. L. Collins, R. M. Chanock, and et al.** 1992. Immunogenicity of recombinant adenovirus-respiratory syncytial virus vaccines with adenovirus types 4, 5, and 7 vectors in dogs and a chimpanzee. *J Infect Dis* **166**:769-75.
141. **Hull, J.** 2007. Genetic susceptibility to RSV disease, p. 115-140. *In* P. A. Cane (ed.), *Respiratory syncytial virus*, vol. 14. Elsevier, Amsterdam.
142. **Hussell, T., A. Georgiou, T. E. Sparer, S. Matthews, P. Pala, and P. J. Openshaw.** 1998. Host genetic determinants of vaccine-induced eosinophilia during respiratory syncytial virus infection. *J Immunol* **161**:6215-22.
143. **Inaba, K., M. Inaba, M. Deguchi, K. Hagi, R. Yasumizu, S. Ikehara, S. Muramatsu, and R. M. Steinman.** 1993. Granulocytes, macrophages, and dendritic cells arise from a common major histocompatibility complex class II-negative progenitor in mouse bone marrow. *Proc Natl Acad Sci U S A* **90**:3038-42.

144. **Inaba, K., M. Inaba, N. Romani, H. Aya, M. Deguchi, S. Ikehara, S. Muramatsu, and R. M. Steinman.** 1992. Generation of large numbers of dendritic cells from mouse bone marrow cultures supplemented with granulocyte/macrophage colony-stimulating factor. *J Exp Med* **176**:1693-702.
145. **Isaacs, D.** 1991. Viral subunit vaccines. *Lancet* **337**:1223-4.
146. **Jackson, M., and R. Scott.** 1996. Different patterns of cytokine induction in cultures of respiratory syncytial (RS) virus-specific human TH cell lines following stimulation with RS virus and RS virus proteins. *J Med Virol* **49**:161-9.
147. **Johnson, P. R., M. K. Spriggs, R. A. Olmsted, and P. L. Collins.** 1987. The G glycoprotein of human respiratory syncytial viruses of subgroups A and B: extensive sequence divergence between antigenically related proteins. *Proc Natl Acad Sci U S A* **84**:5625-9.
148. **Johnston, S. L., P. K. Pattemore, G. Sanderson, S. Smith, F. Lampe, L. Josephs, P. Symington, S. O'Toole, S. H. Myint, D. A. Tyrrell, and et al.** 1995. Community study of role of viral infections in exacerbations of asthma in 9-11 year old children. *Bmj* **310**:1225-9.
149. **Kaech, S. M., E. J. Wherry, and R. Ahmed.** 2002. Effector and memory T-cell differentiation: implications for vaccine development. *Nat Rev Immunol* **2**:251-62.
150. **Kakuk, T. J., K. Soike, R. J. Brideau, R. M. Zaya, S. L. Cole, J. Y. Zhang, E. D. Roberts, P. A. Wells, and M. W. Wathen.** 1993. A human respiratory syncytial virus (RSV) primate model of enhanced pulmonary pathology induced with a formalin-inactivated RSV vaccine but not a recombinant FG subunit vaccine. *J Infect Dis* **167**:553-61.
151. **Kapikian, A. Z., J. A. Bell, F. M. Mastrota, K. M. Johnson, R. J. Huebner, and R. M. Chanock.** 1961. An outbreak of febrile illness and pneumonia associated with respiratory syncytial virus infection. *Am J Hyg* **74**:234-48.
152. **Kelsall, B. L., C. A. Biron, O. Sharma, and P. M. Kaye.** 2002. Dendritic cells at the host-pathogen interface. *Nat Immunol* **3**:699-702.
153. **Kerr, M. H., and J. Y. Paton.** 1999. Surfactant protein levels in severe respiratory syncytial virus infection. *Am J Respir Crit Care Med* **159**:1115-8.
154. **Kim, H. W., J. O. Arrobio, C. D. Brandt, P. Wright, D. Hodes, R. M. Chanock, and R. H. Parrott.** 1973. Safety and antigenicity of temperature sensitive (TS) mutant respiratory syncytial virus (RSV) in infants and children. *Pediatrics* **52**:56-63.
155. **Kim, H. W., J. G. Canchola, C. D. Brandt, G. Pyles, R. M. Chanock, K. Jensen, and R. H. Parrott.** 1969. Respiratory syncytial virus disease in infants despite prior administration of antigenic inactivated vaccine. *Am J Epidemiol* **89**:422-34.
156. **King, J. C., Jr.** 1997. Community respiratory viruses in individuals with human immunodeficiency virus infection. *Am J Med* **102**:19-24; discussion 25-6.
157. **King, J. C., Jr., A. R. Burke, J. D. Clemens, P. Nair, J. J. Farley, P. E. Vink, S. R. Batlas, M. Rao, and J. P. Johnson.** 1993. Respiratory syncytial virus illnesses in human immunodeficiency virus- and noninfected children. *Pediatr Infect Dis J* **12**:733-9.
158. **Kneyber, M. C., A. H. Brandenburg, P. H. Rothbarth, R. de Groot, A. Ott, and H. A. van Steensel-Moll.** 1996. Relationship between clinical severity of respiratory syncytial virus infection and subtype. *Arch Dis Child* **75**:137-40.
159. **Krempl, C. D., and P. L. Collins.** 2004. Reevaluation of the virulence of prototypic strain 15 of pneumonia virus of mice. *J Virol* **78**:13362-5.

160. **Krempl, C. D., E. W. Lamirande, and P. L. Collins.** 2005. Complete sequence of the RNA genome of pneumonia virus of mice (PVM). *Virus Genes* **30**:237-49.
161. **Kristjansson, S., S. P. Bjarnarson, G. Wennergren, A. H. Palsdottir, T. Arnadottir, A. Haraldsson, and I. Jonsdottir.** 2005. Respiratory syncytial virus and other respiratory viruses during the first 3 months of life promote a local TH2-like response. *J Allergy Clin Immunol* **116**:805-11.
162. **Kronin, V., K. Winkel, G. Suss, A. Kelso, W. Heath, J. Kirberg, H. von Boehmer, and K. Shortman.** 1996. A subclass of dendritic cells regulates the response of naive CD8 T cells by limiting their IL-2 production. *J Immunol* **157**:3819-27.
163. **Kurt-Jones, E. A., L. Popova, L. Kwinn, L. M. Haynes, L. P. Jones, R. A. Tripp, E. E. Walsh, M. W. Freeman, D. T. Golenbock, L. J. Anderson, and R. W. Finberg.** 2000. Pattern recognition receptors TLR4 and CD14 mediate response to respiratory syncytial virus. *Nat Immunol* **1**:398-401.
164. **Laemmli, U. K.** 1970. Cleavage of structural proteins during the assembly of the head of bacteriophage T4. *Nature* **227**:680-5.
165. **Laham, F. R., V. Israele, J. M. Casellas, A. M. Garcia, C. M. Lac Prugent, S. J. Hoffman, D. Hauer, B. Thumar, M. I. Name, A. Pascual, N. Taratutto, M. T. Ishida, M. Balduzzi, M. Maccarone, S. Jackli, R. Passarino, R. A. Gaivironsky, R. A. Karron, N. R. Polack, and F. P. Polack.** 2004. Differential production of inflammatory cytokines in primary infection with human metapneumovirus and with other common respiratory viruses of infancy. *J Infect Dis* **189**:2047-56.
166. **Lambrecht, B. N., J. B. Prins, and H. C. Hoogsteden.** 2001. Lung dendritic cells and host immunity to infection. *Eur Respir J* **18**:692-704.
167. **Lanzavecchia, A., and F. Sallusto.** 2001. Regulation of T cell immunity by dendritic cells. *Cell* **106**:263-6.
168. **Laskay, T., A. Diefenbach, M. Rollinghoff, and W. Solbach.** 1995. Early parasite containment is decisive for resistance to *Leishmania major* infection. *Eur J Immunol* **25**:2220-7.
169. **Law, B., E. E. L. Wang, and N. MacDonald.** 1997. Does Ribavirin Impact on the Hospital Course of Children With Respiratory Syncytial Virus (RSV) Infection? An Analysis Using the Pediatric Investigators Collaborative Network on Infections in Canada (PICNIC) RSV Database *PEDIATRICS* **99**: [Online.] <http://pediatrics.aappublications.org/cgi/content/abstract/99/3/e7> [22 November 2007, last date accessed].
170. **Leenen, P. J., K. Radosevic, J. S. Voerman, B. Salomon, N. van Rooijen, D. Klatzmann, and W. van Ewijk.** 1998. Heterogeneity of mouse spleen dendritic cells: in vivo phagocytic activity, expression of macrophage markers, and subpopulation turnover. *J Immunol* **160**:2166-73.
171. **Legg, J. P., I. R. Hussain, J. A. Warner, S. L. Johnston, and J. O. Warner.** 2003. Type 1 and type 2 cytokine imbalance in acute respiratory syncytial virus bronchiolitis. *Am J Respir Crit Care Med* **168**:633-9.
172. **Levy, B. T., and M. A. Graber.** 1997. Respiratory syncytial virus infection in infants and young children. *J Fam Pract* **45**:473-81.
173. **Lipscomb, M. F., and B. J. Masten.** 2002. Dendritic cells: immune regulators in health and disease. *Physiol Rev* **82**:97-130.

174. **Lutz, M. B., N. Kukutsch, A. L. Ogilvie, S. Rossner, F. Koch, N. Romani, and G. Schuler.** 1999. An advanced culture method for generating large quantities of highly pure dendritic cells from mouse bone marrow. *J Immunol Methods* **223**:77-92.
175. **Lydyard M.P., and Grossi E.C.** 2001. Cells, tissues and organs of the immune system, p. 28-29. *In* Roitt I., Brostoff J., and Male D. (ed.), *Immunology*, Sixth ed. Mosby, Edinburgh; NY.
176. **Ma, X.** 2001. TNF-alpha and IL-12: a balancing act in macrophage functioning. *Microbes Infect* **3**:121-9.
177. **Macatonia, S. E., T. M. Doherty, S. C. Knight, and A. O'Garra.** 1993. Differential effect of IL-10 on dendritic cell-induced T cell proliferation and IFN-gamma production. *J Immunol* **150**:3755-65.
178. **MacDonald, N. E., C. B. Hall, S. C. Suffin, C. Alexson, P. J. Harris, and J. A. Manning.** 1982. Respiratory syncytial viral infection in infants with congenital heart disease. *N Engl J Med* **307**:397-400.
179. **Male, D.** 2001. Cell-mediated cytotoxicity, p. 167-168. *In* Roitt I., Brostoff J., and Male D. (ed.), *Immunology*, Sixth ed. Mosby, Edinburgh; NY.
180. **Malley, R., J. DeVincenzo, O. Ramilo, P. H. Dennehy, H. C. Meissner, W. C. Gruber, P. J. Sanchez, H. Jafri, J. Balsley, D. Carlin, S. Buckingham, L. Vernacchio, and D. M. Ambrosino.** 1998. Reduction of respiratory syncytial virus (RSV) in tracheal aspirates in intubated infants by use of humanized monoclonal antibody to RSV F protein. *J Infect Dis* **178**:1555-61.
181. **Martinello, R. A., M. D. Chen, C. Weibel, and J. S. Kahn.** 2002. Correlation between respiratory syncytial virus genotype and severity of illness. *J Infect Dis* **186**:839-42.
182. **Martinez, F. D., W. J. Morgan, A. L. Wright, C. J. Holberg, and L. M. Taussig.** 1988. Diminished lung function as a predisposing factor for wheezing respiratory illness in infants. *N Engl J Med* **319**:1112-7.
183. **Martinez, F. D., A. L. Wright, L. M. Taussig, C. J. Holberg, M. Halonen, and W. J. Morgan.** 1995. Asthma and wheezing in the first six years of life. The Group Health Medical Associates. *N Engl J Med* **332**:133-8.
184. **Matsuno, K., T. Ezaki, S. Kudo, and Y. Uehara.** 1996. A life stage of particle-laden rat dendritic cells in vivo: their terminal division, active phagocytosis, and translocation from the liver to the draining lymph. *J Exp Med* **183**:1865-78.
185. **McIntosh, K., and J. M. Fishaut.** 1980. Immunopathologic mechanisms in lower respiratory tract disease of infants due to respiratory syncytial virus. *Prog Med Virol* **26**:94-118.
186. **Meissner, H. C.** 2003. Selected populations at increased risk from respiratory syncytial virus infection. *Pediatr Infect Dis J* **22**:S40-4; discussion S44-5.
187. **Mejias, A., S. Chavez-Bueno, A. M. Rios, J. Saavedra-Lozano, M. Fonseca Aten, J. Hatfield, P. Kapur, A. M. Gomez, H. S. Jafri, and O. Ramilo.** 2004. Anti-respiratory syncytial virus (RSV) neutralizing antibody decreases lung inflammation, airway obstruction, and airway hyperresponsiveness in a murine RSV model. *Antimicrob Agents Chemother* **48**:1811-22.
188. **Meurman, O., O. Ruuskanen, H. Sarkkinen, P. Hanninen, and P. Halonen.** 1984. Immunoglobulin class-specific antibody response in respiratory syncytial virus infection measured by enzyme immunoassay. *J Med Virol* **14**:67-72.

189. **Meyer, K. C.** 2001. The role of immunity in susceptibility to respiratory infection in the aging lung. *Respir Physiol* **128**:23-31.
190. **Midulla, F., Y. T. Huang, I. A. Gilbert, N. M. Cirino, E. R. McFadden, Jr., and J. R. Panuska.** 1989. Respiratory syncytial virus infection of human cord and adult blood monocytes and alveolar macrophages. *Am Rev Respir Dis* **140**:771-7.
191. **Miyata, H., M. Kishikawa, H. Kondo, C. Kai, Y. Watanabe, K. Ohsawa, and H. Sato.** 1995. New isolates of pneumonia virus of mice (PVM) from Japanese rat colonies and their characterization. *Exp Anim* **44**:95-104.
192. **Monick, M. M., T. O. Yarovinsky, L. S. Powers, N. S. Butler, A. B. Carter, G. Gudmundsson, and G. W. Hunninghake.** 2003. Respiratory syncytial virus up-regulates TLR4 and sensitizes airway epithelial cells to endotoxin. *J Biol Chem* **278**:53035-44.
193. **Morton, C. J., R. Cameron, L. J. Lawrence, B. Lin, M. Lowe, A. Luttick, A. Mason, J. McKimm-Breschkin, M. W. Parker, J. Ryan, M. Smout, J. Sullivan, S. P. Tucker, and P. R. Young.** 2003. Structural characterization of respiratory syncytial virus fusion inhibitor escape mutants: homology model of the F protein and a syncytium formation assay. *Virology* **311**:275-88.
194. **Morton, D. B., and P. H. Griffiths.** 1985. Guidelines on the recognition of pain, distress and discomfort in experimental animals and an hypothesis for assessment. *Vet Rec* **116**:431-6.
195. **Mouse Genome Database (MGD), M. G. I. W. S., The Jackson Laboratory, Bar Harbor, Maine. World Wide Web (URL: http://www.informatics.jax.org/mgihome/other/mouse_facts3.shtml).** last database update: December 27, 2007, posting date. *Mouse Physiology* [Online.]
196. **Mufson, M. A., R. B. Belshe, C. Orvell, and E. Norrby.** 1987. Subgroup characteristics of respiratory syncytial virus strains recovered from children with two consecutive infections. *J Clin Microbiol* **25**:1535-9.
197. **Mufson, M. A., C. Orvell, B. Rafnar, and E. Norrby.** 1985. Two distinct subtypes of human respiratory syncytial virus. *J Gen Virol* **66 (Pt 10)**:2111-24.
198. **Murphy, B. R.** 2005. Mucosal immunity to virusis. *In* J. E. A. Mestecky (ed.), *Mucosal Immunity*. Elsevier Academic Press, Amsterdam.
199. **Murphy, B. R., D. W. Alling, M. H. Snyder, E. E. Walsh, G. A. Prince, R. M. Chanock, V. G. Hemming, W. J. Rodriguez, H. W. Kim, B. S. Graham, and et al.** 1986. Effect of age and preexisting antibody on serum antibody response of infants and children to the F and G glycoproteins during respiratory syncytial virus infection. *J Clin Microbiol* **24**:894-8.
200. **Murphy, B. R., S. L. Hall, A. B. Kulkarni, J. E. Crowe, Jr., P. L. Collins, M. Connors, R. A. Karron, and R. M. Chanock.** 1994. An update on approaches to the development of respiratory syncytial virus (RSV) and parainfluenza virus type 3 (PIV3) vaccines. *Virus Res* **32**:13-36.
201. **Murphy, G. F., D. Messadi, E. Fonferko, and W. W. Hancock.** 1986. Phenotypic transformation of macrophages to Langerhans cells in the skin. *Am J Pathol* **123**:401-6.
202. **Nelson, D. J., C. McMenam, A. S. McWilliam, M. Brenan, and P. G. Holt.** 1994. Development of the airway intraepithelial dendritic cell network in the rat from class II major histocompatibility (Ia)-negative precursors: differential regulation of Ia expression at different levels of the respiratory tract. *J Exp Med* **179**:203-12.

203. **Nicholson, K. G.** 1996. Impact of influenza and respiratory syncytial virus on mortality in England and Wales from January 1975 to December 1990. *Epidemiol Infect* **116**:51-63.
204. **Nicholson, K. G., J. Kent, V. Hammersley, and E. Cancio.** 1997. Acute viral infections of upper respiratory tract in elderly people living in the community: comparative, prospective, population based study of disease burden. *Bmj* **315**:1060-4.
205. **Nicholson, K. G., J. Kent, and D. C. Ireland.** 1993. Respiratory viruses and exacerbations of asthma in adults. *Bmj* **307**:982-6.
206. **Niess, J. H., S. Brand, X. Gu, L. Landsman, S. Jung, B. A. McCormick, J. M. Vyas, M. Boes, H. L. Ploegh, J. G. Fox, D. R. Littman, and H. C. Reinecker.** 2005. CX3CR1-mediated dendritic cell access to the intestinal lumen and bacterial clearance. *Science* **307**:254-8.
207. **Noah, T. L., and S. Becker.** 2000. Chemokines in nasal secretions of normal adults experimentally infected with respiratory syncytial virus. *Clin Immunol* **97**:43-9.
208. **Noah, T. L., and S. Becker.** 1993. Respiratory syncytial virus-induced cytokine production by a human bronchial epithelial cell line. *Am J Physiol* **265**:L472-8.
209. **Noah, T. L., S. S. Ivins, P. Murphy, I. Kazachkova, B. Moats-Staats, and F. W. Henderson.** 2002. Chemokines and inflammation in the nasal passages of infants with respiratory syncytial virus bronchiolitis. *Clin Immunol* **104**:86-95.
210. **Norbury, C. C.** 2006. Drinking a lot is good for dendritic cells. *Immunology* **117**:443-51.
211. **Ogra, P. L.** 2004. Respiratory syncytial virus: the virus, the disease and the immune response. *Paediatr Respir Rev* **5 Suppl A**:S119-26.
212. **Olmsted, R. A., and P. L. Collins.** 1989. The 1A protein of respiratory syncytial virus is an integral membrane protein present as multiple, structurally distinct species. *J Virol* **63**:2019-29.
213. **Olszewska-Pazdrak, B., A. Casola, T. Saito, R. Alam, S. E. Crowe, F. Mei, P. L. Ogra, and R. P. Garofalo.** 1998. Cell-specific expression of RANTES, MCP-1, and MIP-1alpha by lower airway epithelial cells and eosinophils infected with respiratory syncytial virus. *J Virol* **72**:4756-64.
214. **Openshaw, P., S. Edwards, and P. Helms.** 1984. Changes in rib cage geometry during childhood. *Thorax* **39**:624-7.
215. **Openshaw, P. J., and J. S. Tregoning.** 2005. Immune responses and disease enhancement during respiratory syncytial virus infection. *Clin Microbiol Rev* **18**:541-55.
216. **Ostler, T., T. Hussell, C. D. Surh, P. Openshaw, and S. Ehl.** 2001. Long-term persistence and reactivation of T cell memory in the lung of mice infected with respiratory syncytial virus. *Eur J Immunol* **31**:2574-82.
217. **Paccaud, M. F., and C. Jacquier.** 1970. A respiratory syncytial virus of bovine origin. *Arch Gesamte Virusforsch* **30**:327-42.
218. **Panuska, J. R., M. I. Hertz, H. Taraf, A. Villani, and N. M. Cirino.** 1992. Respiratory syncytial virus infection of alveolar macrophages in adult transplant patients. *Am Rev Respir Dis* **145**:934-9.
219. **Parrott, R. H., H. W. Kim, J. O. Arrobio, D. S. Hodes, B. R. Murphy, C. D. Brandt, E. Camargo, and R. M. Chanock.** 1973. Epidemiology of respiratory syncytial virus infection in Washington, D.C. II. Infection and disease with respect to age, immunologic status, race and sex. *Am J Epidemiol* **98**:289-300.

220. **Patterson, S.** 2000. Flexibility and cooperation among dendritic cells. *Nat Immunol* **1**:273-4.
221. **Pearson, H. E., and M.D. Eaton.** 1940. A virus pneumonia of syrian hamsters. *Proceedings of the Society for Experimental Biology and Medicine* **45**:677-679.
222. **Pierre, P., S. J. Turley, E. Gatti, M. Hull, J. Meltzer, A. Mirza, K. Inaba, R. M. Steinman, and I. Mellman.** 1997. Developmental regulation of MHC class II transport in mouse dendritic cells. *Nature* **388**:787-92.
223. **Pinto, R. A., S. M. Arredondo, M. R. Bono, A. A. Gaggero, and P. V. Diaz.** 2006. T helper 1/T helper 2 cytokine imbalance in respiratory syncytial virus infection is associated with increased endogenous plasma cortisol. *Pediatrics* **117**:e878-86.
224. **Plotnicky-Gilquin, H., D. Cyblat-Chanal, J. P. Aubry, T. Champion, A. Beck, T. Nguyen, J. Y. Bonnefoy, and N. Corvaia.** 2002. Gamma interferon-dependent protection of the mouse upper respiratory tract following parenteral immunization with a respiratory syncytial virus G protein fragment. *J Virol* **76**:10203-10.
225. **Poccia, F., R. Cicconi, D. Frasca, C. Mancini, V. Colizzi, and G. Doria.** 1998. Age-related propensity to peripheral expansion of Vgamma3+ gammadelta+ T lymphocytes after irradiation and bone marrow transplantation. *Int Immunol* **10**:547-51.
226. **Power, C. A., D. J. Church, A. Meyer, S. Alouani, A. E. Proudfoot, I. Clark-Lewis, S. Sozzani, A. Mantovani, and T. N. Wells.** 1997. Cloning and characterization of a specific receptor for the novel CC chemokine MIP-3alpha from lung dendritic cells. *J Exp Med* **186**:825-35.
227. **Prince, G. A., S. J. Curtis, K. C. Yim, and D. D. Porter.** 2001. Vaccine-enhanced respiratory syncytial virus disease in cotton rats following immunization with Lot 100 or a newly prepared reference vaccine. *J Gen Virol* **82**:2881-8.
228. **Prince, G. A., V. G. Hemming, R. L. Horswood, P. A. Baron, and R. M. Chanock.** 1987. Effectiveness of topically administered neutralizing antibodies in experimental immunotherapy of respiratory syncytial virus infection in cotton rats. *J Virol* **61**:1851-4.
229. **Prince, G. A., V. G. Hemming, R. L. Horswood, and R. M. Chanock.** 1985. Immunoprophylaxis and immunotherapy of respiratory syncytial virus infection in the cotton rat. *Virus Res* **3**:193-206.
230. **Prince, G. A., R. L. Horswood, J. Berndt, S. C. Suffin, and R. M. Chanock.** 1979. Respiratory syncytial virus infection in inbred mice. *Infect Immun* **26**:764-6.
231. **Prince, G. A., R. L. Horswood, and R. M. Chanock.** 1985. Quantitative aspects of passive immunity to respiratory syncytial virus infection in infant cotton rats. *J Virol* **55**:517-20.
232. **Prince, G. A., A. B. Jenson, V. G. Hemming, B. R. Murphy, E. E. Walsh, R. L. Horswood, and R. M. Chanock.** 1986. Enhancement of respiratory syncytial virus pulmonary pathology in cotton rats by prior intramuscular inoculation of formalin-inactivated virus. *J Virol* **57**:721-8.
233. **Prince, G. A., A. B. Jenson, R. L. Horswood, E. Camargo, and R. M. Chanock.** 1978. The pathogenesis of respiratory syncytial virus infection in cotton rats. *Am J Pathol* **93**:771-91.
234. **Prince, G. A., S. C. Suffin, D. A. Prevar, E. Camargo, D. L. Sly, W. T. London, and R. M. Chanock.** 1979. Respiratory syncytial virus infection in owl monkeys: viral shedding, immunological response, and associated illness caused by wild-type virus and two temperature-sensitive mutants. *Infect Immun* **26**:1009-13.

235. **Pringle, C. R., and R. P. Eglin.** 1986. Murine pneumonia virus: seroepidemiological evidence of widespread human infection. *J Gen Virol* **67 (Pt 6)**:975-82.
236. **Pulendran, B.** 2004. Modulating vaccine responses with dendritic cells and Toll-like receptors. *Immunol Rev* **199**:227-50.
237. **Pulendran, B., J. Lingappa, M. K. Kennedy, J. Smith, M. Teepe, A. Rudensky, C. R. Maliszewski, and E. Maraskovsky.** 1997. Developmental pathways of dendritic cells in vivo: distinct function, phenotype, and localization of dendritic cell subsets in FLT3 ligand-treated mice. *J Immunol* **159**:2222-31.
238. **Pullan, C. R., and E. N. Hey.** 1982. Wheezing, asthma, and pulmonary dysfunction 10 years after infection with respiratory syncytial virus in infancy. *Br Med J (Clin Res Ed)* **284**:1665-9.
239. **Randhawa, J. S., P. Chambers, C. R. Pringle, and A. J. Easton.** 1995. Nucleotide sequences of the genes encoding the putative attachment glycoprotein (G) of mouse and tissue culture-passaged strains of pneumonia virus of mice. *Virology* **207**:240-5.
240. **Richardson, L. S., R. B. Belshe, W. T. London, D. L. Sly, D. A. Prevar, E. Camargo, and R. M. Chanock.** 1978. Evaluation of five temperature-sensitive mutants of respiratory syncytial virus in primates: I. Viral shedding, immunologic response, and associated illness. *J Med Virol* **3**:91-100.
241. **Richardson, L. S., R. B. Belshe, D. L. Sly, W. T. London, D. A. Prevar, E. Camargo, and R. M. Chanock.** 1978. Experimental respiratory syncytial virus pneumonia in cebus monkeys. *J Med Virol* **2**:45-59.
242. **Richter, B. W., J. M. Onuska, S. Niewiesk, G. A. Prince, and M. C. Eichelberger.** 2005. Antigen-dependent proliferation and cytokine induction in respiratory syncytial virus-infected cotton rats reflect the presence of effector-memory T cells. *Virology* **337**:102-10.
243. **Riedl, E., J. Stockl, O. Majdic, C. Scheinecker, W. Knapp, and H. Strobl.** 2000. Ligation of E-cadherin on in vitro-generated immature Langerhans-type dendritic cells inhibits their maturation. *Blood* **96**:4276-84.
244. **Rimoldi, M., M. Chieppa, V. Salucci, F. Avogadri, A. Sonzogni, G. M. Sampietro, A. Nespoli, G. Viale, P. Allavena, and M. Rescigno.** 2005. Intestinal immune homeostasis is regulated by the crosstalk between epithelial cells and dendritic cells. *Nat Immunol* **6**:507-14.
245. **Rimoldi, M., M. Chieppa, M. Vulcano, P. Allavena, and M. Rescigno.** 2004. Intestinal epithelial cells control dendritic cell function. *Ann N Y Acad Sci* **1029**:66-74.
246. **Rossow, K. D., J. E. Collins, S. M. Goyal, E. A. Nelson, J. Christopher-Hennings, and D. A. Benfield.** 1995. Pathogenesis of porcine reproductive and respiratory syndrome virus infection in gnotobiotic pigs. *Vet Pathol* **32**:361-73.
247. **Ruuskanen, O., and P. L. Ogra.** 1993. Respiratory syncytial virus. *Curr Probl Pediatr* **23**:50-79.
248. **Sallusto, F., M. Cella, C. Danieli, and A. Lanzavecchia.** 1995. Dendritic cells use macropinocytosis and the mannose receptor to concentrate macromolecules in the major histocompatibility complex class II compartment: downregulation by cytokines and bacterial products. *J Exp Med* **182**:389-400.
249. **Sallusto, F., J. Geginat, and A. Lanzavecchia.** 2004. Central memory and effector memory T cell subsets: function, generation, and maintenance. *Annu Rev Immunol* **22**:745-63.

250. **Sallusto, F., D. Lenig, R. Forster, M. Lipp, and A. Lanzavecchia.** 1999. Two subsets of memory T lymphocytes with distinct homing potentials and effector functions. *Nature* **401**:708-12.
251. **Sampalis, J. S.** 2003. Morbidity and mortality after RSV-associated hospitalizations among premature Canadian infants. *J Pediatr* **143**:S150-6.
252. **Sato, A., M. Hashiguchi, E. Toda, A. Iwasaki, S. Hachimura, and S. Kaminogawa.** 2003. CD11b⁺ Peyer's patch dendritic cells secrete IL-6 and induce IgA secretion from naive B cells. *J Immunol* **171**:3684-90.
253. **Saunders, D., K. Lucas, J. Ismaili, L. Wu, E. Maraskovsky, A. Dunn, and K. Shortman.** 1996. Dendritic cell development in culture from thymic precursor cells in the absence of granulocyte/macrophage colony-stimulating factor. *J Exp Med* **184**:2185-96.
254. **Scheicher, C., M. Mehlig, R. Zecher, and K. Reske.** 1992. Dendritic cells from mouse bone marrow: in vitro differentiation using low doses of recombinant granulocyte-macrophage colony-stimulating factor. *J Immunol Methods* **154**:253-64.
255. **Schlender, J., B. Bossert, U. Buchholz, and K. K. Conzelmann.** 2000. Bovine respiratory syncytial virus nonstructural proteins NS1 and NS2 cooperatively antagonize alpha/beta interferon-induced antiviral response. *J Virol* **74**:8234-42.
256. **Schlender, J., G. Walliser, J. Fricke, and K. K. Conzelmann.** 2002. Respiratory syncytial virus fusion protein mediates inhibition of mitogen-induced T-cell proliferation by contact. *J Virol* **76**:1163-70.
257. **Schreiber, P., J. P. Matheise, F. Dessy, M. Heimann, J. J. Letesson, P. Coppe, and A. Collard.** 2000. High mortality rate associated with bovine respiratory syncytial virus (BRSV) infection in Belgian white blue calves previously vaccinated with an inactivated BRSV vaccine. *J Vet Med B Infect Dis Vet Public Health* **47**:535-50.
258. **Schrum, S., P. Probst, B. Fleischer, and P. F. Zipfel.** 1996. Synthesis of the CC-chemokines MIP-1alpha, MIP-1beta, and RANTES is associated with a type 1 immune response. *J Immunol* **157**:3598-604.
259. **Schwarze, J., D. R. O'Donnell, A. Rohwedder, and P. J. Openshaw.** 2004. Latency and persistence of respiratory syncytial virus despite T cell immunity. *Am J Respir Crit Care Med* **169**:801-5.
260. **Scott, P., A. Eaton, W. C. Gause, X. di Zhou, and B. Hondowicz.** 1996. Early IL-4 production does not predict susceptibility to *Leishmania major*. *Exp Parasitol* **84**:178-87.
261. **Shay, D. K., R. C. Holman, R. D. Newman, L. L. Liu, J. W. Stout, and L. J. Anderson.** 1999. Bronchiolitis-associated hospitalizations among US children, 1980-1996. *Jama* **282**:1440-6.
262. **Shigeta, S., Y. Hinuma, T. Suto, and N. Ishida.** 1968. The cell to cell infection of respiratory syncytial virus in HEP-2 monolayer cultures. *J Gen Virol* **3**:129-31.
263. **Shimonaski, G., and P. E. Came.** 1970. Plaque assay for pneumonia virus of mice. *Appl Microbiol* **20**:775-7.
264. **Siber, G. R., D. Leombruno, J. Leszczynski, J. McIver, D. Bodkin, R. Gonin, C. M. Thompson, E. E. Walsh, P. A. Piedra, V. G. Hemming, and et al.** 1994. Comparison of antibody concentrations and protective activity of respiratory syncytial virus immune globulin and conventional immune globulin. *J Infect Dis* **169**:1368-73.

265. **Sigurs, N., R. Bjarnason, F. Sigurbergsson, and B. Kjellman.** 2000. Respiratory syncytial virus bronchiolitis in infancy is an important risk factor for asthma and allergy at age 7. *Am J Respir Crit Care Med* **161**:1501-7.
266. **Sigurs, N., P. M. Gustafsson, R. Bjarnason, F. Lundberg, S. Schmidt, F. Sigurbergsson, and B. Kjellman.** 2005. Severe respiratory syncytial virus bronchiolitis in infancy and asthma and allergy at age 13. *Am J Respir Crit Care Med* **171**:137-41.
267. **Silvestri, M., F. Sabatini, A. C. Defilippi, and G. A. Rossi.** 2004. The wheezy infant -- immunological and molecular considerations. *Paediatr Respir Rev* **5 Suppl A**:S81-7.
268. **Simoës, E. A.** 2003. Environmental and demographic risk factors for respiratory syncytial virus lower respiratory tract disease. *J Pediatr* **143**:S118-26.
269. **Simoës, E. A.** 1995. Natural and vaccine induced immunity to RSV primates. NIH publication no R01 AI37271-02. Bethesda, Maryland: National Institutes of Health.
270. **Singleton, R. J., K. M. Petersen, J. E. Berner, E. Schulte, K. Chiu, C. M. Lilly, E. A. Hughes, L. R. Bulkow, and T. L. Nix.** 1995. Hospitalizations for respiratory syncytial virus infection in Alaska Native children. *Pediatr Infect Dis J* **14**:26-30.
271. **Skeen, M. J., M. A. Miller, T. M. Shinnick, and H. K. Ziegler.** 1996. Regulation of murine macrophage IL-12 production. Activation of macrophages in vivo, restimulation in vitro, and modulation by other cytokines. *J Immunol* **156**:1196-206.
272. **Soferman, R., D. Bar-Zohar, U. Jurgenson, and E. Fireman.** 2004. Soluble CD14 as a predictor of subsequent development of recurrent wheezing in hospitalized young children with respiratory syncytial virus-induced bronchiolitis. *Ann Allergy Asthma Immunol* **92**:545-8.
273. **Sparwasser, T., E. S. Koch, R. M. Vabulas, K. Heeg, G. B. Lipford, J. W. Ellwart, and H. Wagner.** 1998. Bacterial DNA and immunostimulatory CpG oligonucleotides trigger maturation and activation of murine dendritic cells. *Eur J Immunol* **28**:2045-54.
274. **Stark, J. M., S. A. McDowell, V. Koenigsnecht, D. R. Prows, J. E. Leikauf, A. M. Le Vine, and G. D. Leikauf.** 2002. Genetic susceptibility to respiratory syncytial virus infection in inbred mice. *J Med Virol* **67**:92-100.
275. **Stein, R. T., D. Sherrill, W. J. Morgan, C. J. Holberg, M. Halonen, L. M. Taussig, A. L. Wright, and F. D. Martinez.** 1999. Respiratory syncytial virus in early life and risk of wheeze and allergy by age 13 years. *Lancet* **354**:541-5.
276. **Steinman, R. M., M. Pack, and K. Inaba.** 1997. Dendritic cells in the T-cell areas of lymphoid organs. *Immunol Rev* **156**:25-37.
277. **Steinman, R. M., and J. Swanson.** 1995. The endocytic activity of dendritic cells. *J Exp Med* **182**:283-8.
278. **Stensballe, L. G., J. K. Devasundaram, and E. A. Simoës.** 2003. Respiratory syncytial virus epidemics: the ups and downs of a seasonal virus. *Pediatr Infect Dis J* **22**:S21-32.
279. **Sterner, G., S. Wolontis, B. Bloth, and G. de Hevesy.** 1966. Respiratory syncytial virus. An outbreak of acute respiratory illnesses in a home for infants. *Acta Paediatr Scand* **55**:273-9.
280. **Straliootto, S. M., B. Roitman, J. B. Lima, G. B. Fischer, and M. M. Siqueira.** 1994. Respiratory syncytial virus (RSV) bronchiolitis: comparative study of RSV groups A and B infected children. *Rev Soc Bras Med Trop* **27**:1-4.
281. **Stumbles, P. A., J. A. Thomas, C. L. Pimm, P. T. Lee, T. J. Venaille, S. Proksch, and P. G. Holt.** 1998. Resting respiratory tract dendritic cells preferentially stimulate T helper

- cell type 2 (Th2) responses and require obligatory cytokine signals for induction of Th1 immunity. *J Exp Med* **188**:2019-31.
282. **Suffin, S. C., G. A. Prince, K. B. Muck, and D. D. Porter.** 1979. Immunoprophylaxis of respiratory syncytial virus infection in the infant ferret. *J Immunol* **123**:10-4.
283. **Sullender, W. M., M. A. Mufson, L. J. Anderson, and G. W. Wertz.** 1991. Genetic diversity of the attachment protein of subgroup B respiratory syncytial viruses. *J Virol* **65**:5425-34.
284. **Suss, G., and K. Shortman.** 1996. A subclass of dendritic cells kills CD4 T cells via Fas/Fas-ligand-induced apoptosis. *J Exp Med* **183**:1789-96.
285. **Svensson, M., B. Stockinger, and M. J. Wick.** 1997. Bone marrow-derived dendritic cells can process bacteria for MHC-I and MHC-II presentation to T cells. *J Immunol* **158**:4229-36.
286. **Tal, G., A. Mandelberg, I. Dalal, K. Cesar, E. Somekh, A. Tal, A. Oron, S. Itskovich, A. Ballin, S. Hour, A. Beigelman, O. Lider, G. Rechavi, and N. Amariglio.** 2004. Association between common Toll-like receptor 4 mutations and severe respiratory syncytial virus disease. *J Infect Dis* **189**:2057-63.
287. **Teichtahl, H., N. Buckmaster, and E. Pertnikovs.** 1997. The incidence of respiratory tract infection in adults requiring hospitalization for asthma. *Chest* **112**:591-6.
288. **Tekkanat, K. K., H. Maassab, A. Miller, A. A. Berlin, S. L. Kunkel, and N. W. Lukacs.** 2002. RANTES (CCL5) production during primary respiratory syncytial virus infection exacerbates airway disease. *Eur J Immunol* **32**:3276-84.
289. **The, I.-R. S. V. S. G.** 1998. Palivizumab, a Humanized Respiratory Syncytial Virus Monoclonal Antibody, Reduces Hospitalization From Respiratory Syncytial Virus Infection in High-risk Infants. *Pediatrics* **102**:531-537.
290. **Thompson, W. W., D. K. Shay, E. Weintraub, L. Brammer, N. Cox, L. J. Anderson, and K. Fukuda.** 2003. Mortality associated with influenza and respiratory syncytial virus in the United States. *Jama* **289**:179-86.
291. **Thorpe, L. C., and A. J. Easton.** 2005. Genome sequence of the non-pathogenic strain 15 of pneumonia virus of mice and comparison with the genome of the pathogenic strain J3666. *J Gen Virol* **86**:159-69.
292. **Tripp, R. A., L. Jones, and L. J. Anderson.** 2000. Respiratory syncytial virus G and/or SH glycoproteins modify CC and CX3C chemokine mRNA expression in the BALB/c mouse. *J Virol* **74**:6227-9.
293. **Tripp, R. A., L. P. Jones, L. M. Haynes, H. Zheng, P. M. Murphy, and L. J. Anderson.** 2001. CX3C chemokine mimicry by respiratory syncytial virus G glycoprotein. *Nat Immunol* **2**:732-8.
294. **Tripp, R. A., D. Moore, L. Jones, W. Sullender, J. Winter, and L. J. Anderson.** 1999. Respiratory syncytial virus G and/or SH protein alters Th1 cytokines, natural killer cells, and neutrophils responding to pulmonary infection in BALB/c mice. *J Virol* **73**:7099-107.
295. **Tsutsumi, H., M. Onuma, K. Suga, T. Honjo, Y. Chiba, S. Chiba, and P. L. Ogra.** 1988. Occurrence of respiratory syncytial virus subgroup A and B strains in Japan, 1980 to 1987. *J Clin Microbiol* **26**:1171-4.
296. **Vainionpaa, R., O. Meurman, and H. Sarkkinen.** 1985. Antibody response to respiratory syncytial virus structural proteins in children with acute respiratory syncytial virus infection. *J Virol* **53**:976-9.

297. **Valarcher, J. F., H. Bourhy, A. Lavenu, N. Bourges-Abella, M. Roth, O. Andreoletti, P. Ave, and F. Schelcher.** 2001. Persistent infection of B lymphocytes by bovine respiratory syncytial virus. *Virology* **291**:55-67.
298. **Valdovinos, M. R., and B. Gomez.** 2003. Establishment of respiratory syncytial virus persistence in cell lines: association with defective interfering particles. *Intervirology* **46**:190-8.
299. **Vallbracht, S., H. Unsold, and S. Ehl.** 2006. Functional impairment of cytotoxic T cells in the lung airways following respiratory virus infections. *Eur J Immunol* **36**:1434-42.
300. **van Drunen Littel-van den Hurk, S., J. W. Mapletoft, N. Arsic, and J. Kovacs-Nolan.** 2007. Immunopathology of RSV infection: prospects for developing vaccines without this complication. *Rev Med Virol* **17**:5-34.
301. **van Schaik, S. M., N. Obot, G. Enhorning, K. Hintz, K. Gross, G. E. Hancock, A. M. Stack, and R. C. Welliver.** 2000. Role of interferon gamma in the pathogenesis of primary respiratory syncytial virus infection in BALB/c mice. *J Med Virol* **62**:257-66.
302. **van Schaik, S. M., D. A. Tristram, I. S. Nagpal, K. M. Hintz, R. C. Welliver, 2nd, and R. C. Welliver.** 1999. Increased production of IFN-gamma and cysteinyl leukotrienes in virus-induced wheezing. *J Allergy Clin Immunol* **103**:630-6.
303. **Varga, S. M., X. Wang, R. M. Welsh, and T. J. Braciale.** 2001. Immunopathology in RSV infection is mediated by a discrete oligoclonal subset of antigen-specific CD4(+) T cells. *Immunity* **15**:637-46.
304. **Walsh, E. E., K. M. McConnochie, C. E. Long, and C. B. Hall.** 1997. Severity of respiratory syncytial virus infection is related to virus strain. *J Infect Dis* **175**:814-20.
305. **Wang, S. Z., and K. D. Forsyth.** 2000. The interaction of neutrophils with respiratory epithelial cells in viral infection. *Respirology* **5**:1-10.
306. **Ward, K. A., P. R. Lambden, M. M. Ogilvie, and P. J. Watt.** 1983. Antibodies to respiratory syncytial virus polypeptides and their significance in human infection. *J Gen Virol* **64 (Pt 9)**:1867-76.
307. **Waris, M. E., C. Tsou, D. D. Erdman, D. B. Day, and L. J. Anderson.** 1997. Priming with live respiratory syncytial virus (RSV) prevents the enhanced pulmonary inflammatory response seen after RSV challenge in BALB/c mice immunized with formalin-inactivated RSV. *J Virol* **71**:6935-9.
308. **Waris, M. E., C. Tsou, D. D. Erdman, S. R. Zaki, and L. J. Anderson.** 1996. Respiratory syncytial virus infection in BALB/c mice previously immunized with formalin-inactivated virus induces enhanced pulmonary inflammatory response with a predominant Th2-like cytokine pattern. *J Virol* **70**:2852-60.
309. **Waterston, R. H., K. Lindblad-Toh, E. Birney, J. Rogers, J. F. Abril, P. Agarwal, R. Agarwala, R. Ainscough, M. Alexandersson, P. An, S. E. Antonarakis, J. Attwood, R. Baertsch, J. Bailey, K. Barlow, S. Beck, E. Berry, B. Birren, T. Bloom, P. Bork, M. Botcherby, N. Bray, M. R. Brent, D. G. Brown, S. D. Brown, C. Bult, J. Burton, J. Butler, R. D. Campbell, P. Carninci, S. Cawley, F. Chiaromonte, A. T. Chinwalla, D. M. Church, M. Clamp, C. Clee, F. S. Collins, L. L. Cook, R. R. Copley, A. Coulson, O. Couronne, J. Cuff, V. Curwen, T. Cutts, M. Daly, R. David, J. Davies, K. D. Delehaunty, J. Deri, E. T. Dermitzakis, C. Dewey, N. J. Dickens, M. Diekhans, S. Dodge, I. Dubchak, D. M. Dunn, S. R. Eddy, L. Elnitski, R. D. Emes, P. Esvara, E. Eyraas, A. Felsenfeld, G. A. Fewell, P. Flicek, K. Foley, W. N. Frankel, L. A. Fulton, R. S. Fulton, T. S. Furey, D. Gage, R. A. Gibbs, G. Glusman, S. Gnerre, N.**

- Goldman, L. Goodstadt, D. Grafham, T. A. Graves, E. D. Green, S. Gregory, R. Guigo, M. Guyer, R. C. Hardison, D. Haussler, Y. Hayashizaki, L. W. Hillier, A. Hinrichs, W. Hlavina, T. Holzer, F. Hsu, A. Hua, T. Hubbard, A. Hunt, I. Jackson, D. B. Jaffe, L. S. Johnson, M. Jones, T. A. Jones, A. Joy, M. Kamal, E. K. Karlsson, et al.** 2002. Initial sequencing and comparative analysis of the mouse genome. *Nature* **420**:520-62.
310. **Weisman, L. E.** 2003. Populations at risk for developing respiratory syncytial virus and risk factors for respiratory syncytial virus severity: infants with predisposing conditions. *Pediatr Infect Dis J* **22**:S33-7; discussion S37-9.
311. **Welliver, R. C., T. N. Kaul, and P. L. Ogra.** 1980. The appearance of cell-bound IgE in respiratory-tract epithelium after respiratory-syncytial-virus infection. *N Engl J Med* **303**:1198-202.
312. **Welliver, R. C., T. N. Kaul, T. I. Putnam, M. Sun, K. Riddlesberger, and P. L. Ogra.** 1980. The antibody response to primary and secondary infection with respiratory syncytial virus: kinetics of class-specific responses. *J Pediatr* **96**:808-13.
313. **Welliver, R. C., T. N. Kaul, M. Sun, and P. L. Ogra.** 1984. Defective regulation of immune responses in respiratory syncytial virus infection. *J Immunol* **133**:1925-30.
314. **Welliver, R. C., D. T. Wong, M. Sun, E. Middleton, Jr., R. S. Vaughan, and P. L. Ogra.** 1981. The development of respiratory syncytial virus-specific IgE and the release of histamine in nasopharyngeal secretions after infection. *N Engl J Med* **305**:841-6.
315. **Welliver, T. P., R. P. Garofalo, Y. Hosakote, K. H. Hintz, L. Avendano, K. Sanchez, L. Velozo, H. Jafri, S. Chavez-Bueno, P. L. Ogra, L. McKinney, J. L. Reed, and R. C. Welliver, Sr.** 2007. Severe human lower respiratory tract illness caused by respiratory syncytial virus and influenza virus is characterized by the absence of pulmonary cytotoxic lymphocyte responses. *J Infect Dis* **195**:1126-36.
316. **West, K., L. Petrie, D. M. Haines, C. Konoby, E. G. Clark, K. Martin, and J. A. Ellis.** 1999. The effect of formalin-inactivated vaccine on respiratory disease associated with bovine respiratory syncytial virus infection in calves. *Vaccine* **17**:809-20.
317. **Whimbey, E., and S. Ghosh.** 2000. Respiratory syncytial virus infections in immunocompromised adults. *Curr Clin Top Infect Dis* **20**:232-55.
318. **Wilkinson, T. M., G. C. Donaldson, S. L. Johnston, P. J. Openshaw, and J. A. Wedzicha.** 2006. Respiratory syncytial virus, airway inflammation, and FEV1 decline in patients with chronic obstructive pulmonary disease. *Am J Respir Crit Care Med* **173**:871-6.
319. **World Health Organization (WHO). World Wide Web (URL:http://www.who.int/vaccine_research/diseases/ari/en/index3.html). Last Accessed March 03 2008, posting date. WHO Acute Respiratory Infections. [Online.]**
320. **Wright, A. L., C. Holberg, F. D. Martinez, and L. M. Taussig.** 1991. Relationship of parental smoking to wheezing and nonwheezing lower respiratory tract illnesses in infancy. *Group Health Medical Associates. J Pediatr* **118**:207-14.